Maastricht University

Nerve fibers in the tumor microenvironment

Citation for published version (APA):

Tan, X. (2023). *Nerve fibers in the tumor microenvironment: a novel prognostic biomarker in CCA and PDAC*. [Doctoral Thesis, Maastricht University]. Maastricht University.
https://doi.org/10.26481/dis.20230524xt

Document status and date:
Published: 01/01/2023

DOI:
10.26481/dis.20230524xt

Document Version:
Publisher's PDF, also known as Version of record

Please check the document version of this publication:

• A submitted manuscript is the version of the article upon submission and before peer-review. There can be important differences between the submitted version and the official published version of record. People interested in the research are advised to contact the author for the final version of the publication, or visit the DOI to the publisher's website.
• The final author version and the galley proof are versions of the publication after peer review.
• The final published version features the final layout of the paper including the volume, issue and page numbers.

Link to publication

General rights
Copyright and moral rights for the publications made accessible in the public portal are retained by the authors and/or other copyright owners and it is a condition of accessing publications that users recognise and abide by the legal requirements associated with these rights.

• Users may download and print one copy of any publication from the public portal for the purpose of private study or research.
• You may not further distribute the material or use it for any profit-making activity or commercial gain
• You may freely distribute the URL identifying the publication in the public portal.

If the publication is distributed under the terms of Article 25fa of the Dutch Copyright Act, indicated by the “Taverne” license above, please follow below link for the End User Agreement:

www.umlib.nl/taverne-license

Take down policy
If you believe that this document breaches copyright please contact us at:

repository@maastrichtuniversity.nl

providing details and we will investigate your claim.

Download date: 02 May. 2024

MAASTRICHT UNIVERSITY

NERVE FIBERS IN THE TUMOR MICROENVIRONMENT: A NOVEL PROGNOSTIC BIOMARKER IN CCA AND PDAC

Xiuxiang Tan

Nerve fibers in the tumor microenvironment:
a novel prognostic biomarker in CCA and PDAC

Dissertation

to obtain the degree of Doctor at Maastricht University,

on the authority of Rector Magnificus,

Prof. Pamela Habibovic,

according to the decision of the Board of Deans,

to be defended in public on

24-May-2023 at 1pm

By

Xiuxiang Tan

Promotor

Prof. dr. Ulf P. Neumann

Co-promotor

Dr. Lara Heij

Assessment Committee

Prof. dr. Manon van Engeland (Chair, Maastricht University)

Prof. dr. Heike Grabsch (Maastricht University)

Prof. dr. Danny Jonigk (RWTH Aachen University, Germany)

Prof. dr. Edgar Dahl (RWTH Aachen University, Germany)

Contents

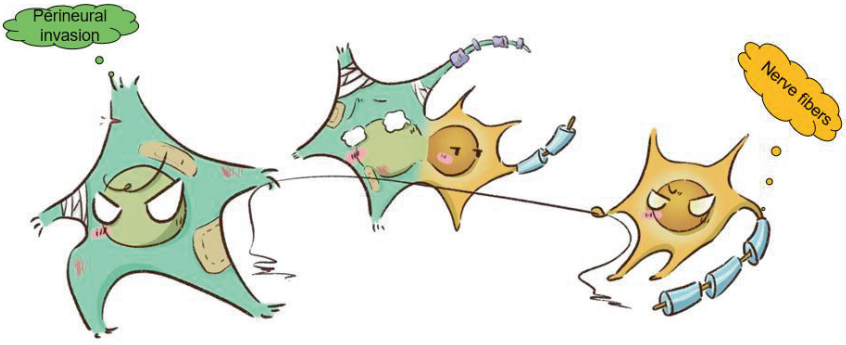
Perineural invasion
Nerve fibers

CHAPTER 1

General introduction, aim and outline of the thesis

Chapter 1

General introduction

Nerve fibers in the tumor microenvironment

The Tumor Microenvironment (TME) is regarded as a complex "ecosystem" in which a heterogeneous population of tumor cells is surrounded by stroma (figure 1). The term "stroma" is broadly defined and here interaction between infiltrating cancer cells, secretion factors and extracellular matrix proteins takes place. In addition, immune cells, fibroblasts, blood vessels, lymphatics and nerve fibers are part of the TME as well. Neuronal nerve processes have been described as being a part of the TME recently in several cancers as colorectal carcinoma[1], breast cancer[2] and head and neck cancers[3].
Interestingly different nerve fibers exist, the peripheral nervous system (PNS) is a transportation
system of signals through nerve fibers connecting the body and the brain. The autonomic part of the PNS is described to play an important role in regeneration when tissue is damaged[4]. The autonomic nervous system is divided in a sympathetic and parasympathetic nervous system. Sympathetic nerve fibers drive the tumor angiogenesis and the parasympathetic nerve fibers stimulate cancer stem cells and potentially can inhibit cancer progression[5].

Some solid cancers are characterized by perineural invasion (PNI), defined as cancer cells invading the perineurium or endoneurium of the nerve fiber[6,7]. PNI is usually associated with a poor outcome and is considered an aggressive feature[8]. In the past years it has been proposed that nerve fibers have a dual role in the TME and besides the PNI another type of nerve fiber growth
pattern exists. Some data on solid tumors demonstrate a potential beneficiary effect of nerve fibers on outcome. By using special staining, small nerve fibers can be visualized, usually these small nerve fibers are not invaded by cancer cells. These small nerve fibers interact with the host and the cancer, but not much is known about the mechanism behind this. The presence of small nerve fibers in the TME can have a potential good effect on outcome. The rationale behind this phenomenon needs further investigation and underlying pathways are not identified yet.

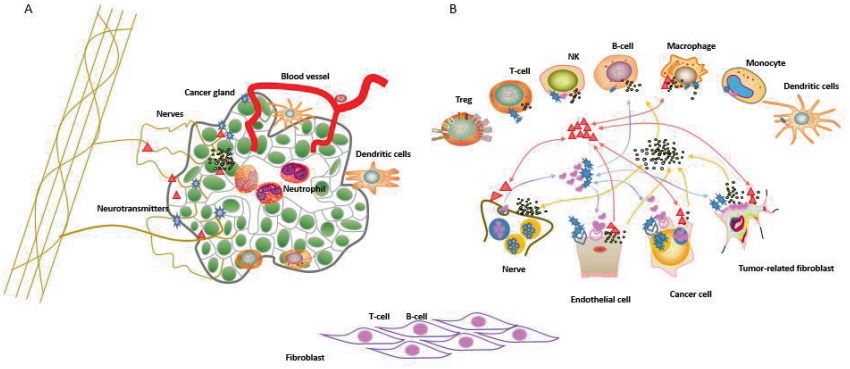

Fig. 1: Overview of tumor microenvironment. (A) the tumor microenvironment consists of cancer cells, nerves, and stromal cells which include fibroblasts, endothelial cells and immune cells like dendric cells, neutrophils and lymphocytes (T- and B-cell) and the non-cellular components of extracellular matrix such as neurotransmitters amongst others. **(B)** cancer cells control the function of cellular and non-cellular components through complex signaling networks of cytokines, chemokines, growth factors, inflammatory mediators, and matrix remodeling enzymes. Figure courtesy of X. Tan.

What is pancreatic ductal adenocarcinoma and cholangiocarcinoma?

Pancreatic Ductal Adenocarcinoma (PDAC) and cholangiocarcinoma (CCA) both are aggressive tumors with a comparable histomorphology[9]. Both cancer types are characterized

by an abundant desmoplastic stroma, common invasion of cancer cells in the lymphatic and blood vessels and spread of cancer cells through the nerves.

Pancreatic Cancer (PCA)

Different types of pancreatic cancer exist (see Fig. 2), in our study cohorts we have included PDAC patients only. Here the tumor glands originate from the exocrine part of the pancreas, giving rise to PDAC. This cancer type is often located at the head of the pancreas. Another type of pancreatic cancer exists, where the neuroendocrine cells in the pancreas can be the origin of a neuroendocrine tumor. This cancer type has a different morphology and is not typically associated with PNI; therefore, this cancer type was not included in our study cohorts.

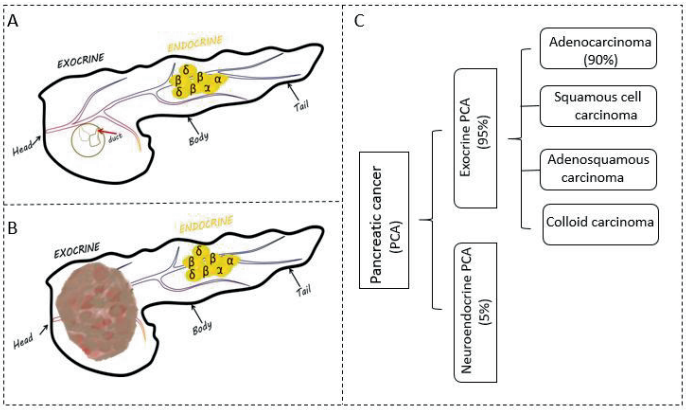

Fig. 2: Anatomy of the pancreas and pancreatic cancer. (A) the pancreas plays an important role in
digestion. The pancreas is a mixed gland with an endocrine and an exocrine function, the largest
compartment is exocrine (about 99%). During digestion, pancreatic enzymes are transported through the ducts into the duodenum, which breaks down sugars, proteins, and fat in the food. In addition, the pancreas also regulates blood sugar levels and secretes hormones, such as somatostatin, and glucagon. (B) pancreatic cancer can arise in the exocrine or the endocrine part. (C) a short summary of different histological subtypes of pancreatic cancer. Figure courtesy of X. Tan.

Cholangiocarcinoma

CCA is considered an incurable and rapidly lethal disease, unless the tumor can be fully resected. However, most cases of CCA present as unresectable carcinoma unfortunately meaning patients usually die from liver failure, biliary sepsis, and cancer cachexia within 6-12 months after the diagnosis. The 5-year survival rate is <5% in general[10]. The patients who are not eligible for surgery are treated by combination treatment of chemotherapy, with or without radiotherapy. The knowledge of the biology of this aggressive behavior and therapy resistance is limited. One reason for this is the fact that CCA is a rare cancer and samples to conduct research in large cohorts often are missing.

CCA is a malignant cancer from which the cancer cells arise from the biliary tract epithelium. CCA is classified into 3 subtypes based on their location (See fig. 3):

1) Intrahepatic cholangiocarcinoma (iCCA) in which the primary cancer is located within liver.
2) Perihilar cholangiocarcinoma (pCCA) (also known as Klatskin tumor) in which the cancer is located at the bifurcation of hepatic duct.
3) Distal cholangiocarcinoma (dCCA) in which the cancer is located at the bile ducts outside the liver.

PCCA is the most common type, accounting for ~60%-70%, followed by dCCA comprising ~20%-30% and iCCA being responsible for 5%-10% of the CCA cases[11].

Cholangiocarcinoma is characterized by frequent PNI. In our study cohorts we included pCCA and iCCA patients, because of their location within the liver parenchyma. In case of dCCA the cancer is sometimes located in the pancreas or the common bile duct, and these cases have a different TME and are therefore not included in our study cohorts.

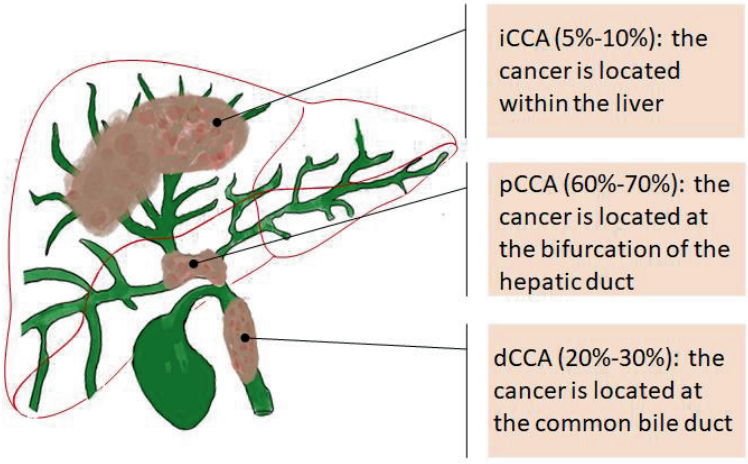

Fig. 3: Three main types of cholangiocarcinoma: iCCA: intrahepatic cholangiocarcinoma, pCCA: perihilar cholangiocarcinoma, dCCA: distal cholangiocarcinoma. Figure courtesy of X. Tan.

Current existing and used predictive and prognostic biomarkers PDAC and CCA

PDAC is often discovered in an advanced stage and therefore treatment options are limited. In consideration of the performance status, different chemotherapy regimens are established in metastatic or locally advanced PDAC[12]. In case of a good performance status (defined by ECOG 0-1) FOLFIRINOX (5-FU, leucovorin, irinotecan, oxaliplatin) and gemcitabine/nab-paclitaxel have shown highest potency regarding survival times[13]. For gemcitabine/nab-paclitaxel response a CA19-9 association was shown, with the greatest reduction in the risk of death in patients with CA19-9 levels ≥ 59xULN and in those with a serum level decrease over 90%. Therefore CA19-9 currently is used in the clinical field as a biomarker during treatment to monitor response and risk for the patient. In case of a poor perfomance status Capacitabine monotherapy can be considered or best supportive care. Immunotherapeutical agents are offered in clinical trial setting but efficacy is limited. For CCA, Durvalumab in combination with Gemcitabine/Cisplatin has received FDA approval in America recently. Results from the TOPAZ-1 trial are promosing but still only a subset, approximately 30%, of patients seem to respond[14]. Biomarkers to predict a response to immuntherapy up to now fail.

For diagnosis and or prognosis in PDAC, other carbohydrate antigens can be used, but with less sensitivity then CA19-9, serum levels of CA125, CA72.4[15] and CEA[16] have been identified as a potential biomarker for an early diagnosis. A solitary diagnostic potential for these antigens does not exist, therefore their value is more used as a prognostic marker.

PDAC precursor lesions, acinar to ductal metaplasia (ADM) and pancreatic intraepithelial neoplasia (PanIN) have the potential to develop into an invasive malignancy. These precursor lesions harbour specific genetic alterations that ultimately lead to the development of an invasive malignancy[17,18].

Biomarkers to identify these precursor lesions are very much needed, so screening methods can
discover PDAC in an early stage. Intraductal papillary mucinous neoplasms (IPMNs) represent
precursor lesions with a special status, since they are detectable on imaging techniques and therefore can be risk classified based on imaging criteria[19]. The development of new non-invasive biomarkers is crucial to improve early diagnosis and surveillance of precursor lesions of PDAC.

Elevated levels of serum carcinoembryonic antigen (CEA) and CA19-9 in CCA have been observed in approximately 31% and 59%, respectively. Increased levels were mainly found in patients with locally advanced disease or metastatic disease. These markers are used in clinical care when the CCA

diagnosis is suspected. While CA19-9 offers prognostic value as a biomarker, CEA fails to do so[20]. Tissue collection can be problematic and if a biopsy is performed for a histological diagnosis, the tissue is usually sparse. This limits the discovery of tissue related biomarkers and the ideal biomarker would be detectable in blood or other liquids (bile, stool, or urine).

Ongoing research in these cancer types to identify novel biomarkers and treatment options

Biomarkers can be based on any biospecimen and ongoing research is focused on multiple different technologies and different tissues. In tumor tissue research has been done on molecular alterations and potential prognostic proteins. The potential of liquid biopsies has been widely investigated and prognostic proteins can be detected in blood samples. Also, urine and bile samples potentially harbour biomarkers. Recently the development of artificial intelligence has opened new possibilities to use computer-based models in combination with neural networks for a diagnosis or prediction of prognosis.

Due to the high importance to find new biomarkers for early diagnosis of occurrence and recurrence of PDAC and CCA, as well as treatment response in advanced stage tumor disease, this has been a field of interest over the past years. The clinical need for personalised care and development of biomarkers to allow treatment stratification is high.

Hypothesis

We hypothesized that nerve fibers in the TME play a dual role and the small nerve fibers are predictive of a good prognosis for the patients outcome in CCA and PDAC.

Choice of study cohorts, type of material and methodology to investigate the research question

During this PhD trajectory, research cohorts from the University Hospital RWTH Aachen were designed. In collaboration with the pathology department and the surgery department extended databases were created with clinical data and histology slides and FFPE blocks from the pathology archive were collected. Patients without previous treatment were included and for CCA only patients with iCCA and pCCA were included, as mentioned before. For iCCA and pCCA we aimed to select slides with the same surrounding tissue, the liver parenchyma.

The methods used for our research projects were mainly single immunohistochemistry and multiplexed immunohistochemistry. Outcomes were correlated with clinical data as overall survival and disease-free survival. Also, lymph node metastasis was used as a parameter for a poor outcome and aggressive biology of the disease.

Chapter 2 consists of a review of the literature; this chapter provides a background on the existing literature in 2019 on nerve fibers in neurotropic cancer.

Summary

Nerve fibers are a component of the TME in CCA and PDAC and although PNI is a well-known feature in these cancer types, the role of small nerve fibers is under investigated. PNI is a known aggressive feature and the large with cancer invaded nerve trunks are located in and around the tumor. Research on the role of small nerve fibers in the TME in cancer is evolving. CCA and PDAC both are cancer types with frequent PNI and a large stromal component. The diagnosis of CCA and PDAC often takes place in advanced stage of the disease and therefore treatment options are limited. Depending on the performance status, chemotherapeutical agents alone or in combination are the current standard of care. For both, treatment is done either before or after surgery. Ongoing research to identify biomarkers, either for early detection of the disease, prognosis, treatment stratification for personalized care and the development of new potential therapeutically agents, are of high clinical importance.

Aims and outline

Nerve fibers are a pivotal component of the TME in CCA as well as PDAC. Nerve fibers can play a dual role in the TME. Nerve fibers infiltrated with cancer are a sign of an aggressive tumor biology. Small nerve fibers however have a good prognosis for the patients outcome.

The aim of this thesis is to gain more in-depth knowledge about the role of nerve fibers within the TME of CCA and PDAC and to explore new predictive and prognostic biomarkers. The following aims will be addressed within this thesis. **Chapter 2. Nerve fibers in the tumor microenvironment in neurotropic cancer—pancreatic cancer and cholangiocarcinoma** gives an overview of current knowledge of nerve fibers participating in the progress of neurotropic cancer. Further, it provides insight in the potential for nerve fibers to be used as powerful biomarker for prognosis. Also, nerve fibers can be used as a tool to stratify patients for therapy and/or nerve fibers can be used to target in a (combination) therapy. **Chapter 3. Nerve fibers in the tumor microenvironment are co-localized with lymphoid aggregates in pancreatic cancer** aims to define the role of small nerve fibers in the TME and their spatial arrangement to immune cells within TME of PDAC. **Chapter 4. Nerve fibers in the tumor microenvironment as a novel biomarker for oncological outcome in patients undergoing surgery for perihilar cholangiocarcinoma** explores nerve fiber density in correlation to survival of pCCA patients. **Chapter 5. The presence of small nerve fibers in the tumor microenvironment as predictive biomarker of oncological outcome following partial hepatectomy for intrahepatic cholangiocarcinoma** demonstrate nerve fibers as a novel and important prognostic biomarker in iCCA patients. **Chapter 6. PD1+ T-cells correlate with Nerve Fiber Density as a prognostic biomarker in patients with resected perihilar cholangiocarcinoma** explores differences in immune cell populations and survival of pCCA patients.

Finally, in **Chapter 7. General discussion** the key findings and novelty of this thesis are discussed in the context of these two "neurotropic cancers" along with a perspective view on its potential application biomarker discovery and potentially therapeutic targets.

Abbreviations

ADM Acinar to ductal metaplasia

AFP α-fetoprotein

CCA Cholangiocarcinoma

DCCA Distal cholangiocarcinomas

ICCA Intrahepatic cholangiocarcinomas

IPMN Intraductal papillary mucinous neoplasm

PanIN Pancreatic intraepithelial neoplasia

PCA Pancreatic cancer

PCCA Perihilar cholangiocarcinoma

PDAC Pancreatic ductal adenocarcinoma

PNI Perineural Invasion

PNS Peripheral nervous system

TME Tumor microenvironment

Reference

1. Vaes N, Idris M, Boesmans W, Alves MM, Melotte V. Nerves in gastrointestinal cancer: from mechanism to modulations. *Nat Rev Gastroenterol Hepatol* 2022.
2. Li D, Hu LN, Zheng SM, et al. High nerve density in breast cancer is associated with poor patient outcome. *FASEB Bioadv* 2022; **4**(6): 391-401.
3. Amit M, Takahashi H, Dragomir MP, et al. Loss of p53 drives neuron reprogramming in head and neck cancer. *Nature* 2020; **578**(7795): 449-54.
4. Guillot J, Dominici C, Lucchesi A, et al. Sympathetic axonal sprouting induces changes in macrophage populations and protects against pancreatic cancer. *Nature communications* 2022; **13**(1): 1985.
5. Faulkner S, Jobling P, March B, Jiang CC, Hondermarck H. Tumor Neurobiology and the War of Nerves in Cancer. *Cancer Discov* 2019; **9**(6): 702-10.
6. Tan X, Sivakumar S, Bednarsch J, et al. Nerve fibers in the tumor microenvironment in neurotropic cancer-pancreatic cancer and cholangiocarcinoma. *Oncogene* 2021; **40**(5): 899-908.
7. Bapat AA, Hostetter G, Von Hoff DD, Han H. Perineural invasion and associated pain in pancreatic cancer. *Nat Rev Cancer* 2011; **11**(10): 695-707.
8. Wang W, Li L, Chen N, et al. Nerves in the Tumor Microenvironment: Origin and Effects. *Frontiers in Cell and Developmental Biology* 2020; **8**.
9. Liu H, Ma Q, Xu Q, et al. Therapeutic potential of perineural invasion, hypoxia and desmoplasia in pancreatic cancer. *Curr Pharm Des* 2012; **18**(17): 2395-403.
10. Yusoff AR, Razak MM, Yoong BK, Vijeyasingam R, Siti ZM. Survival analysis of cholangiocarcinoma: a 10-year experience in Malaysia. *World journal of gastroenterology* 2012; **18**(5): 458-65.
11. Krishna M. Pathology of Cholangiocarcinoma and Combined Hepatocellular-Cholangiocarcinoma. *Clin Liver Dis (Hoboken)* 2021; **17**(4): 255-60.
12. Ducreux M, Cuhna AS, Caramella C, et al. Cancer of the pancreas: ESMO Clinical Practice Guidelines for diagnosis, treatment and follow-up. *Ann Oncol* 2015; **26 Suppl 5**: v56-68.
13. Conroy T, Desseigne F, Ychou M, et al. FOLFIRINOX versus gemcitabine for metastatic pancreatic cancer. *N Engl J Med* 2011; **364**(19): 1817-25.
14. Oh D-Y, He AR, Qin S, et al. Durvalumab plus Gemcitabine and Cisplatin in Advanced Biliary Tract Cancer. *NEJM Evidence*; **0**(0): EVIDoa2200015.
15. Wang Z, Tian YP. Clinical value of serum tumor markers CA19-9, CA125 and CA72-4 in the diagnosis of pancreatic carcinoma. *Mol Clin Oncol* 2014; **2**(2): 265-8.
16. Nazli O, Bozdag AD, Tansug T, Kir R, Kaymak E. The diagnostic importance of CEA and CA 19-9 for the early diagnosis of pancreatic carcinoma. *Hepatogastroenterology* 2000; **47**(36): 1750-2.
17. Ren B, Liu X, Suriawinata AA. Pancreatic Ductal Adenocarcinoma and Its Precursor Lesions: Histopathology, Cytopathology, and Molecular Pathology. *Am J Pathol* 2019; **189**(1): 9-21.
18. Matthaei H, Schulick RD, Hruban RH, Maitra A. Cystic precursors to invasive pancreatic cancer. *Nat Rev Gastroenterol Hepatol* 2011; **8**(3): 141-50.
19. Tanaka M, Fernandez-Del Castillo C, Kamisawa T, et al. Revisions of international consensus Fukuoka guidelines for the management of IPMN of the pancreas. *Pancreatology* 2017; **17**(5): 738-53.
20. Izquierdo-Sanchez L, Lamarca A, La Casta A, et al. Cholangiocarcinoma landscape in Europe: Diagnostic, prognostic and therapeutic insights from the ENSCCA Registry. *Journal of hepatology* 2022; **76**(5): 1109-21.

Chapter 1

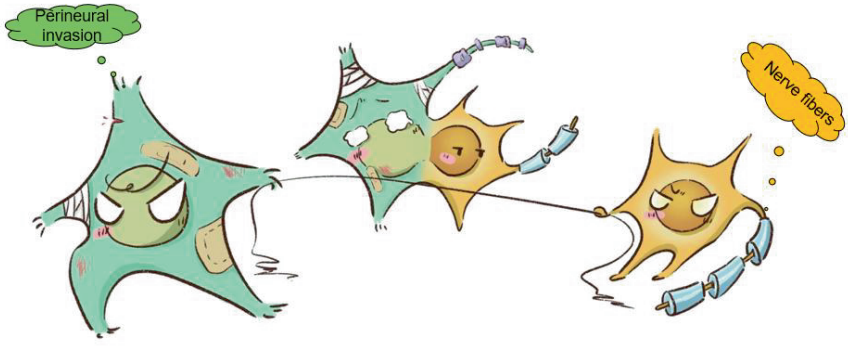

CHAPTER 2

Nerve fibers in the Tumor Microenvironment in neurotropic cancer - Pancreatic Cancer and Cholangiocarcinoma

Xiuxiang Tan, Shivan Sivakumar, Jan Bednarsch, Georg Wiltberger, Jakob Nikolas Kather, Jan Niehues, Judith de Vos-Geelen, Liselot Valkenburg-van Iersel, Svetlana Kintsler, Anjali Roeth, Guangshan Hao, Sven Lang, Mariëlle E. Coolsen, Marcel den Dulk, Merel R. Aberle, Jarne Koolen, Nadine T. Gaisa, Steven W.M. Olde Damink, Ulf Neumann, Lara R. Heij

1ST author

Oncogene, 07 December 2020, 40, pages 899–908 (2021)

Chapter 2

Abstract

Pancreatic ductal adenocarcinoma (PDAC) and Cholangiocarcinoma (CCA) are both deadly cancers and they share many biological features besides their close anatomical location. One of the main histological features is neurotropism, which results in frequent perineural invasion. The underlying mechanism of cancer cells favoring growth by and through the nerve fibers is not fully understood.

In this review, we provide knowledge of these cancers with frequent perineural invasion. We discuss nerve fiber crosstalk with the main different components of the Tumor Microenvironment (TME), the immune cells and the fibroblasts. Also we discuss the crosstalk between the nerve fibers and the cancer. We highlight the shared signaling pathways of the mechanisms behind perineural invasion in PDAC and CCA. Hereby we have focused on signaling neurotransmitters and neuropeptides which may be a target for future therapies. Furthermore, we have summarized retrospective results of the previous literature about nerve fibers in PDAC and CCA patients.

We provide our point of view in the potential for nerve fibers to be used as powerful biomarker for prognosis, as a tool to stratify patients for therapy or as a target in a (combination)therapy. Taking the presence of nerves into account can potentially change the field of personalized care in these neurotropic cancers.

Keywords: perineural invasion, immune cells, cancer-related neurogenesis, tumor microenvironment, pancreatic ductal adenocarcinoma, cholangiocarcinoma, cancer associated stroma, nerve fibers.

List of abbreviations

Ach	Acetylcholine
AJCC	American Joint Committee on Cancer
ANS	Autonomic nervous system
CAFs	Cancer-associated fibroblasts
cAMP	Cyclic 3′-5′ AdenosineMonophosphate
CCA	Cholangiocarcinoma
CHRM1	Muscarinic type 1 receptor
DFS	Disease Free Survival
EGF	Epidermal growth factor signalling
GAP-43	Growth-associated protein-43
H&E	Hematoxylin and Eosin
JAK2	Janus kinase2
M3	Acetylcholine receptor 3
MMP	Matrix metalloproteases
nAChRs	Nicotinic acetylcholine receptors
NE	Norepinephrine
NGF	Nerve growth factor
NICUs	Neuro-immune cell units
OS	Overall Survival
p75NTR	p75 neurotrophin receptor
PDAC	Pancreatic ductal adenocarcinoma

PGP9.5	Protein gene product 9.5
PKA	Protein kinaseA
PLCγ	Phospholipase Cγ
PNI	Perineural invasion
PSNS	Parasympathetic nervous system
SNS	Sympathetic nervous system
TME	Tumor Microenvironment
TRKA	Tropomyosin receptor kinase A

Introduction

Pancreatic ductal adenocarcinoma (PDAC) and cholangiocarcinoma (CCA) are aggressive cancers with only a limited response to chemotherapy. PDAC mortality is estimated to exceed the total breast, prostate, and colorectal cancer deaths and be the second leading cancer-related death by 2030[1,2]. PDAC and CCA share many clinical characteristics, which include high mortality rates and low treatment efficacy[3]. Unfortunately, survival rates have not improved even from recent novel therapeutic targets such as immune checkpoints[3-7]. Biologically PDAC and CCA are characterized by desmoplastic stroma and this stromal compartment is thought to be held responsible for the poor efficacy of chemotherapy. Today, surgery combined with chemotherapy is the only chance of cure[8].

The tumor microenvironment (TME) is a fervent area of research interest as it contains a host of non-malignant cells that play an important role in carcinogenesis such as fibroblasts, immune cells, blood- and lymphatic vessels and nerve fibers. In this review, we will focus on the pathways involved in neurogenesis and the interaction between nerve fibers and the other components of the TME.

Internal organs are innervated by the autonomic nervous system (ANS), which is composed of two components: the sympathetic nervous system (SNS) and the parasympathetic nervous system (PSNS). Increasing evidence shows that not only the internal organs are innervated by the PSNS, but solid tumors also depend on the development of nerves in the TME for growth and invasion in adjacent tissue [9-11].

Besides the aggressive behaviour and poor response to treatment, another shared feature of these two cancer types is perineural invasion (PNI), which is defined as cancer cells surrounding at least 33% of the epineurial, perineural and endoneurial space of the nerve sheath[12]. Perineural invasion describes the process of cancer cells invading the nerve, crossing all layers of the nerve sheath. Once the cancer cells are invaded in the nerve, they have reached a favourable environment to travel intraneural and contribute to progression of the disease. Over time different definitions for perineural invasion have been used. It has been described as cancer cells located in the endoneurium associated with the Schwann cells[13] or later on as the presence of cancer cells along one of the layers of the nerve sheath[12,14-16]. For pathologists invasion in one of these nerve sheath layers is used to report perineural invasion and often a mixture of invasion in different layers is seen in one histological slide. Intraneural invasion in PDAC has been associated with higher frequency of local/distant recurrence when compared to cases with PNI but without intraneural invasion[17]. This provides some evidence that defining the level of perineural invasion matters clinically but up to now this is not recommended in the guidelines for the pathologists. The exact underlying mechanism of PNI remains unknown [12,18]. A hypothesis is that the nerve fibers choose the path of "least resistance" and the cancer cells move along this low resistance path[14,15]. A recent insight showed that PNI was activating signaling pathways when cancer cells attacked the perineural spaces of the surrounding nerves[12]. Even though PNI commonly occurs in many solid tumors[19-22], PDAC and CCA are "neurotropic cancers" and have a high frequency of perineural invasion[23]. It has been reported that almost all PDAC lesions contain PNI and about 75% of CCA lesions showed PNI[23-25] (Figure 1 presents the classical PNI pathological characteristics of PDAC and CCA).

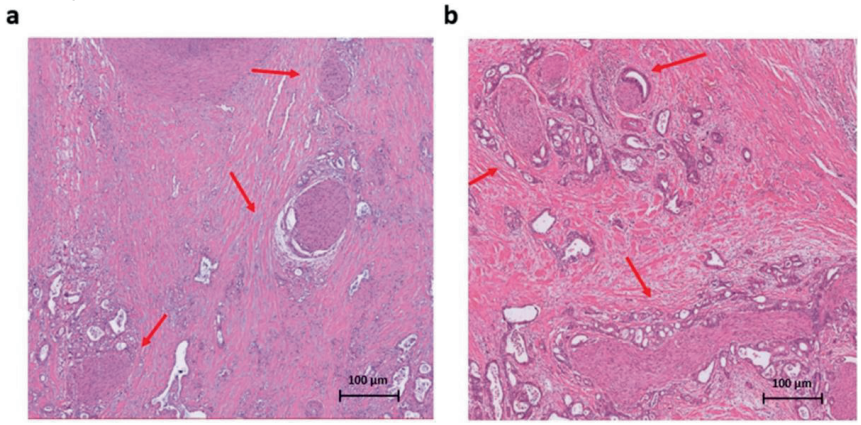

Fig. 1: Histology of perineural invasion in neurotropic cancer. Histology slide of PDAC (**a**) and CCA (**b**) in Hematoxylin and Eosin (H&E) showing PNI, which is one of the shared pathological characteristics of both cancers. a PDAC slide with extended PNI and an almost identical histomorphology as CCA. (**b**) CCA with tumor cells massively invading the perineural space, surrounded by desmoplastic stroma and few small tumor glands in the stroma.

A novel biological phenomenon is the cancer-related neurogenesis, which is described in prostate cancer. The nerve fiber density is increased in paraneoplastic and neoplastic prostate lesions[26]. It is not known whether this cancer-related neurogenesis also occurs in PDAC or CCA. Exploring the role of alterations in nerve fibers in PDAC and CCA has the potential to be of importance in developing
personalised medicine and finding an effective novel treatment strategy.

In this review, we aim to provide an overview of the current knowledge about nerve fiber crosstalk with cancer, and other components of the TME in PDAC and CCA.

Innervation and neurotransmitters

There is a complex nerve fiber network distributed around the pancreas, retroperitoneum and the biliary tree. Nerve fibers in the PDAC TME include axons originating from the sympathetic, parasympathetic, enteropancreatic or hepatic plexus, afferent nerve fibers and newly developed nerve fibers[27]. The nerve fibers of the SNS are derived from the lateral horn of the spinal cord whilst PSNS fibers originate from the brainstem (Figure 2)[28-31]. A rich nerve network facilitates peripheral nerve invasion by cancer cells. Direct contact between cancer cells and nerves leads to a fertile ground for perineural invasion. In addition, numerous signal transduction pathways, neurotransmitters, and neuropeptides regulate the pathophysiology of cancer cells[32-34]. Neurotransmitters can interact with cancer cells and in exchange the cancer cells can also release neurotransmitters which can activate receptors on nerve fibers. This stimulation possibly causes dysregulation of the nerve fiber network and acceleration of PNI[35].

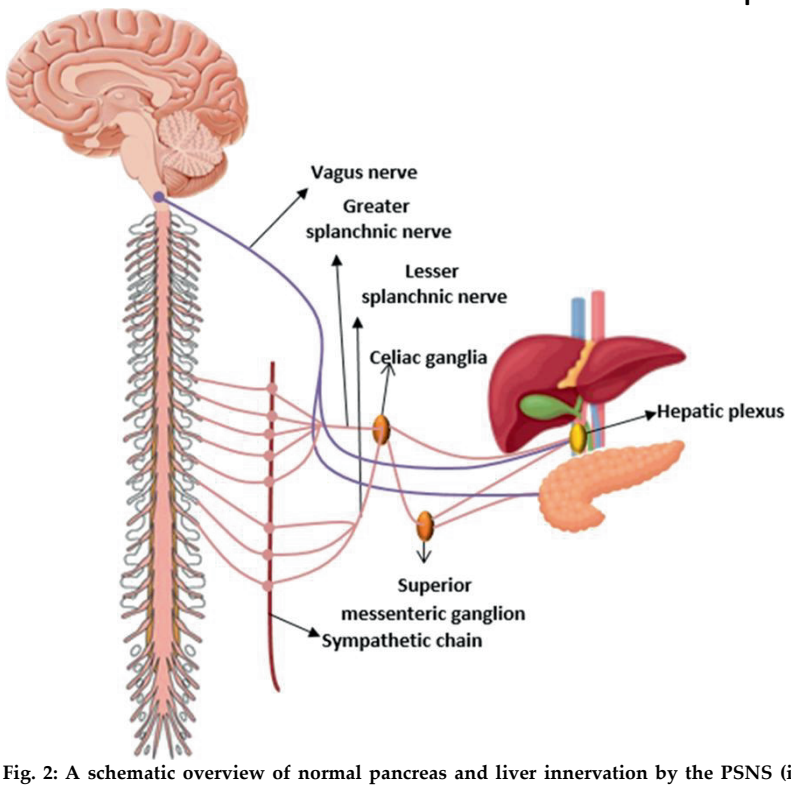

Fig. 2: A schematic overview of normal pancreas and liver innervation by the PSNS (in purple) and the SNS (in pink). SNS innervation of the liver and pancreas is derived from the lateral horn of the spinal cord (liverT7-T12, pancreas C8-L3) across through sympathetic chain primarily via the splanchnic nerve to prevertebral ganglia including the celia and superior ganglion entering hepatic plexus. The PSNS supporting the liver and pancreas originates from the brainstem (dorsal motor nucleus of the n. vagus in the medulla) and activates parasympathetic postganglionic neurons in the liver or the pancreatic ganglia [28,29,30,31].

Norepinephrine (NE)

NE is an indispensable neurotransmitter released by the postganglionic sympathetic neurons that is involved in cell migration activity[36]. The migration of tumor cells is needed for the development of cancer metastases[37]. Migration activity mediated by norepinephrine occurs via acting on β-2 adrenergic receptors and this can be influenced by using β-blockers [38]. A study in mice demonstrated that when NE is induced in development, the secretion of neurotrophins is accelerated. The inhibition of neurotrophins receptors improved the effect of gemcitabine's treatment (gemcitabine is a chemotherapy commonly used in pancreatic cancer)[39]. In CCA cell lines (Mz-ChA-1 cells), using immunocytochemistry and immunoblotting α-2-adrenergic receptor was stimulated by NE, causing an upregulation of cAMP. cAMP stimulates or inhibits mitosis depending on the cell type. By prolonged EGF stimulation, by NE or cAMP, an increase of RAF-1 and B-RAF was achieved. This opens new possible therapeutic targets because the inhibition of growth occurred downstream of RAS[40]. The study demonstrated that β-2 and α-2 adrenergic receptors were significantly down-regulated in a differentiation signature involved in the above process and promote cancer progression. Thereby, p53 mutation was linked to poor survival. Deficiency of p53 can lead to cancer associated neurogenesis with an adrenergic phenotype and a poor survival in head and neck cancer[41].

Acetylcholine (Ach)

Ach and its ligands nicotinic acetylcholine receptors (nAChRs) participate as functional neurotransmitters in the cholinergic system and they play a stimulating role in progression of PDAC and CCA[42-44]. In CD18/HPAF pancreatic cell implantation in mice, nicotine treatment stimulated the α7 subunit of nicotinic acetylcholine receptor (7-nAChR) and enhanced cancer metastasis. This stimulation of 7-nAChR resulted in an activation of Janus kinase2 (JAK2)/STAT3 signalling cascade together with the protein kinase (Ras/Raf/MEK/ERK1/2) pathway[45]. Also, higher densities of muscarinic acetylcholine receptor 3 (M3) showed an association with high grade differentiation of PDAC, more lymph node metastasis and a shorter patient overall survival[44]. In CCA, the presence of the cholinergic system plays a role in CCA cell proliferation and growth[46,47].

Nerve growth factor (NGF)

NGF has been extensively studied and it has been shown that NGF not only acts directly on the peripheral and central nervous system, but also on the components of the TME[48]. NGF treatment can trigger the cancer cells to stay in a more differentiated cell phenotype and thus reduce tumor growth[48,49]. Besides the effect on the cancer cell phenotype there is a possible interaction between the immune cells in the TME. NGF is able to act on immune cell activities and this enables NGF to play an important role in the immunity against cancer. Two important cell surface receptors on neurotrophins have been described: tropomyosin receptor kinase A (TRKA) and p75 neurotrophin receptor (p75NTR)[50-52]. In CCA patients, high levels of NGF and high levels of TRKA have been shown to be a marker for poor prognosis[53]. In PDAC, overexpression of NGF promoted pancreatic cell proliferation and invasiveness and was associated with poor prognosis of PDAC[54]. Saloman et al. injected NGF antibodies in a xenograft mouse model of PDAC. It appeared that anti-NGF treatment reduced neural inflammation, neural invasion, and metastasis in this model only after recent onset of the disease. This indicates that the timing of treatment would be critical[55]. Furthermore, in the biliary system in rats it was shown that cholangiocytes secrete NGF and express NGF receptors. NGF promoted cholangiocyte proliferation in synergy with estrogen[56]. It has been shown in human cholangiocarcinoma cell lines (QBC939) that NGF-β induced progression of disease[57]. Other studies also confirmed that the role of NGF-β in human hilar cholangiocarcinoma was associated with lymph node metastasis and nerve infiltration[58].

Crosstalk between neural systems and cancer

Two recent reviews reveal the importance of nerves in cancer and describe the bidirectional crosstalk of the nervous system. The nerves are able to control cancer initiation, growth and metastasis, whereas the cancer induces functional alterations of the nervous system (Figure 3 shows an overview of the bidirectional crosstalk)[49,59]. Nerves often travel together with blood vessels, mainly arterioles and capillaries, and share the same distribution[60]. In addition, adrenergic nerves can activate and initiate angiogenesis in the early stage of cancer[9]. For the tissue to make the transition from hyperplasia to neoplasia there is a need for angiogenic activity and neovascularization[61]. Evidence showed that adrenergic nerves, through the ß-adrenergic receptor pathway, are important in facilitating tumor growth and cancer cell dissemination in prostate cancer[62,63]. Hence pharmacological blockade of adrenergic-ß-blockers can improve survival[62]. Previous work suggests that a ß-blocker therapy could show lower recurrence and lower mortality in many types of cancer including PDAC[63-66]. Nerves contribute to the development of a new vascular network and they help in supplying the TME for oxygen, nutrients and removal of waste products[9]. Neurogenesis is driven by neural progenitors in the TME which are strongly associated with tumor infiltration and dissemination[67]. An increased density of nerve fibers in the tumor lesion is correlated with high-grade disease and increased pathological stage, including for cancers of head and neck[68], breast[69], lung[70], stomach[71], prostate[26,62], colon and rectum[72]. For PDAC it is suggested to be the other way around: a low nerve fiber density correlates with a poorer survival[73]. In another study, a high nerve fiber density of the parasympathetic nerve fibers correlated with tumor budding and a poor survival[74].

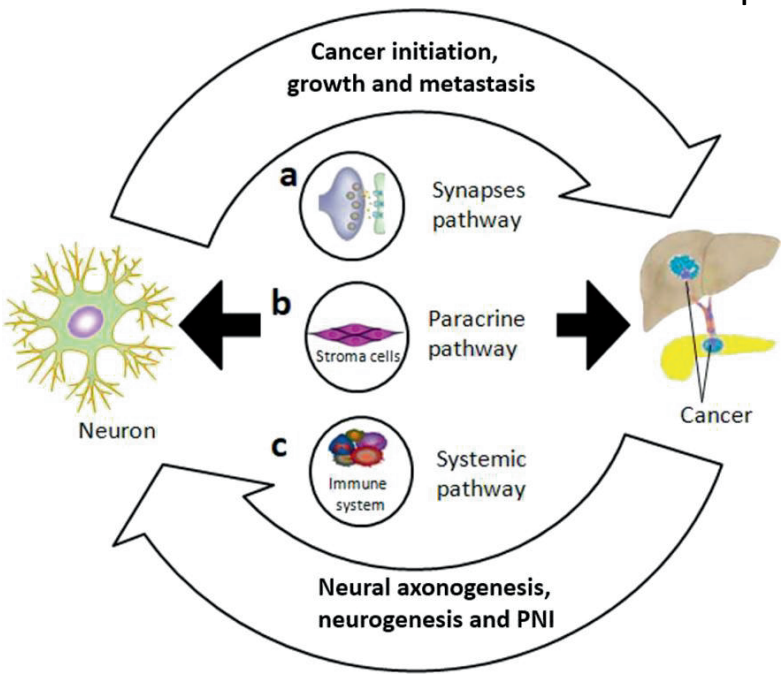

Fig. 3: A bidirectional crosstalk between nerves and cancer in pancreas and liver. Nerve fibers as branches of neuron infiltrate the TME and control cancer cells initiation, growth and metastasis mainly through three interactions pathways: **a** Direct contact in a synapse pathway, neuron as presynaptic cell via secretion of neurotransmitters and neuropeptides such as acetylcholin act on neurotransmitter receptors such as acetylcholin receptors on postsynaptic cell to regulate epithelial proliferation, stem cell activity, both nerve and liver or pancreatic cancer cells can be as pre- or post-synaptic cells in this communication. **b** Paracrine pathway, within TME, addition to direct influence, nerves communication with cancer can be mediated by regulation of tumor-related stroma cells. And the paracrine signals (neurotrophic growth factors) derived by cancer cell promote nerve axonogenesis or neurogenesis in TME. **c** Systemic pathway, nervous system can influence cancer cells activities through regulation the function of immune system mediated by elevated systemic circulating catecholamines. PNI can also be a consequence of circulating signals from cancer cells [42, 59].

Nerve fibers from different origins have a different influence and can be indicative of a protective or aggressive role. Previous work has investigated the role of adrenergic nerves in prostate cancer, this work illustrates that the adrenergic nerve fibers are important in the "angiogenic switch", which activates endothelial cells to support exponential tumor growth[9]. Analysis of clinical outcome in 43 prostate cancer patients showed that parasympathetic nerve fibers are involved in early tumor development and the parasympathetic nerve fibers play a role in the tumor progression and more disseminated disease[62]. A retrospective study of PDAC specimens found consistent results and in PDAC the parasympathetic neurogenesis is highly associated with a poor prognosis[74]. PDAC mouse model experiments have investigated the role of nerves in the TME, multiple studies have shown that targeting the nerves in the TME could contribute to the prevention of paraneoplastic lesions to develop into cancer [75-77].

In one of these experiments, xenograft mouse models and genetically engineered mouse models of PDAC are used to investigate the role of peripheral nerves in the paraneoplastic lesion, where neonatal capsaicin is administered to ablate the sensory innervation of the pancreas. The results show that in the early stage of cancer, denervation of the pancreas slows pancreatic intraepithelial neoplasia progression and ultimately increases survival[76].

Denervation treatment has been shown to be effective in early stages of cancer. However, in a metastatic PDAC mouse model, mice with vagotomy (with a part of the PSNS) have an accelerated tumorigenesis. Systemic administration of a muscarinic agonist reduced this effect in the mice that underwent vagotomy[7]. These results indicate that denervation treatment combined with another therapy can be effective.

During the tumor formation process, tumor cells may attract neural progenitors which induce neurogenesis to support their growth and metastasis. Adrenergic nerve fibers and newly formed neural networks develop and infiltrate into the cancer-related stroma, providing signals to regulate tumor progression[78]. Previous studies have presented that newly formed adrenergic nerve fibers are participators involved in prostate carcinogenesis and progression and this was associated with a poor clinical outcome[9,26,62]. Recently it was shown that p53 mutation status in head and neck cancer was related with a adrenergic transdifferentiating of the nerves in the tumor and this was associated with a poor clinical outcome[78].

Crosstalk between nerves and immune cells

Previous literature shows that communication and interaction between the nervous system and the immune system exists. The autonomic nervous system has a regulatory effect on the inflammatory response[79]. The peripheral nervous system interacts by efferent and afferent nerves which innervate primary and secondary lymphoid organs such as the spleen and lymph nodes. T cells originate in the thymus and then spread to peripheral organs[80]. During the process of T cell development and differentiation, neuro-immune communications in the thymus play a key role[81]. A current study reveals the distribution of nerve fibers in mouse thymus venules: there is a dense network of nerve fibers present in all thymic compartments. Inside the thymus, nerve fibers are closely associated with the blood vessels including postcapillary venules. This indicates that neural regulation may be involved in lymphocyte transport since T cell precursors and mature lymphocytes enter the peripheral organs through postcapillary venules[82]. In our own recent study, we show in our cohort of PDAC patients, that nerve fibers are co-localized with clusters of lymphocytes. These clusters are mainly CD20 positive B cells, CD4+CD8+ T cells and CD21+ follicular dendritic cells (unpublished data).

Besides the co-localization of nerve fibers with immune cells, the patients with a high nerve fiber density show a better survival. This phenomenon is described as neuro-immune cell units (NICUs), in other studies: immune cell and nerve fiber co-localization and their interaction can drive tissue protection and can play a critical immune-regulatory role[83,84]. NICUs are present in many tissues around the body and are shown to be important in many physiological processes such as tissue repair, inflammation and organogenesis[85,86]. However, the current knowledge of NICUs is limited. In conclusion, exploring this prominent novel field in cancer research will unravel future pathways for a better response to novel therapy strategies and may make PDAC and CCA patients more primed for a better response to immunotherapy.

Crosstalk between nerves and fibroblasts

Within the TME, cancer-associated fibroblasts (CAFs) are the major stromal cell type (up to 80% of the tumor mass in PDAC). The remodelling of the stromal compartment contributes to cancer growth and progression by activation of secretion of cytokines[87,88]. PDAC and CCA are typically characterized by a significant desmoplastic reaction. The desmoplastic stroma creates a physical and chemical barrier to prevent therapeutics and immune cells to infiltrate and reach the cancer. This results in an immune cell depleted TME and could be an explanation for failure of response to immunotherapy[89]. In addition, during the ECM remodelling, a type I collagen predominate phenotype, tends to stimulate angiogenesis and neurogenesis facilitating neo-vessel formation, which is beneficial for tumor dissemination[49]. In PDAC and CCA, CAFs are differentiated from stellate cells, these stellate cells play an essential role in the desmoplastic reaction through the expression of alpha-smooth muscle actin (α-SMA) and co-localization with procollagen, contributing to

ECM remodelling[3]. Furthermore, stellate cells favor nerve outgrowth during tumor development by supporting growth and elongation of neurons and communicate via Ach signaling pathways[90]. A few studies have described that hepatic stellate cells regulate nerve growth via the alteration of ECM composition and up-expression of several factors such as tumor growth factor beta, which stimulates angiogenesis and with this influences axons in the TME[91]. Abundant ECM components such as hyaluronic acid, fibronectin and collagen are predominately present within the TME in PDAC and CCA. Those ECM components influence neuron growth[92,93]. Hence, stellate cells regulate the composition of ECM components and therefore affect nerve growth in PDAC and CCA[90].

CAFs can secrete matrix metalloproteases (MMPs), the MMP family is an ECM protein and they are reported to be regulators of neural development[94]. It was described that some MMPs (MT1-MMP) are shown to degrade the ECM and promote pancreatic cancer expansion, invasion and progression to an advanced stage[95,96]. It is reported that MMP9 is associated with more lymph node metastasis and a poorer survival in breast cancer[97]. PDAC cells in vivo undergoing chronic stress, were sensitive to neural signaling and pancreatic stromal cells were increased. This promoted tumor metastasis and cancer progression, β-adrenergic receptor blockade intervention therapy can block this neural signaling and be part of a combination therapy for PDAC[63].

Pathological features of nerve fibers in pdac and cca

PNI is considered as an important factor for poor prognosis in PDAC and CCA[24,98]. It has been shown that PNI can be the reason for curative resection failure (shown in table 1). Chatterjee al showed by examination of 212 PDAC slides, that the presence of PNI was directly correlated with tumor size, margin status, lymph node metastasis and AJCC stages and inversely associated with disease free survival (DFS) and overall survival (OS)[17]. Shimada et al found that the degree of intrapancreatic nerve invasion can be used as a predictor for recurrence of disease after surgery[99]. A phenomenon termed as "neural remodelling" is postulated in PDAC, characterized by the alterations in morphology of the nerve[18,100-102]. It was shown that nerve fiber alterations including hypertrophic nerves, increased nerve fiber density and pancreatic neuritis were strongly associated with GAP-43 overexpression and abdominal pain[103]. In the perineural space, PNI induces reactive alterations in the morphology and function of the nerves. Morphological changes include changes of the nerve trunk and thickness[102]. The aggressiveness of PNI is related to neural remodelling, desmoplasia and cancer pain. Severe and enduring pain was strongly associated with poor survival in PDAC patients. However, these neural alterations did not have a significant association with survival[103]. NGF and Artemin play a fundamental role in neural modelling in pancreatic adenocarcinoma.

Table 1 Summary of current research neural remodeling in PDAC and CCA.

Authors	Samples	Neural marker	Key results	Cancer types
Iwasaki 2019[119]	256	GAP-43	Neural hypertrophic, neural density and number decreased;	Pancreatic carcinoma
Fisher 2012[120]	58		Present of PNI is was associated with a reduction of OS	Cholangiocarcinoma
Chatterjee 2012[121]	212		Present of PNI was directly correlated with tumor size, margin status, lymph node metastasis, pathologic tumor and AJCC stages, and shorter DFS and OS	Pancreatic Carcinoma
Lenz 2011[122]	177		80.3 % of PDAC detected PNI; Neural remodeling progress can be a reason of pancreatic neuropathy;	Pancreatic Carcinoma
Shimada 2011[114]	153		Degree of PNI was directly related to node metastases, surgical margin and tumor sides, and inversely associated with DFS	Pancreatic Carcinoma
Ceyhan 2010[123]	97	GAP-43 NGF PGP9.5 Artemin	There were enlarged nerves and dense neural networks in pancreatic carcinoma slides; Neurotrophic characteristics GAP-43, NGF and Artemin increased in pancreatic carcinoma and have close relevancy with intrapancreatic neuropathy.	Pancreatic Carcinoma
Ceyhan 2009[124]	149	GAP-43 PGP9.5 NGF	Neural hypertrophic, neural density increased; Neuropathic alteration was not correlated with survival in pancreatic carcinoma, these changes includes neural thickness, hypertrophy, density. Only the severity of pain significantly affects survival.	Pancreatic Carcinoma
Ceyhan 2009[118]	564	GAP-43	Neural density increased and nerves enlarged in pancreatic carcinoma, the severity of PNI was linked to neuropathic changes and pain.	Pancreatic Carcinoma
Shirai 2008[125]	59		80% of CCC samples detected PNI; 5 years survival rates of patients with or without PNI were 17% and 70%, respectively.	Cholangiocarcinoma

Interestingly, lower intrapancreatic neural density in the tumor area was linked to shorter OS with multivariate analysis[73]. Related research in cholangiocarcinoma mainly focused on PNI prevalence and patient survival[45,99,104]. In summary, these studies consistently showed that the presence of PNI was linked to shorter survival in patients with PDAC or CCA. The significance that PNI is an independent prognostic factor of poor outcome has been demonstrated. However, the influence of nerve remodelling especially the new outgrown small nerve fibers has not been fully explained.

Conclusions and future directions

With its frequent PNI, PDAC and CCA are two neurotropic cancers. The neurotropism of these cancers could be an explanation of their aggressiveness and poor response to treatment. In this review, the progress of recent research in the mechanism of PNI in PDAC and CCA is discussed. However, the crosstalk between the nervous system in PDAC and CCA is undiscovered. Different nerve fibers have a different function and the interaction with the components of the TME and the cancer are important to investigate.

In PDAC, the role of nerve fibers is divergent and nerves from the PSNS and SNS have a cancer stimulating and cancer inhibiting effect. To our current knowledge, detailed understanding of the underlying mechanisms of tumor and nerve fiber interaction is critical for the development of innovative therapeutic strategies for patients with these highly lethal cancers. The nerve outgrowth is part of the TME, in which cancer to stroma crosstalk takes place. It is likely that other components of the TME also influence the nerve outgrowth and immune cells and fibroblasts are key components in this process. Targeting nerves has the potential to be a new strategy for therapy for PDAC and CCA patients by influencing the TME, immune cells and fibroblasts, potentially influencing sensitivity to therapeutics. The newly formed nerve fibers are different from the more commonly used PNI. From our perspective, PNI originates in the pre-existing nerve fiber networks and the cancer uses the distribution network for cancer growth. This is a well-known sign of aggressive disease and is associated with poor survival. Small nerve fiber outgrowth can be used as a biomarker for a better survival, as a tool to stratify patients for treatment and as a target for therapeutics.

More research is needed to investigate whether sensitivity to already existing immunotherapy can be achieved by targeting nerves.

Reference

1. Rahib L, Smith BD, Aizenberg R, Rosenzweig AB, Fleshman JM, Matrisian LM. Projecting cancer incidence and deaths to 2030: the unexpected burden of thyroid, liver, and pancreas cancers in the United States. *Cancer Res* 2014; **74**(11): 2913-21.
2. Bertuccio P, Malvezzi M, Carioli G, et al. Global trends in mortality from intrahepatic and extrahepatic cholangiocarcinoma. *Journal of Hepatology* 2019; **71**(1): 104-14.
3. Liu H, Ma Q, Xu Q, et al. Therapeutic potential of perineural invasion, hypoxia and desmoplasia in pancreatic cancer. *Current pharmaceutical design* 2012; **18**(17): 2395-403.
4. Maisonneuve P. Epidemiology and burden of pancreatic cancer. *La Presse Médicale* 2019; **48**(3, Part 2): e113-e23.
5. Khan SA, Tavolari S, Brandi G. Cholangiocarcinoma: Epidemiology and risk factors. *Liver International* 2019; **39**(S1): 19-31.
6. McClements S, Khan SA. Epidemiology and Pathogenesis of Cholangiocarcinoma. In: Cross T, Palmer DH, eds. Liver Cancers: From Mechanisms to Management. Cham: Springer International Publishing; 2019: 179-86.
7. Renz BW, Tanaka T, Sunagawa M, et al. Cholinergic Signaling via Muscarinic Receptors Directly and Indirectly Suppresses Pancreatic Tumorigenesis and Cancer Stemness. *Cancer discovery* 2018; **8**(11): 1458-73.
8. Farrow B, Albo D, Berger DH. The Role of the Tumor Microenvironment in the Progression of Pancreatic Cancer. *Journal of Surgical Research* 2008; **149**(2): 319-28.
9. Zahalka AH, Arnal-Estapé A, Maryanovich M, et al. Adrenergic nerves activate an angio-metabolic switch in prostate cancer. *Science* 2017; **358**(6361): 321-6.
10. Hondermarck H, Jobling P. The Sympathetic Nervous System Drives Tumor Angiogenesis. *Trends Cancer* 2018; **4**(2): 93-4.
11. March B, Faulkner S, Jobling P, et al. Tumour innervation and neurosignalling in prostate cancer. *Nat Rev Urol* 2020; **17**(2): 119-30.
12. Bapat AA, Galen H, Hoff DD, Von, Haiyong H. Perineural invasion and associated pain in pancreatic cancer. *Nature Reviews Cancer* 2011; **11**(10): 695.
13. Bockman DE, Büchler M, Beger HG. Interaction of pancreatic ductal carcinoma with nerves leads to nerve damage. *Gastroenterology* 1994; **107**(1): 219-30.
14. Liebig C, Ayala G, Wilks JA, Berger DH, Albo D. Perineural invasion in cancer: a review of the literature. *Cancer* 2009; **115**(15): 3379-91.
15. Batsakis JG. Nerves and neurotropic carcinomas. *The Annals of otology, rhinology, and laryngology* 1985; **94**(4 Pt 1): 426-7.
16. Gasparini G, Pellegatta M, Crippa S, et al. Nerves and Pancreatic Cancer: New Insights into a Dangerous Relationship. *Cancers* 2019; **11**(7).
17. Chatterjee D, Katz MH, Rashid A, et al. Perineural and intraneural invasion in posttherapy pancreaticoduodenectomy specimens predicts poor prognosis in patients with pancreatic ductal adenocarcinoma. *The American journal of surgical pathology* 2012; **36**(3): 409-17.
18. Demir IE, Ceyhan GO, Liebl F, D'Haese JG, Maak M, Friess H. Neural invasion in pancreatic cancer: the past, present and future. *Cancers (Basel)* 2010; **2**(3): 1513-27.
19. Shen F-Z, Zhang B-Y, Feng Y-J, et al. Current research in perineural invasion of cholangiocarcinoma. *J Exp Clin Cancer Res* 2010; **29**(1): 24-.
20. Liang D, Shi S, Xu J, et al. New insights into perineural invasion of pancreatic cancer: More than pain. *Biochimica et Biophysica Acta (BBA) - Reviews on Cancer* 2016; **1865**(2): 111-22.
21. Pundavela J, Roselli S, Faulkner S, et al. Nerve fibers infiltrate the tumor microenvironment and are associated with nerve growth factor production and lymph node invasion in breast cancer. *Molecular Oncology* 2015; **9**(8): 1626-35.
22. Zareba P, Flavin R, Isikbay M, et al. Perineural Invasion and Risk of Lethal Prostate Cancer. *Cancer Epidemiol Biomarkers Prev* 2017; **26**(5): 719-26.
23. Chen S-H, Zhang B-Y, Zhou B, Zhu C-Z, Sun L-Q, Feng Y-J. Perineural invasion of cancer: a complex crosstalk between cells and molecules in the perineural niche. *Am J Cancer Res* 2019; **9**(1): 1-21.

24. Ren K, Yi SQ, Dai Y, Kurosawa K, Miwa Y, Sato I. Clinical Anatomy of the Anterior and Posterior Hepatic Plexuses, Including Relations with the Pancreatic Plexus: A Cadaver Study. *Clinical anatomy (New York, NY)* 2019.
25. Mavros MN, Economopoulos KP, Alexiou VG, Pawlik TM. Treatment and Prognosis for Patients With Intrahepatic Cholangiocarcinoma: Systematic Review and Meta-analysis. *JAMA surgery* 2014; **149**(6): 565-74.
26. Ayala GE, Dai H, Powell M, et al. Cancer-related axonogenesis and neurogenesis in prostate cancer. *Clinical cancer research : an official journal of the American Association for Cancer Research* 2008; **14**(23): 7593-603.
27. Zuo H-D, Zhang X-M, Li C-J, et al. CT and MR imaging patterns for pancreatic carcinoma invading the extrapancreatic neural plexus (Part I): Anatomy, imaging of the extrapancreatic nerve. *World journal of radiology* 2012; **4**(2): 36-43.
28. Li W, Yu G, Liu Y, Sha L. Intrapancreatic Ganglia and Neural Regulation of Pancreatic Endocrine Secretion. *Front Neurosci* 2019; **13**: 21-.
29. Mizuno K, Ueno Y. Autonomic Nervous System and the Liver. *Hepatology Research* 2017; **47**(2): 160-5.
30. Rodriguez-Diaz R, Caicedo A. Neural control of the endocrine pancreas. *Best Pract Res Clin Endocrinol Metab* 2014; **28**(5): 745-56.
31. Travagli TBaRA. Neural Control of the Pancreas. *Pancreapedia: Exocrine Pancreas Knowledge Base* 2016.
32. Franchitto A, Onori P, Renzi A, et al. Recent advances on the mechanisms regulating cholangiocyte proliferation and the significance of the neuroendocrine regulation of cholangiocyte pathophysiology. *Ann Transl Med* 2013; **1**(3): 27-.
33. Sha M, Cao J, Sun H-y, Tong Y, Xia Q. Neuroendocrine regulation of cholangiocarcinoma: A status quo review. *Biochimica et Biophysica Acta (BBA) - Reviews on Cancer* 2019; **1872**(1): 66-73.
34. Dang N, Meng X, Song H. Nicotinic acetylcholine receptors and cancer. *Biomed Rep* 2016; **4**(5): 515-8.
35. Liu H-P, Tay S-S-W, Leong S-K, Schemann M. Colocalization of ChAT, DβH and NADPH-d in the pancreatic neurons of the newborn guinea pig. *Cell and Tissue Research* 1998; **294**(2): 227-31.
36. O'Donnell J, Zeppenfeld D, McConnell E, Pena S, Nedergaard M. Norepinephrine: a neuromodulator that boosts the function of multiple cell types to optimize CNS performance. *Neurochem Res* 2012; **37**(11): 2496-512.
37. Campbell K, Rossi F, Adams J, et al. Collective cell migration and metastases induced by an epithelial-to-mesenchymal transition in Drosophila intestinal tumors. *Nature communications* 2019; **10**(1): 2311.
38. Barbieri A, Bimonte S, Palma G, et al. The stress hormone norepinephrine increases migration of prostate cancer cells in vitro and in vivo. *International journal of oncology* 2015; **47**(2): 527-34.
39. Renz BW, Takahashi R, Tanaka T, et al. β2 Adrenergic-Neurotrophin Feedforward Loop Promotes Pancreatic Cancer. *Cancer cell* 2018; **33**(1): 75-90.e7.
40. Kanno N, LeSage G, Phinizy JL, Glaser S, Francis H, Alpini G. Stimulation of α2-adrenergic receptor inhibits cholangiocarcinoma growth through modulation of Raf-1 and B-Raf activities. *Hepatology* 2002; **35**(6): 1329-40.
41. Amit M, Takahashi H, Dragomir MP, et al. Loss of p53 drives neuron reprogramming in head and neck cancer. *Nature* 2020; **578**(7795): 449-54.
42. Jobling P, Pundavela J, Oliveira SM, Roselli S, Walker MM, Hondermarck H. Nerve-Cancer Cell Cross-talk: A Novel Promoter of Tumor Progression. *Cancer Res* 2015; **75**(9): 1777-81.
43. Feng Y-J, Zhang B-Y, Yao R-Y, Lu Y. Muscarinic acetylcholine receptor M3 in proliferation and perineural invasion of cholangiocarcinoma cells. *Hepatobiliary & Pancreatic Diseases International* 2012; **11**(4): 418-23.
44. Zhang L, Xiu D, Zhan J, et al. High expression of muscarinic acetylcholine receptor 3 predicts poor prognosis in patients with pancreatic ductal adenocarcinoma. *Onco Targets Ther* 2016; **9**: 6719-26.
45. Momi N, Ponnusamy MP, Kaur S, et al. Nicotine/cigarette smoke promotes metastasis of pancreatic cancer through alpha7nAChR-mediated MUC4 upregulation. *Oncogene* 2013; **32**(11): 1384-95.

46. Amonyingcharoen S, Suriyo T, Thiantanawat A, Watcharasit P, Satayavivad J. Taurolithocholic acid promotes intrahepatic cholangiocarcinoma cell growth via muscarinic acetylcholine receptor and EGFR/ERK1/2 signaling pathway. *International journal of oncology* 2015; **46**(6): 2317-26.
47. Martínez AK, Jensen K, Hall C, et al. Nicotine Promotes Cholangiocarcinoma Growth in Xenograft Mice. *The American Journal of Pathology* 2017; **187**(5): 1093-105.
48. Aloe L, Rocco ML, Balzamino BO, Micera A. Nerve growth factor: role in growth, differentiation and controlling cancer cell development. *Journal of experimental & clinical cancer research : CR* 2016; **35**(1): 116-.
49. Zahalka AH, Frenette PS. Nerves in cancer. *Nature Reviews Cancer* 2020; **20**(3): 143-57.
50. Roux PP, Barker PA. Neurotrophin signaling through the p75 neurotrophin receptor. *Progress in neurobiology* 2002; **67**(3): 203-33.
51. Schecterson LC, Bothwell M. Neurotrophin receptors: Old friends with new partners. *Developmental neurobiology* 2010; **70**(5): 332-8.
52. Molloy NH, Read DE, Gorman AM. Nerve growth factor in cancer cell death and survival. *Cancers (Basel)* 2011; **3**(1): 510-30.
53. Yang XQ, Xu YF, Guo S, et al. Clinical significance of nerve growth factor and tropomyosin-receptor-kinase signaling pathway in intrahepatic cholangiocarcinoma. *World J Gastroenterol* 2014; **20**(14): 4076-84.
54. Ma J, Jiang Y, Jiang Y, Sun Y, Zhao X. Expression of nerve growth factor and tyrosine kinase receptor A and correlation with perineural invasion in pancreatic cancer. *J Gastroenterol Hepatol* 2008; **23**(12): 1852-9.
55. Saloman JL, Singhi AD, Hartman DJ, Normolle DP, Albers KM, Davis BM. Systemic Depletion of Nerve Growth Factor Inhibits Disease Progression in a Genetically Engineered Model of Pancreatic Ductal Adenocarcinoma. *Pancreas* 2018; **47**(7): 856-63.
56. Gigliozzi A, Alpini G, Baroni GS, et al. Nerve growth factor modulates the proliferative capacity of the intrahepatic biliary epithelium in experimental cholestasis. *Gastroenterology* 2004; **127**(4): 1198-209.
57. Yue XJ, Xu LB, Zhu MS, Zhang R, Liu C. Over-expression of nerve growth factor-beta in human cholangiocarcinoma QBC939 cells promote tumor progression. *PloS one* 2013; **8**(4): e62024.
58. Xu LB, Liu C, Gao GQ, Yu XH, Zhang R, Wang J. Nerve growth factor-beta expression is associated with lymph node metastasis and nerve infiltration in human hilar cholangiocarcinoma. *World journal of surgery* 2010; **34**(5): 1039-45.
59. Monje M, Borniger JC, D'Silva NJ, et al. Roadmap for the Emerging Field of Cancer Neuroscience. *Cell* 2020; **181**(2): 219-22.
60. Eichmann A, Brunet I. Arterial Innervation in Development and Disease. *Science Translational Medicine* 2014; **6**(252): 252ps9-ps9.
61. Folkman J, Watson K, Ingber D, Hanahan D. Induction of angiogenesis during the transition from hyperplasia to neoplasia. *Nature* 1989; **339**(6219): 58-61.
62. Magnon C, Hall SJ, Lin J, et al. Autonomic Nerve Development Contributes to Prostate Cancer Progression. *Science* 2013; **341**(6): 713-4.
63. Kim-Fuchs C, Le CP, Pimentel MA, et al. Chronic stress accelerates pancreatic cancer growth and invasion: a critical role for beta-adrenergic signaling in the pancreatic microenvironment. *Brain Behav Immun* 2014; **40**: 40-7.
64. Kamiya A, Hayama Y, Kato S, et al. Genetic manipulation of autonomic nerve fiber innervation and activity and its effect on breast cancer progression. *Nature neuroscience* 2019; **22**(8): 1289-305.
65. Barron TI, Connolly RM, Sharp L, Bennett K, Visvanathan K. Beta blockers and breast cancer mortality: a population- based study. *J Clin Oncol* 2011; **29**(19): 2635-44.
66. Grytli HH, Fagerland MW, Fossa SD, Tasken KA. Association between use of beta-blockers and prostate cancer-specific survival: a cohort study of 3561 prostate cancer patients with high-risk or metastatic disease. *Eur Urol* 2014; **65**(3): 635-41.
67. Mauffrey P, Tchitchek N, Barroca V, et al. Progenitors from the central nervous system drive neurogenesis in cancer. *Nature* 2019; **569**(7758): 672-8.
68. Raju B, Haug SR, Ibrahim SO, Heyeraas KJ. Sympathectomy decreases size and invasiveness of tongue cancer in rats. 2007; **149**(3): 715-25.

69. Huang D, Su S, Cui X, et al. Nerve fibers in breast cancer tissues indicate aggressive tumor progression. *Medicine* 2014; **93**(27): e172.
70. Shao JX, Wang B, Yao YN, Pan ZJ, Shen Q, Zhou JY. Autonomic nervous infiltration positively correlates with pathological risk grading and poor prognosis in patients with lung adenocarcinoma. *Thoracic cancer* 2016; **7**(5): 588-98.
71. Zhao CM, Hayakawa Y, Kodama Y, et al. Denervation suppresses gastric tumorigenesis. *Sci Transl Med* 2014; **6**(250): 250ra115.
72. Albo D, Akay CL, Marshall CL, et al. Neurogenesis in colorectal cancer is a marker of aggressive tumor behavior and poor outcomes. *Cancer* 2011; **117**(21): 4834-45.
73. Iwasaki T, Hiraoka N, Ino Y, et al. Reduction of intrapancreatic neural density in cancer tissue predicts poorer outcome in pancreatic ductal carcinoma. *Cancer science* 2019; **110**(4): 1491-502.
74. Zhang L, Guo L, Tao M, Fu W, Xiu D. Parasympathetic neurogenesis is strongly associated with tumor budding and correlates with an adverse prognosis in pancreatic ductal adenocarcinoma. *Chinese journal of cancer research = Chung-kuo yen cheng yen chiu* 2016; **28**(2): 180-6.
75. Sinha S, Fu YY, Grimont A, et al. PanIN Neuroendocrine Cells Promote Tumorigenesis via Neuronal Cross-talk. *Cancer Res* 2017; **77**(8): 1868-79.
76. Saloman JL, Albers KM, Li D, et al. Ablation of sensory neurons in a genetic model of pancreatic ductal adenocarcinoma slows initiation and progression of cancer. *Proc Natl Acad Sci U S A* 2016; **113**(11): 3078-83.
77. Bai H, Li H, Zhang W, et al. Inhibition of chronic pancreatitis and pancreatic intraepithelial neoplasia (PanIN) by capsaicin in LSL-KrasG12D/Pdx1-Cre mice. *Carcinogenesis* 2011; **32**(11): 1689-96.
78. Amit M, Takahashi H, Dragomir MP, et al. Loss of p53 drives neuron reprogramming in head and neck cancer. *Nature* 2020.
79. Soto‐Tinoco E, Guerrero‐Vargas NN, Buijs RM. Interaction between the hypothalamus and the immune system. *Experimental Physiology* 2016; **101**.
80. Thome JJ, Bickham KL, Ohmura Y, et al. Early-life compartmentalization of human T cell differentiation and regulatory function in mucosal and lymphoid tissues. *Nature medicine* 2016; **22**(1): 72-7.
81. Mignini F, Sabbatini M, Mattioli L, Cosenza M, Artico M. Neuro-immune modulation of the thymus microenvironment (Review). *International journal of molecular medicine* 2014; **33**.
82. Al-Shalan HAM, Hu D, Nicholls PK, Greene WK, Ma B. Immunofluorescent characterization of innervation and nerve-immune cell neighborhood in mouse thymus. 2019; **378**(2): 239-54.
83. Veiga-Fernandes H, Pachnis V. Neuroimmune regulation during intestinal development and homeostasis. *Nature Immunology* 2017; **18**.
84. Godinho-Silva C, Cardoso F, Veiga-Fernandes H. Neuro-Immune Cell Units: A New Paradigm in Physiology. *Annual review of immunology* 2019; **37**: 19-46.
85. Veiga-Fernandes H, Mucida D. Neuro-Immune Interactions at Barrier Surfaces. *Cell* 2016; **165**(4): 801-11.
86. Chesne J, Cardoso V, Veiga-Fernandes H. Neuro-immune regulation of mucosal physiology. *Mucosal immunology* 2019; **12**(1): 10-20.
87. Cirri P, Chiarugi P. Cancer associated fibroblasts: the dark side of the coin. *Am J Cancer Res* 2011; **1**(4): 482-97.
88. Yu M, Tannock IF. Targeting tumor architecture to favor drug penetration: a new weapon to combat chemoresistance in pancreatic cancer? *Cancer Cell* 2012; **21**(3): 327-9.
89. Joyce JA, Fearon DT. T cell exclusion, immune privilege, and the tumor microenvironment. *Science* 2015; **348**(6230): 74-80.
90. Apte MV, Wilson JS, Lugea A, Pandol SJ. A starring role for stellate cells in the pancreatic cancer microenvironment. *Gastroenterology* 2013; **144**(6): 1210-9.
91. Coulouarn C, Clément B. Stellate cells and the development of liver cancer: therapeutic potential of targeting the stroma. *Journal of hepatology* 2014; **60**(6): 1306-9.
92. Gritsenko PG, Ilina O, Friedl P. Interstitial guidance of cancer invasion. *J Pathol* 2012; **226**(2): 185-99.
93. Preston M, Sherman LS. Neural stem cell niches: roles for the hyaluronan-based extracellular matrix. *Front Biosci (Schol Ed)* 2011; **3**: 1165-79.

94. Ulrich R, Gerhauser I, Seeliger F, Baumgartner W, Alldinger S. Matrix metalloproteinases and their inhibitors in the developing mouse brain and spinal cord: a reverse transcription quantitative polymerase chain reaction study. *Dev Neurosci* 2005; **27**(6): 408-18.
95. Maatta M, Soini Y, Liakka A, Autio-Harmainen H. Differential expression of matrix metalloproteinase (MMP)-2, MMP-9, and membrane type 1-MMP in hepatocellular and pancreatic adenocarcinoma: implications for tumor progression and clinical prognosis. *Clin Cancer Res* 2000; **6**(7): 2726-34.
96. Liu T, Zhou L, Li D, Andl T, Zhang Y. Cancer-Associated Fibroblasts Build and Secure the Tumor Microenvironment. *Front Cell Dev Biol* 2019; **7**: 60-.
97. Roy R, Yang J, Moses MA. Matrix metalloproteinases as novel biomarkers and potential therapeutic targets in human cancer. *J Clin Oncol* 2009; **27**(31): 5287-97.
98. Yamada Y, Mori H, Hijiya N, et al. Extrahepatic bile duct cancer: invasion of the posterior hepatic plexuses--evaluation using multidetector CT. *Radiology* 2012; **263**(2): 419-28.
99. Shimada K, Nara S, Esaki M, Sakamoto Y, Kosuge T, Hiraoka N. Intrapancreatic nerve invasion as a predictor for recurrence after pancreaticoduodenectomy in patients with invasive ductal carcinoma of the pancreas. *Pancreas* 2011; **40**(3): 464-8.
100. Nakao A, Harada A, Nonami T, Kaneko T, Takagi H. Clinical significance of carcinoma invasion of the extrapancreatic nerve plexus in pancreatic cancer. *Pancreas* 1996; **12**(4): 357-61.
101. Liu B, Lu KY. Neural invasion in pancreatic carcinoma. *Hepatobiliary & pancreatic diseases international : HBPD INT* 2002; **1**(3): 469-76.
102. Demir IE, Friess H, Ceyhan GO. Neural plasticity in pancreatitis and pancreatic cancer. *Nature reviews Gastroenterology & hepatology* 2015; **12**(11): 649-59.
103. Ceyhan GO, Bergmann F, Kadihasanoglu M, et al. Pancreatic Neuropathy and Neuropathic Pain—A Comprehensive Pathomorphological Study of 546 Cases. *Gastroenterology* 2009; **136**(1): 177-86.e1.
104. Shirai K, Ebata T, Oda K, et al. Perineural invasion is a prognostic factor in intrahepatic cholangiocarcinoma. *World journal of surgery* 2008; **32**(11): 2395-402.

Chapter 2

2

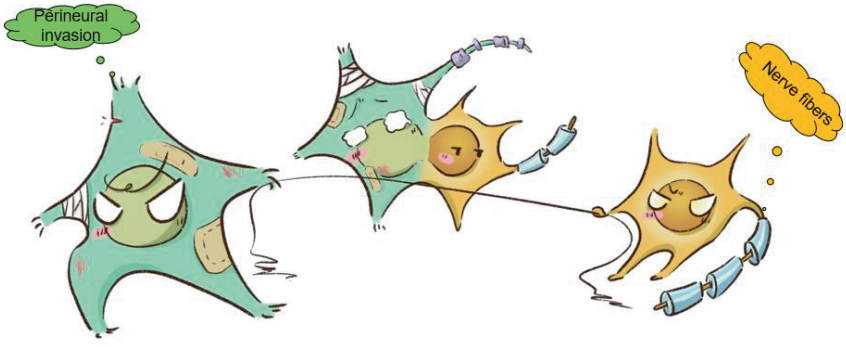

CHAPTER 3

Nerve fibers in the Tumor Microenvironment are co-localized with Lymphoid Aggregates in Pancreatic Cancer

Lara R. Heij, **Xiuxiang Tan,** Jakob N. Kather, Jan M. Niehues, Shivan Sivakumar, Nicole Heussen, Gregory van der Kroft, Steven W.M. Olde Damink, Sven Lang, Merel R. Aberle, Tom Luedde, Nadine T. Gaisa, Jan Bednarsch, Drolaiz H.W. Liu, Jack P.M. Cleutjens, Dominik P. Modest, Ulf P. Neumann and Georg J. Wiltberger

2nd author

Journal of Clinical Medicine, 30 January 2021, 40, 10(3):490

Chapter 3

Abstract: B cells and tertiary lymphoid structures (TLS) are reported to be important in survival in cancer. Pancreatic Cancer (PDAC) is one of the most lethal cancer types and currently it is the seventh leading cause of cancer-related death worldwide[1]. A better understanding of the tumor biology is pivotal to improve clinical outcome. The desmoplastic stroma is a complex system in which crosstalk takes place between cancer-associated fibroblasts, immune cells and the cancer cells. Indirect and direct cellular interactions within the tumor microenviroment (TME) drive key processes such as tumor progression, metastasis formation and treatment resistance. In order to understand the aggressiveness of PDAC and its resistance to therapeutics the TME needs to be further unraveled. There is some limited data about the influence of nerve fibers on cancer progression. Here we show that small nerve fibers are located at lymphoid aggregates in PDAC. This unravels future pathways and has potential to improve clinical outcome by a rational development of new therapeutic strategies.

Keywords: Tumor Microenvironment; Machine Learning; Nerve Fiber Density; Spatial Arrangements; Tertiary Lymphoid Structures; Pancreatic Cancer

Abbreviations

LA	Lymphoid aggregates
NFD	Nerve fiber density
PDAC	Pancreatic cancer
ROI	Region of Interest
TC	Tumor cellularity
TIL-B	Tumor-infiltrating lymphocytic B cell
TLS	Tertiary lymphoid structures
TME	Tumor microenvironment
WHO	World health organization

Introduction

In order to understand the aggressiveness of Pancreatic Ductal Adenocarcinoma (PDAC) and its resistance to therapeutics, the components within the cancer stroma need to be further unraveled. PDAC arises in a tumor microenvironment (TME) that is characterized by extensive communication between tumor cells and non-malignant cells. Specifically, stromal components have been mechanistically implied in immune evasion in the context of cancer therapy, including immunotherapy[2,3]. The role of nerve fibers within the cancer-associated stroma has not really been investigated. The aim of this study was to define the role of small nerve fibers in the cancer stroma and their spatial arrangement to immune cells. We hypothesized that small nerve fibers are one of the key components in cancer progression.

Recent publications show that B cells play an important role in survival of cancer patients and response to immunotherapy[4-8] and this is not limited to T cells only[9-11]. Furthermore, B cells play an important role in the tumor formation of PDAC[12]. Tertiary lymphoid structures (TLS) have been recognized as ectopic lymphoid organs that reside in inflamed tissue and also in cancer[13,14]. These structures show differences in maturation stage and sometimes results in formation of a germinal center[14-16]. The different maturation stages of TLS show expression of different cells: early-TLS without the formation of a germinal center, primary follicle-TLS with CD21 positive follicular dendritic cells without the formation of a germinal center and secondary follicle-TLS with presence of a germinal center (also CD23 positive)[17]. TLS presence is described in multiple cancer types and is variably present in cancer types and patients and is a favorable prognostic factor[18,19].

Methods

Ethics statement

All experiments were conducted in accordance with the Declaration of Helsinki and the International Ethical Guidelines for Biomedical Research Involving Human Subjects. Pathology blocks from the University Hospital of Aachen (RWTH Aachen) were retrieved (institutional ethics EK 106/18). Written human patient consent was not necessary, because this study was based on retrospective chart review and archived pathology material. Nevertheless most patients have signed informed consent, in some cases informed consent was waived due to the lack of risk for the patient and the fact that those patients were unable to provide informed consent. Images from tissue specimens are entirely unidentifiable and no details on individuals are reported within the manuscript.

Patient Cohort

Histological slides from 166 patients with PDAC were selected and used to cut tissue sections for the immunostaining Protein Gene Product 9.5 (PGP9.5).

Of the 188 patients included in the cohort 15 were excluded due to in hospital-mortality, 3 due to a loss to follow up, and 4 were excluded due to poor quality pathology slides. Analysis was performed on 166 cases. Clinical data for this cohort are listed in Table 1.

Table 1. Results from univariate and multivariate Cox regression analysis adjusted for age, gender and BMI of prognostic factors associated with overall survival.

		Univariate analyses (adjusted for age, gender, BMI)		Multivariate analysis (adjusted for age, gender, BMI)	
Variable	Mean (SD) or Frequency (%)	Hazard ratio [95%-C])	p-value	Hazard ratio (95%-CI)	p-value
Age	66 (10)			1.024 [1.002; 1.047]	0.0356
Gender					
female	80 (48.19)			1.173 [0.789; 1.745]	0.4297
male	86 (51.81)				
BMI	25.7 (4.3)			0.996 [0.954; 1.040]	0.8547
ASA					
< 3	62 (37.35)	0.909 [0.607, 1.362]	0.6449		
≥ 3	104 (62.65)				
Tumour grade					
G2	94 (56.63)	1.954 [1.342, 2.844]	0.0005		
G3	72 (56.63)				
Extent of tumour					
T1/T2	26 (15.66)	2.116 [1.015, 4.410]	0.0455		
T3/T4	140 (84.34)				

Perineural invasion					
Absent	28 (16.87)	2.239	0.0056	2.409	0.0034
Present	138 (83.13)	[1.265, 3.961]		[1.337; 4.340]	
Lymph node metastasis					
Absent	39 (23.49)	2.322	0.0010		
Present	127 (76.51)	[1.407, 3.834]			
Lymphatic invasion					
Absent	114 (68.67)	2.080	0.0002	1.763	0.0064
Present	52 (31.33)	[0.418, 3.050]		[1.173; 2.651]	
Venous invasion					
Absent	136 (81.93)	1.452	0.1068		
Present	30 (81.93)	[0.923, 2.284]			
Surgical margin status					
Negative	106 (63.86)	1.962	0.0005		
Positive	60 (36.14)	[1.342, 2.868]			
Nerve fiber density					
High	72 (43.37)	1.597	0.0155	1.676	0.0109
Low	94 (56.63)	[1.093, 2.336]		[1.126, 2.495]	
Lymphoid Aggregates					
< 5	95 (57.23)	1.084	0.6723		
≥ 5	71 (42.77)	[0.745, 1.577]			
Tumor cellularity	0.36 (0.20)	5.280 [1.952, 14.282]	0.0010	4.287 [1.460; 12.589]	0.0081
Interaction between Lymph node metastasis and surgical margin status					0.0053
lymph node metastasis present at surgical margin status positive				0.587 [0.272; 1.266]	
lymph node metastasis present at surgical margin status negative				2.618 [1.260; 5.437]	

Pathological Examination

The clinic-pathological parameters, including tumor size, differentiation, positive lymph node status, R0/R1, were carefully reviewed in the original report. All PDAC lesions were pathologically examined and classified according to World Health Organization (WHO) classification using the 8th edition of the TNM Classification for Malignant Tumors.

Nerve fiber density (NFD)

Immunohistochemistry was performed on formalin-fixed, paraffin embedded tissue sections. Sections (2.5μm thick) were cut, deparaffinized in xylene and rehydrated in graded alcohols. Slides were boiled in citrate buffer (pH 6.0) at 95 - 100°C for 5 minutes and were cooled for 20 minutes. Endogenous peroxide in methanol for 10 minutes. Sections were incubated with rabbit anti-human PGP 9.5 (DAKO 1:100) overnight at 4°C.

A single digital image was uploaded in Qupath 0.1.6 which is a flexible software platform suitable for a range of digital pathology applications. NFD was evaluated by counting the number of nerve fascicles with diameters of <100 μm in 20 continuous fields at x 200 magnification.

Nerve fiber density results were grouped into 3 categories: 1) negative, no nerve fibers, 2) weak expression, 1-10 nerve fibers and 3) moderate/strong expression >10 nerve fibers, according to existing literature on breast cancer[20].

Tumor Cellularity (TC)

Every immunostained slide was scanned and on whole slide imaging the tumor glands, normal pancreatic tissue and atrophic pancreatic tissue were manually annotated in QuPath 0.1.6 by a senior pathologist[18]. Stromal area was measured by following formula: total tissue - (normal tissue + atrophic pancreas+ tumor) = stroma surface. Tumor cellularity was measured as (tumor surface / (tumor surface + stroma surface).

Phenotyping of Immune Cells

Based on H&E the pre-dominant type of immune cells was judged manually by the PhD student and the senior pathologist. The H&E slide and the slide used for immunostaining were cut directly after each other. The dominant type of immune cells was determined and manually scored into three categories: 1) lymphocyte predominant, 2) neutrophil predominant or 3) no immune cells.

Single Immunohistochemistry

To further define the type of immune cell, we performed immunohistochemistry on 10 patients with histologically confirmed lymphoid aggregates on HE staining and a high NFD based on the PGP9.5 staining. We used CD20 (B cells), CD4, CD8 (T cell markers), FOXP3 (which can be expressed by T cells), according to previous literature that CD20+ B cells were located in the TLS and were colocalized with CD4+, CD8+, and FOXP3+ T cells[6]. To illustrate the presence of follicular dendritic cells we also stained for CD21. These staining's were compared to the H&E routine staining and PGP9.5 nerve fiber staining.

Sections were stained with mouse or rabbit anti-human monoclonal antibodies against CD20 (Dako, L26, 1:200), CD21 DAKO, 1:25, CD23 (Leica, CD23-1B12, 1:50), CD4 (DAKO, 4B12 1:50), CD8 (DAKO, C8/144B, 1:50), FOXP3 (DAKO, PCH101, 1:50). All sections were counterstained with hematoxylin, dehydrated and mounted. All sections were cover slipped using Vectashield Hardset 1500 mounting medium with DAPI and slides were scanned and digitalized using the Roche Ventana scanner. Immunohistochemistry staining was interpreted in conjunction with H&E stained sections.

Multiplex immunofluorescence assay and analysis

For immunofluorescence multiplex staining, we followed the staining method for the following markers: CD20 (Dako, L26, 1:500) with subsequent visualization using fluorescein Cy3 (1:100); FOXP3 (DAKO, PCH101, 1:300) with subsequent visualization using fluorescein

FITC (1:100); PGP9.5 (DAKO 1:300) with subsequent visualization using fluorescein TEX RED (1:100) and nuclei visualized with DAPI.

The slides were scanned using the TissueFAXS slide scanner (supplier TissueGnostics). For each marker, the mean fluorescent intensity per case was then determined as a base point from which positive cells could be established. For multispectral analysis, each of the individually stained sections was used to establish the spectral library of the fluorophores. The senior pathologist selected the Region of Interest (ROI) at 20× magnification.

Lymphoid aggregate count using Machine Learning

By using the annotations on the immunostained slide (PGP9.5), the distance from each immune cell to tumor gland was measured. The spatial arrangement of the immune cells was determined by a semi-automated machine learning workflow, which comprised cell segmentation, feature computation and stroma- and immune cell identification. To facilitate high trough put of thousands of immune cells on multiple images, QuPath enables interactive training of cell classification, after which the classifier can be saved and run over multiple slides. The senior pathologist trained a cell detection classifier to recognize immune cells and fibroblasts in a certain Region of Interest (ROI). This ROI was annotated by the senior pathologist and contained tumor glands and stroma only, it was avoided to include normal tissue and/or atrophic tissue in order to achieve the best detection results. Application of this workflow resulted in both fine grained cell-by-cell analysis and overall summary scores of the spatial arrangements of the immune cells within the ROI in relation to the annotated tumor glands. The results are visualized via color-coded markup images.

To obtain estimates for immune cell densities a kernel-density estimate using Gaussian kernels as implemented in the gaussian_kde class from SciPy is applied. First kernels are fitted from immune cells positions and calculated for points on a 100x100 grid for each slide. Subsequently the results are displayed as a heat map together with the slides tumor annotations (see Figure 3). From this heat map regions of high immune cell density can be identified manually that correspond to a lymphoid aggregate.

Statistics

Continuous variables were summarized by means and corresponding standard deviations (SD). Categorical data were presented by frequencies and percentages. Cox regression models were used to analyze the joint relation between clinical variables (coded by 0 and 1 for binary variables) on overall mortality. All exploratory variables were studied in an univariate Cox regression model adjusted for age, gender and BMI. Exploratory variables were assessed as relevant to be mutually included in our final model if the p-value was below 0.05. Relevant variables were studied further for pairwise interaction. In doing so, we used again the significance margin of 5%. Then a multivariate Cox regression model adjusted for age, gender and BMI with backward selection was fitted to the previously identified variables and interactions. During this final step, the significance level for removing a variable or interaction from the model was set to 0.05. For the final Cox model, graphical and numerical methods according to Lin et al. were performed to establish the validity of the proportionality assumption [21]. No deviation from model assumption could be observed. We report our results by hazard ratios, corresponding 95% confidence limits and p-values, where a p-value of less or equal than 0.05 could be interpreted as statistically significant test results. Forest plots were chosen for graphical visualization and Kaplan-Meier plots for comparison of subgroups. All analyses were performed using SAS®statistical software, V9.4 (SAS Institute, Cary, NC, USA).

Results

High Nerve Fiber Density is associated with a better survival in Pancreatic Cancer

To gain deeper insight of the influence of nerve fibers on survival we used the neuronal immunohistochemistry staining PGP9.5 on our cohort of patients with pancreatic cancer (n=166). A multivariate Cox regression model adjusting for age, gender and BMI, revealed

high Nerve Fiber Density (NFD) (more than 10 positive nerve fibers with diameters of <100 μm in 20 continuous fields at x 200 magnification) to be associated significantly with prolonged overall survival (HR 1.676 (95%CI 1.126,2.495) for low vs. high NFD, p-value 0.0109) as compared to low NFD. We have used small nerve fiber innervation of the blood vessels in the normal tissue as an internal positive control in case of a low NFD tumor. (see Supplementary Figure S1 en S2).

The lymphocyte predominant immunophenotype mainly in a low cellular tumor

To further understand to which extent immune cells and nerve fibers may interact, each routine H&E slide was scored manually into a lymphocyte predominant, neutrophil predominant or immune cell depleted phenotype[22]. The scoring was done by a senior pathologist and the PhD and based on the most dominant immune cell on one tumor slide only by viewing the histology on HE staining. In this evaluation, abundant stromal phenotype, so a low cellular tumor, was associated with lymphocyte predominant phenotype. High tumor cellularity was significantly associated with poor survival (HR 4.287 (95%CI 1.460,12.589), p-value 0.0081 for one unit increase). All results are summarized in Table 1.

Immune cells located at the nerve fibers are mainly B cells

Single immunohistochemistry was used to define which immune cells are co-localized with the nerve fibers. The immune cells that presented in the direct surroundings of the nerve fibers were mainly CD20 positive. Definition of TLS differs based on maturation stage but commonly accepted is that TLS are composed of a B cell zone and a T cell zone and may show the presence of a germinal center. To evaluate the maturity of the TLS we used CD21 to define follicular dendritic cells. In our cohort we found clusters of B lymphocytes with and without a T cell zone and follicular dendritic cells corresponding to different maturation stages of TLS. Multiplex immunofluorescence shows the architecture of a TLS in Pancreatic Cancer (see Figure 1) and this image provides an overview of the distribution of the immune cell aggregates at the edge of the tumor.

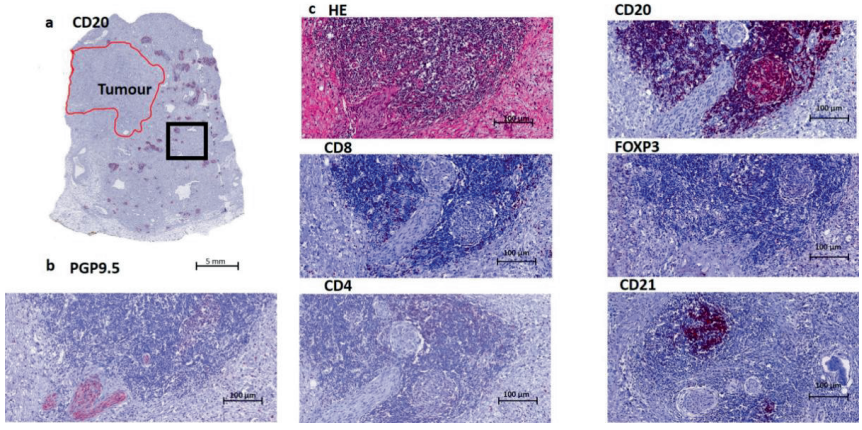

Figure 1. Overview of a TLS in Pancreatic Cancer. ***A.*** *Overview of a CD20 staining (B cells) in a PDAC patient, The red annotated area indicates the tumor region and the black box indicates the area of magnification for image 1B-D.* ***B****. Nerve fiber staining PGP9.5 which is a pan-neuronal marker. This image shows the presence of nerve fibers at the edge of a lymphoid aggregate.* ***C****. Routine HE staining, containing B cells (CD20), T cells (here mostly CD8 and CD4), and follicular dendritic cells (CD21). Treg cells (FOXP3) are mostly absent , just as CD4 in this image. CD8 shows a few positive cells at the border of this structure.* ***D****. Multiplex imaging: T cells (FOXP3 green), B cells (CD20 yellow), Nerves (PGP9.5 red) and nucleus (DAPI blue).*

Machine learning for quantification of lymphoid aggregates

Chapter 3

To gain insight in the spatial arrangements of the immune cells we used machine learning to further measure the distance from the immune cells to the tumor glands. The slides were scanned first and annotations were made in QuPath 0.1.6. A cell detection classifier was trained to recognize immune cells within a region of interest and separate the immune cells from fibroblasts (See Figure 2). To obtain estimates for immune cell densities a kernel-density was applied. The results are displayed as a heat map together with the slides tumor annotations (see Figure 3). To examine the predictive power of the number of lymphoid aggregates (LA) in combination with nerve fiber density and tumor cellularity on overall survival, an additional exploratory Cox regression model with LA, NFD and TC as well as the interaction between LA and NFD or TC respectively was evaluated. As the interaction between LA and TC was non-significant at a 5% level, the interaction was removed from the model. Thus, the exploratory model contains LA, NFD, TC and the interaction between LA and NFD as explanatory factors. The significant NFD*LA interaction (p-value 0.0220) suggests that the effect of NFD is different by LA. For LA number greater or equal to 5 mortality is significantly lower in patients with high NFD compared to patients with low NFD (20% (n=14) vs. 10% (n=7); HR 0.388 (95%CI 0.218, 0.689)). Whereas for LA number less than 5 no significant difference between patients with high or low NFD could be shown (14% (n=13) vs. 19% (n=18); HR 0.959 (95%CI 0.573, 1.604)) which is also apparent in the corresponding Kaplan-Meier plot (See Figure 3).

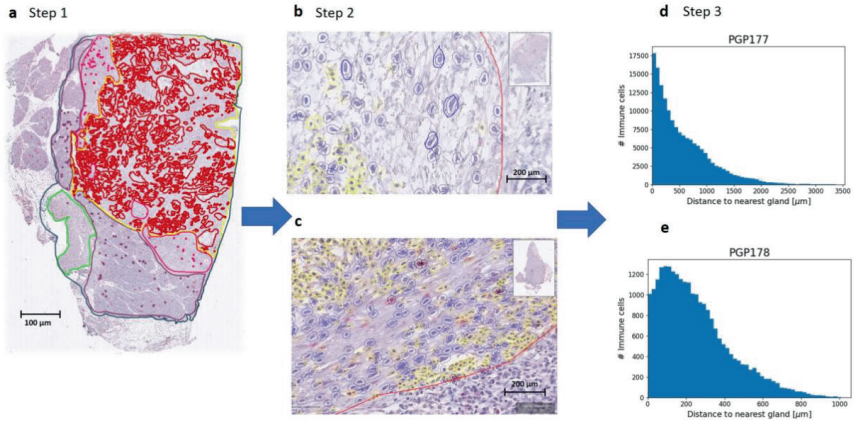

Figure 2. *Process using Machine Learning to determine Immune Cell spatiality. A.Step 1. Defining the ROI (yellow line). Every scanned slide was annotated in: total tissue (dark blue), normal pancreas (purple), atrophic pancreas (pink), normal duodenum (green) and tumor (red). For the machine learning classifier a Region of Interest (ROI) was also annotated (yellow). In this area only the cell detection classifier was used to detect the stromal cells in fibroblasts and immune cells. B+C. Step 2. The cell classifier was trained by the pathologist to recognize fibroblasts (blue annotations) and immune cells (yellow annotations). The tumor glands were all annotated manually gland by gland and are shown in red annotation. D+E. Step 3. Measurement of distance of Immune Cell to Tumor gland. From each slide a plot was made with amount of immune cells (y-axis) and the distance to nearest tumor gland (x-axis). These plots were used to measure the mean distance from immune cell to tumor gland in micrometer. Some slides showed immune cells at a greater distance from the tumor and some slides showed immune cells nearby the tumor. With this technique we could identify immune cell aggregates; so groups of immune cells located close to each other.*

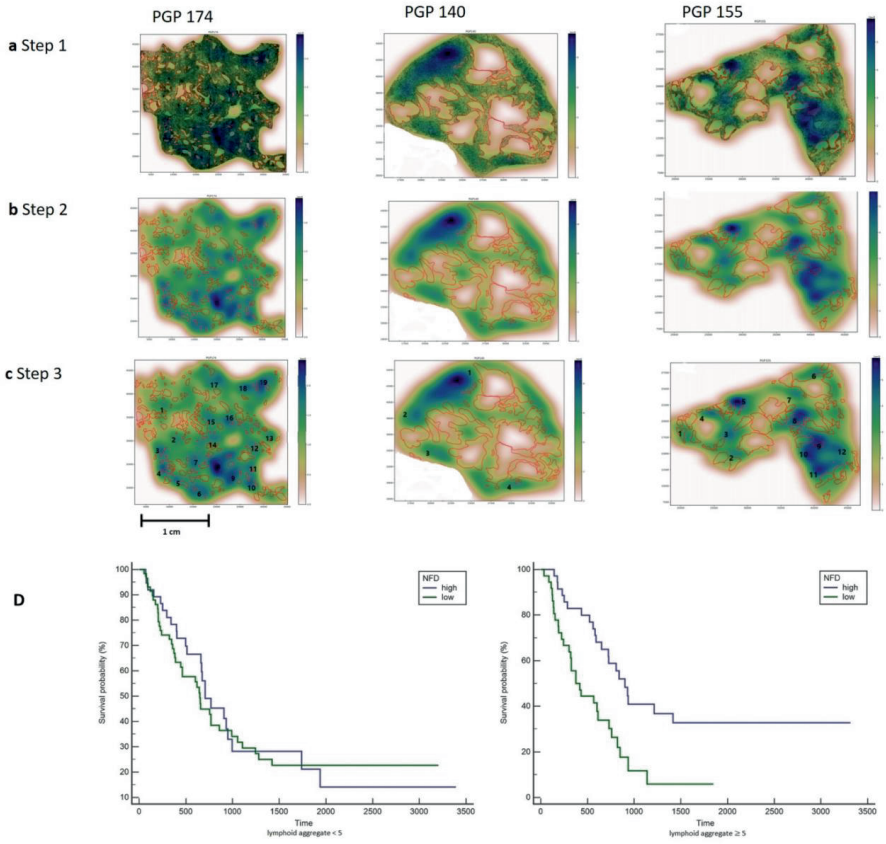

Figure 3. *Counting the number of lymphoid aggregates in patients with Pancreatic Cancer. **A**. Step 1 all immune cells are plotted by using the x- and y coordinates. Tumor glands annotated in red. Three patients are shown with a different distribution pattern of the immune cells. PGP 174 is immune cell rich and shows aggregates at the edge and in between the tumor glands. PGP 140 only shows a few immune cell aggregates at the edge of the tumor. PGP 155 shows a few immune cell aggregates mainly located at the edge of the tumor. **B.** Step 2 A heat map is created by using a 2D Kernel Density. The color blue was used because of the already red annotations for tumor glands. Dark blue areas show a high density of immune cells. **C.** Step 3 The heat map clusters with a dark blue and light blue color were interpreted as lymphoid aggregates and counted manually. **D**. Left: Kaplan-Meier plot for patients with less than 5 lymphoid aggregates show no significance in survival. Right: Kaplan-Meier plot for patients with 5 or more Lymphoid Aggregates and a high NFD show a significantly better survival.*

Discussion

PDAC is known for its significant cancer associated stroma or so-called tumor microenvironment. The large stromal component is a significant area of investigation and it is held responsible for poor treatment response. In this study we show that nerve fibers also play a role in the TME. Nerves are emerging regulators of cancer initiation, progression, and metastasis[23]. Previous data described by Renz et al. suggest that cholinergic signaling by the parasympathetic nerves can suppress the growth of pancreatic cancer cells, where the sympathetic nerves stimulate the growth of pancreatic cells. Therefore, in pancreatic cancer cells there is a balance of neural influence[24]. Immune cells also play a role in nerves in cancer and are a potential target. There are many levels of neuroimmune interactions, including regulation of inflammation, that play a role in cancer growth and dissemination[25].

Neural invasion by tumor cells is one of the most striking characteristics of PDAC and is a sign of aggressive behavior. Surprisingly in this study we found that a high NFD is associated with a better survival in patients with PDAC. We observed perineural tumor invasion of the bigger nerve trunks, also staining positive in PGP9.5 but these nerves were not counted due to exclusion based on their size. The smaller nerve fibers were not associated with tumor invasion and these nerve fibers were included in the counting method for NFD. So NFD is determined as the amount of small nerve fibers not to be confused by nerves invaded by tumor cells. We found that these small nerve fibers are located around lymphoid aggregates and predict a better survival in patients with 5 or more lymphoid aggregates and a high NFD. The definition of TLS differs in the literature depending on the maturation stage. The presence or absence of a germinal center shows different maturation stages of the TLS[15]. Mature TLS show the presence of germinal centers with expression of CD21 and CD23. With the use of machine learning we could only be certain of the presence of lymphoid aggregates and to specify these aggregates as real TLS further immunohistochemistry is needed.

Supplementary Materials: The following are available online at www.mdpi.com/xxx/s1, Figure S1: title, Table S1: title, Video S1: title.

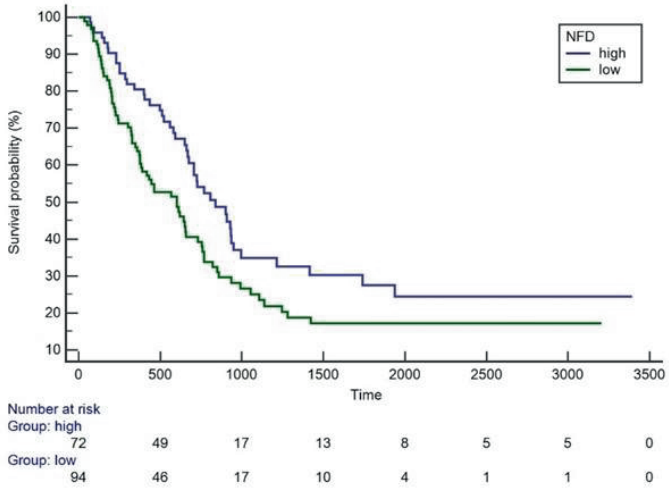

Figure S1: *Kaplan-Meier plot of the survival probabilities of patients with high and low NFD*

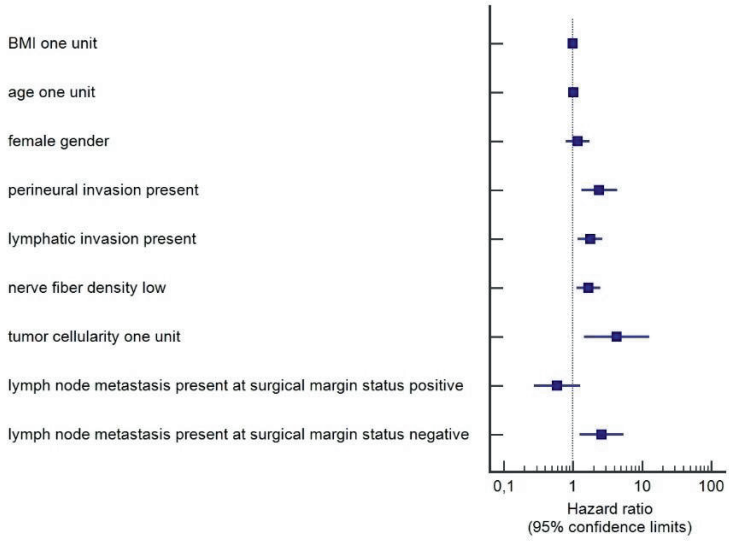

Figure S2: *Forest plot of hazard ratios and corresponding 95% confidence limits*

Code availability: Source codes are available at https://github.com/janniehues/PGP-pancreas/

References

1. Bray, F., *et al.* Global cancer statistics 2018: GLOBOCAN estimates of incidence and mortality worldwide for 36 cancers in 185 countries. *CA: a cancer journal for clinicians* **68**, 394-424 (2018).
2. Chen, D.S. & Mellman, I. Elements of cancer immunity and the cancer-immune set point. *Nature* **541**, 321-330 (2017).
3. Feig, C., *et al.* Targeting CXCL12 from FAP-expressing carcinoma-associated fibroblasts synergizes with anti-PD-L1 immunotherapy in pancreatic cancer. *Proceedings of the National Academy of Sciences of the United States of America* **110**, 20212-20217 (2013).
4. Petitprez, F., *et al.* B cells are associated with survival and immunotherapy response in sarcoma. *Nature* **577**, 556-560 (2020).
5. Helmink, B.A., *et al.* B cells and tertiary lymphoid structures promote immunotherapy response. *Nature* **577**, 549-555 (2020).
6. Cabrita, R., *et al.* Tertiary lymphoid structures improve immunotherapy and survival in melanoma. *Nature* **577**, 561-565 (2020).
7. Yuen, G.J., Demissie, E. & Pillai, S. B lymphocytes and cancer: a love-hate relationship. *Trends in cancer* **2**, 747-757 (2016).
8. Germain, C., Gnjatic, S. & Dieu-Nosjean, M.C. Tertiary Lymphoid Structure-Associated B Cells are Key Players in Anti-Tumor Immunity. *Frontiers in immunology* **6**, 67 (2015).
9. Sarvaria, A., Madrigal, J.A. & Saudemont, A. B cell regulation in cancer and anti-tumor immunity. *Cellular & molecular immunology* **14**, 662-674 (2017).
10. Tsou, P., Katayama, H., Ostrin, E.J. & Hanash, S.M. The Emerging Role of B Cells in Tumor Immunity. *Cancer research* **76**, 5597-5601 (2016).
11. Chen, P.L., *et al.* Analysis of Immune Signatures in Longitudinal Tumor Samples Yields Insight into Biomarkers of Response and Mechanisms of Resistance to Immune Checkpoint Blockade. *Cancer discovery* **6**, 827-837 (2016).
12. Pylayeva-Gupta, Y., *et al.* IL35-Producing B Cells Promote the Development of Pancreatic Neoplasia. *Cancer discovery* **6**, 247-255 (2016).
13. Carragher, D.M., Rangel-Moreno, J. & Randall, T.D. Ectopic lymphoid tissues and local immunity. *Seminars in immunology* **20**, 26-42 (2008).
14. Colbeck, E.J., Ager, A., Gallimore, A. & Jones, G.W. Tertiary Lymphoid Structures in Cancer: Drivers of Antitumor Immunity, Immunosuppression, or Bystander Sentinels in Disease? *Frontiers in immunology* **8**, 1830 (2017).
15. Sautes-Fridman, C., Petitprez, F., Calderaro, J. & Fridman, W.H. Tertiary lymphoid structures in the era of cancer immunotherapy. *Nature reviews. Cancer* **19**, 307-325 (2019).

16. Dieu-Nosjean, M.C., Goc, J., Giraldo, N.A., Sautes-Fridman, C. & Fridman, W.H. Tertiary lymphoid structures in cancer and beyond. *Trends in immunology* **35**, 571-580 (2014).
17. Siliņa, K.*, et al.* Germinal Centers Determine the Prognostic Relevance of Tertiary Lymphoid Structures and Are Impaired by Corticosteroids in Lung Squamous Cell Carcinoma. *Cancer research* **78**, 1308-1320 (2018).
18. Hiraoka, N.*, et al.* Intratumoral tertiary lymphoid organ is a favourable prognosticator in patients with pancreatic cancer. *British journal of cancer* **112**, 1782-1790 (2015).
19. Fukunaga, A.*, et al.* CD8+ tumor-infiltrating lymphocytes together with CD4+ tumor-infiltrating lymphocytes and dendritic cells improve the prognosis of patients with pancreatic adenocarcinoma. *Pancreas* **28**, e26-31 (2004).
20. Zhao, Q.*, et al.* The clinicopathological significance of neurogenesis in breast cancer. *BMC cancer* **14**, 484 (2014).
21. Lin, D.Y., Wei, L.J. & Ying, Z. Checking the Cox Model with Cumulative Sums of Martingale-Based Residuals. *Biometrika* **80**, 557-572 (1993).
22. de Santiago, I.*, et al.* Immunophenotypes of pancreatic ductal adenocarcinoma: Meta-analysis of transcriptional subtypes. *International journal of cancer* (2019).
23. Faulkner, S., Jobling, P., March, B., Jiang, C.C. & Hondermarck, H. Tumor Neurobiology and the War of Nerves in Cancer. *Cancer discovery* **9**, 702-710 (2019).
24. Renz, B.W.*, et al.* Cholinergic Signaling via Muscarinic Receptors Directly and Indirectly Suppresses Pancreatic Tumorigenesis and Cancer Stemness. *Cancer discovery* **8**, 1458-1473 (2018).
25. Dantzer, R. Neuroimmune Interactions: From the Brain to the Immune System and Vice Versa. *Physiological reviews* **98**, 477-504 (2018).
26. Balachandran, V.P.*, et al.* Identification of unique neoantigen qualities in long-term survivors of pancreatic cancer. *Nature* **551**, 512-516 (2017).
27. Karamitopoulou, E. Tumour microenvironment of pancreatic cancer: immune landscape is dictated by molecular and histopathological features. *British journal of cancer* **121**, 5-14 (2019).
28. Roghanian, A., Fraser, C., Kleyman, M. & Chen, J. B Cells Promote Pancreatic Tumorigenesis. *Cancer discovery* **6**, 230-232 (2016).

Chapter 3

Chapter 3

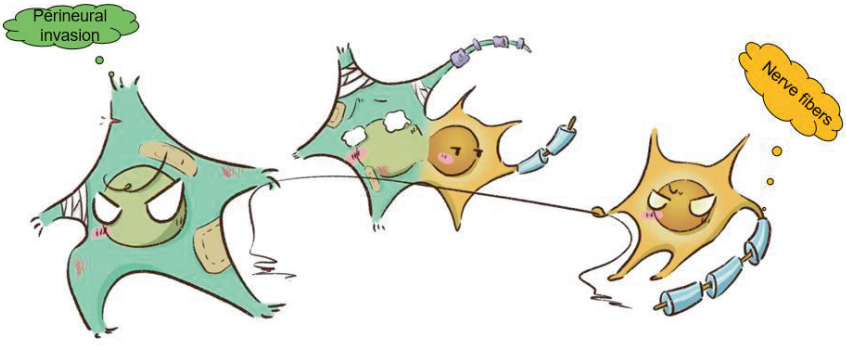

CHAPTER 4

Nerve Fibers in the Tumor Microenvironment as a novel biomarker for oncological outcome in patients undergoing surgery for perihilar

Jan Bednarsch, Jakob Kather, **Xiuxiang Tan,** Shivan Sivakumar, Claudio Cacchi, Georg Wiltberger, Zoltan Czigany, Florian Ulmer, Ulf Peter Neumann, Lara Heij

3rd author

Liver Cancer, 6 May 2021, 10:260–274

Chapter 4

Abstract: *Introduction:* Perihilar cholangiocarcinoma (pCCA) is a biliary tract cancer with a dismal prognosis, with surgery being the only chance of cure. A characteristic aggressive biological feature of pCCA is perineural growth which is defined by the invasion of cancers cells to nerves and nerve fibers. Recently, nerve fiber density (NFD) was linked to oncological outcomes in various malignancies, however, its prognostic role in pCCA remains to be elucidated. *Material and Methods:* Data of 101 pCCA patients who underwent curative intent surgery between 2010 and 2019 were included in this study. Extensive group comparisons between patients with high and low NFD were carried out and the association of cancer-specific survival (CSS), recurrence-free survival (RFS) with NFD and other clinico-pathological characteristics were assessed using univariate and multivariable cox regression models. *Results:* Patients with high NFD showed a median CSS of 90 months (95% CI: 48-132, 3-year-CSS=77%, 5-year-CSS=72%) compared to 33 months (95% CI: 19-47, 3-year-CSS=46%, 5-year-CSS=32%) in patients with low NFD (p=0.006 log rank). Further, N1 category (HR=2.84, p=0.001) and high NFD (HR=0.41, p=0.024) were identified as independent predictors of CSS in multivariable analysis. Patients with high NFD and negative lymph nodes, showed a median CSS of 90 months (3-year-CSS=88%, 5-year-CSS=80%), while patients either positive lymph nodes or low NFD displayed a median CSS of 51 months (3-year-CSS=59%, 5-year-CSS=45%) and patients with both positive lymph nodes and low NFD a median CSS of 24 months (3-year-CSS=26%, 5-year-CSS=16%, p=0.001 log rank). *Conclusion:* NFD has been identified as an important novel prognostic biomarker in pCCA patients. NFD alone and in combination with nodal status in particular, allow to stratify pCCA patients based on their risk for inferior oncological outcomes after curative-intent surgery.

Abbreviations

ALPPS	Associating liver partition and portal vein ligation for staged hepatectomy
ALT	Alanine aminotransferase
AP	Alkaline phosphatase
ASA	American society of anesthesiologists
AST	Aspartate aminotransferase
BMI	Body mass index
CA 19-9	Carbohydrate antigen 19-9
CAF	Cancer-associated fibroblasts
CCA	Cholangiocellular carcinoma
CCI	Comprehensive complication index
CI	Confidence interval
CRP	C reactive protein
CSS	Cancer-specific survival
CT	Computed tomography
EBD	Endoscopic biliary drainage
ECM	Extracellular matrix
ERCP	Endoscopic retrograde cholangiopancreatography
FFP	Fresh frozen plasma
FFPE	Formalin-fixed paraffin-embedded

FLR Future liver remnant

GGT Gamma glutamyltransferase

H&E Hematoxylin and Eosin

INR International normalized ratio

LiMAx Maximum liver function capacity

MRCP Magnetic resonance cholangiopancreatography

MRI Magnetic resonance imaging

NFD Nerve fiber density

NPY Neuropeptide Y

OS Overall Survival

PBD Percutaneous biliary drainage

PDAC Pancreatic ductal adenocarcinoma

PET-CT Positron emission tomography–computed tomography

pCCA Perihilar cholangiocarcinoma

RFS Recurrence-free survival

RWTH Rheinisch-Westfälische Technische Hochschule

VIP Vasoactive intestinal peptide

Introduction

Perihilar cholangiocarcinoma (pCCA) is the commonest subtype among biliary tract tumors and is associated with a poor prognosis [1-3]. Liver resection with vascular reconstructions and radical lymphadenectomy emerged as the gold standard of therapy in resectable disease, this yielded improved survival rates in selected cohorts. [3-9]. Despite these encouraging outcomes, surgical therapy remains challenging and often displays significant perioperative mortality rates exceeding 10% due to the distinct anatomic location of the tumor and the close proximity to major vascular structures [8-11].

As the prognosis spans from poor prognosis to good prognosis, there is significant value in being able to identify prognostic features [3]. Tumor differentiation, R0 status and lymph node status have been previously reported as important prognostic factors by Nagino et al. [12]. Our group and others have confirmed perioperative blood transfusion, serum albumin and lymphovascular invasion (LVI) as independent variables predicting adverse outcomes following surgery for pCCA [3,13,14].

PCCA is characterized by a large desmoplastic stroma component which might explain systemic therapy resistance [15]. Nerve fibers are a component of the tumor microenvironment (TME) and a significant proportion of cholangiocarcinoma patients display a tumor infiltration of the epineural, perineural and endoneural space of the neural sheath [16,17]. These features are termed perineural infiltration (PNI). PNI can be recognized on Hematoxylin and Eosin (H&E) staining and appears to be an independent predictor of prognosis in cholangiocarcinoma (CCA). In contrast, the prognostic role of nerve fiber density (NFD) referring to small nerve fibers in the TME which are usually not visible on H&E staining and do not show invasion of cancer cells remains to be determined in pCCA patients [18,19]. Therefore, we aimed to investigate NFD as a prognostic marker in a large European cohort of pCCA patients undergoing surgical resection.

Material and Methods

Patients

All consecutive patients with pCCA who underwent surgical resection at the University Hospital RWTH Aachen (UH-RWTH) between 2010 and 2019 were eligible for this study. Of

these patients (n=127), 20 individuals were excluded (n=14 perioperative mortality; n=6 with missing NFD data). Subsequently, a cohort of 101 patients were included in this analysis (Figure 1B). The study was conducted in accordance with the requirements of the Institutional Review Board of the RWTH-Aachen University (EK 106/18), the Declaration of Helsinki, and good clinical practice guidelines (ICH-GCP). A written informed consent was obtained from all patients.

Staging and surgical technique

All patients who were referred for surgical treatment for pCCA to our institution underwent a detailed clinical work-up as previously described [9,20]. In brief, tumor anatomy and localization were assessed by endoscopic retrograde cholangiopancreatography (ERCP) or magnetic resonance cholangiopancreatography (MRCP), while the presence of distant metastases was ruled out by multiphase computed tomography (CT). Additionally, the vascular anatomy as well as the potential invasion of major vessels at the liver hilum were also assessed by multiphase CT.

Our preoperative work-up included a unilateral stenting strategy as standard of care to relieve the future liver remnant (FLR) from cholestasis and bilateral stenting in cases with persisting cholangitis. Endoscopic biliary drainage (EBD) was generally preferred over percutaneous biliary drainage (PBD). In patients with insufficient FLR scheduled for right-sided hepatectomy, a right portal vein embolization (PVE) was conducted 2 to 4 weeks before surgery. The decision for surgery as primary treatment for the cancer was made by an experienced hepatobiliary surgeon and approved by the local multidisciplinary tumor board in all cases.

The surgical procedure was carried out as previously described by Neuhaus et al. [3,8,9,21,22]. Briefly, a "no-touch" hilar en-bloc resection approach, as defined by liver resection with mandatory portal vein resection and reconstruction, was carried out in all cases. Additional arterial resection and reconstruction as well as the concomitant resection of the pancreatic head (hepatoduodenopancreatectomy) was necessary in selected cases (table 1). Lymphadenectomy comprising the pericholedochal, the periportal, the common hepatic lymph nodes, the posterior pancreaticoduodenal and the celiac lymph nodes was routinely performed. All surgical specimens were evaluated by an experienced staff pathologist.

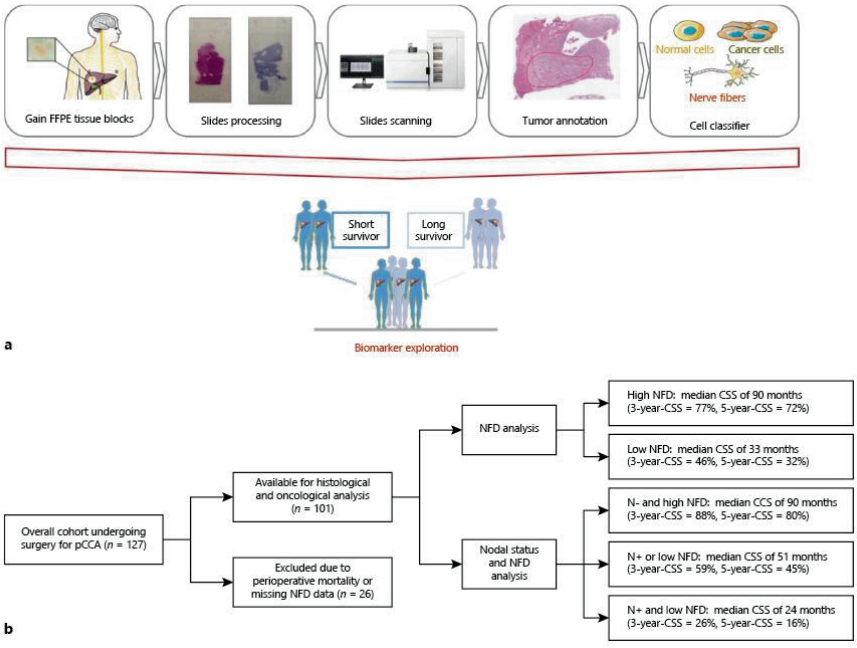

Figure 1: Workflow and study cohort. ***A:*** *Overview of all steps from tissue to biomarker. FFPE, formalin-fixed paraffin-embedded.* ***B:*** *Study cohort. CSS, cancer-specific survival; NFD, nerve fiber density; pCCA, perihilar cholangiocarcinoma.*

Follow-up

Adjuvant therapy was recommended for patients displaying high risk features (e.g. positive nodal status or R1 resection) from 2010 to 2017 and later in every individual in accordance to the results of the BILCAP trial [23]. Each patient underwent a regular follow-up including clinical examinations, standard laboratory blood tests with tumor markers (CA 19-9) and cross-sectional imaging by the referring oncologist or the local outpatient clinic. If tumor recurrence was suspected, additional imaging and/or biopsy was performed to confirm the diagnosis.

Assessment of nerve fiber density

Immunohistochemistry was performed on formalin-fixed, paraffin embedded (FFPE) tissue sections as previously described [19]. Briefly, sections (2.5µm thick) were cut, deparaffinized in xylene and rehydrated in graded alcohols. Slides were boiled in citrate buffer (pH 6.0) at 95 - 100°C for 5 minutes and were cooled for 20 minutes. Endogenous peroxide in methanol for 10 minutes. Sections were incubated with rabbit anti-human PGP 9.5 (DAKO 1:100) overnight at 4°C. A single digital image was uploaded in Qupath 0.1.6. As previously described, all slides were assessed by a trained pathologist who was blinded to the clinical outcomes of the individual patients and NFD was evaluated by manually counting the number of nerve fascicles with diameters of <100 µm in 20 continuous visual fields at x200 magnification [19]. An overview of the workflow is presented in figure 1A. Based on NFD results, patients were categorized into a low NFD group (<10 nerve fibers) and a high NFD group (≥10 nerve fibers).

Assessment of origin of the small nerve fibers

Immunohistochemistry was performed on formalin-fixed, paraffin embedded tissue sections as previously described. Sections were incubated with NPY (Abcam 1:200) and VIP (Abcam 1:50) overnight at 4°C.

Statistical analysis

The primary endpoint of this study was cancer-specific survival (CSS), which was defined from the date of resection to the date of tumor specific death. Deaths not associated with the tumor, e.g. cardiovascular events etc. were censored at the time of death. The secondary endpoint was recurrence-free survival (RFS), which was defined as the period from surgery to the date of first recurrence. Patients without tumor recurrence were censored at the time of death or at the last follow-up. Perioperative mortality was defined as in-hospital mortality. The cut-off level for NFD categorization was determined by the receiver operating characteristic (ROC)-analysis of CCS with respect to NFD as previously described [19]. Group comparisons were conducted by the Mann-Whitney-U-Test in case of continuous variables, while the chi-squared test, fisher's exact test or linear-by-linear association in accordance to scale and number count were used in case of categorical variables. The associations of CSS and RFS with clinico-pathological characteristics were assessed using univariate and multivariable Cox regression analyses in a backward selection model. Survival curves were generated by the Kaplan-Meier method and compared with the log-rank test. Median follow up was assessed with the reverse Kaplan-Meier method. The level of significance was set to $p < 0.05$ and p-values were given for two-sided testing. Analyses were performed using SPSS Statistics 24 (IBM Corp., Armonk, NY, USA)).

Results

Patient cohort

The study cohort consisted of 68 men (67%) and 33 women (33%) with a median age of 68 years. The majority of patients presented with Bismuth Type III (55%, 55/101) or IV (32%, 32/101) tumors and were assessed as ASA (American Society of Anesthesiologists classification) III or higher (53%, 53/101). Neoadjuvant therapy was applied in a small number of patients (4%, 4/101), while preoperative portal vein embolization (PVE) was carried out in a significant proportion of patients (43%, 43/101). Mandatory portal vein resection and reconstruction was carried out in every patient (101/101), while additional arterial reconstruction was necessary in 7% (7/101). Also, the concomitant resection of the pancreatic head was needed in 6% (6/101) of the patients to achieve clear tumor margins. Accordingly, R1 resection was confirmed in 12% (12/101) of the overall cohort. Major complications after surgery were frequently observed with 33% (33/101) of the patients presenting with complications ≥ Clavien-Dindo IIIb. Cases with perioperative mortality were excluded from the analysis as stated above. Further demographic and clinico-pathological details of the cohort are outlined in table 1.

Table 1. Patients' characteristics

Demographics	Overall cohort (n = 101)	High NFD (n = 31)	Low NFD (n = 70)	p value
Gender, male/female (%)	68 (67)/33 (33)	22 (71)/9 (29)	46 (66)/24 (34)	0.604
Age, years	68 (57–74)	68 (56–72)	68 (57–74)	0.968
BMI, kg/m^2	25 (22–29)	25 (23–30)	25 (22–28)	0.439
Neoadjuvant therapy, n (%)	4 (4)	3 (10)	1 (1)	0.050
PVE, n (%)	43 (43)	12 (39)	31 (44)	0.601
ASA, n (%)				
I	4 (4)	1 (3)	3 (4)	
II	44 (44)	16 (52)	28 (40)	
III	50 (50)	13 (42)	37 (53)	0.740
IV	3 (3)	1 (3)	2 (3)	
V	0	0		
Bismuth classification, n (%)				
I	4 (4)	4 (13)	4 (6)	
II	10 (10)	0	6 (9)	
IIIa	28 (28)	8 (26)	20 (29)	0.675
IIIb	27 (27)	9 (29)	18 (26)	
IV	32 (32)	10 (32)	22 (31)	
Preoperative cholangitis, n (%)	27 (27)	5 (16)	22 (31)	0.109
Preoperative PBD, n (%)	23 (23)	5 (16)	18 (26)	0.289
Preoperative EBD, n (%)	78 (77)	23 (74)	55 (79)	0.628
Clinical chemistry				
Albumin, g/dL	37 (33–42)	39 (34–42)	37 (32–41)	0.268
AST, U/L	47 (36–81)	49 (32–135)	47 (36–77)	0.932
ALT, U/L	68 (37–133)	88 (43–161)	63 (37–120)	0.318
GGT, U/L	451 (221–774)	554 (240–982)	441 (209–756)	0.304
Total bilirubin, mg/dL	1.2 (0.6–2.8)	1.2 (0.8–2.6)	1.2 (0.5–2.8)	0.805
Platelet count, /nL	296 (228–393)	292 (212–392)	297 (230–399)	0.548
Alkaline phosphatase, U/L	254 (169–396)	251 (160–445)	254 (183–372)	0.747
Prothrombin time, %	96 (81–105)	99 (79–107)	96 (82–104)	0.868
INR	1.02 (0.96–1.12)	1.01 (0.97–1.13)	1.03 (0.96–1.12)	0.839
Hemoglobin, g/dL	12.5 (11.3–13.4)	13 (11.5–13.6)	12.3 (11.1–13.2)	0.165
CRP, mg/L	12 (6–35)	12 (6–35)	12 (6–36)	0.759
Operative data				
Operative time, min	404 (356–474)	415 (355–465)	400 (355–483)	0.947
Operative procedure, n (%)				
Limited bile duct resection	1 (1)	0	1 (1)	
Right hepatectomy	11 (11)	2 (7)	9 (13)	
Left hepatectomy	11 (11)	5 (16)	6 (9)	
Extended right hepatectomy	18 (18)	6 (19)	12 (17)	
Extended left hepatectomy	28 (28)	9 (29)	19 (27)	0.475
Right trisectionectomy	20 (20)	6 (19)	14 (20)	
Left trisectionectomy	5 (5)	3 (10)	2 (3)	
Hepatoduodenoectomy	6 (6)	0	6 (9)	
ALPPS	1 (1)	0	1 (1)	
Portal vein reconstruction	101 (100)	31 (100)	70 (100)	0.999
Arterial reconstruction	7 (7)	2 (7)	5 (7)	0.900
Intraoperative blood transfusion	0 (0–2)	0 (0–2)	1 (0–2)	0.368
Intraoperative FFP	3 (0–5)	3 (0–4)	3 (0–6)	0.463
Pathological examination				
R1 resection, n (%)	12 (12)	3 (10)	9 (13)	0.606
pT category, n (%)				
1	7 (7)	2 (7)	5 (7)	
2	62 (61)	18 (58)	44 (63)	0.678
3	26 (26)	10 (32)	16 (23)	
4	6 (6)	1 (3)	5 (7)	
pN category				
N0	62 (61)	21 (68)	41 (59)	0.383
N1	39 (39)	10 (32)	29 (41)	
Tumor grading, n (%)				
G1	6 (6)	2 (7)	4 (6)	
G2	73 (75)	27 (90)	46 (68)	0.099
G3	18 (18)	1 (3)	17 (25)	
G4	1 (1)	0	1 (2)	
MVI, n (%)	71 (73)	4 (13)	21 (32)	0.100
LVI, n (%)	21 (22)	7 (23)	14 (22)	0.938
PNI, n (%)	66 (81)	18 (82)	48 (80)	0.854
Postoperative data				
Intensive care, days	1 (1–3)	1 (1–2)	2 (1–3)	0.233
Hospitalization, days	20 (13–36)	14 (12–31)	24 (13–42)	**0.017**
Postoperative complications, n (%)				
No complications	14 (14)	6 (19)	8 (11)	
Clavien-Dindo I	8 (8)	3 (10)	5 (7)	
Clavien-Dindo II	27 (27)	10 (32)	17 (24)	
Clavien-Dindo IIIa	19 (19)	2 (7)	17 (24)	0.272
Clavien-Dindo IIIb	22 (22)	7 (23)	15 (21)	
Clavien-Dindo IVa	7 (7)	3 (10)	4 (6)	
Clavien-Dindo IVb	4 (4)	0	4 (6)	
Clavien-Dindo V	0	0	0	
CCI	35 (21–50)	23 (8–54)	39 (20–49)	0.124
Oncologic data				
Adjuvant therapy	23 (23)	6 (19)	17 (25)	0.562
Median RFS, months (95% CI)	37 (18–56)	83 (34–132)	24 (13–35)	**0.004**
Median CSS, months (95% CI)	49 (29–69)	90 (48–132)	33 (19–47)	**0.006**

Data are presented as median and interquartile range if not noted otherwise. Bold numbers indicate statistical significance ($p < 0.05$). NFD, nerve fiber density; ALT, alanine aminotransferase; ASA, American Society of Anesthesiologists classification; AST, aspartate aminotransferase; CCI, comprehensive complication index; CSS, cancer-specific survival; EBD, endoscopic biliary drainage; FFP, fresh frozen plasma; GGT, gamma glutamyltransferase; INR, international normalized ratio; LVI, lymphovascular invasion; MVI, microvascular invasion; PBD, percutaneous biliary drainage; PNI, perineural invasion, RFS, recurrence-free survival; PVE, portal vein embolization.

Group categorization and comparative analysis with respect to nerve fiber density

A receiver operating characteristic analysis evaluating the total number of nerve fibers

for patients who survived at least 4 years versus patients who died during follow-up was conducted. The corresponding area under the curve was 0.618 (95% confidence interval [CI]: 0.480–0.756). A cutoff value for NFD was determined with respect to optimized accuracy and equal weight for sensitivity and specificity errors (<10 nerve fibers and ≥10 nerve fibers). Using the established cutoff value, the median CSS was 90 months in patients with high NFD (≥10 nerve fibers) and 33 months in patients with low NFD (<10 nerve fibers, p = 0.006 log rank)

A comparative group analysis regarding NFD was further carried out between patients with high NFD (n=31) and low NFD (n=70). Extensive group comparisons revealed no significant differences in clinical characteristics expect a longer median hospitalization time in the low NFD group (14 vs. 21 days, p=0.017). Of note, no statistical differences in pT category (p=0.678), pN category (p=0.383), tumor grading (p=0.099), lymphovascular invasion (LVI, p=0.938), microvascular invasion (MVI, p=0.100) and perineural invasion (PNI, p=0.854) were observed between the groups. However, the median CSS (90 months (95% CI: 48- 132) vs. 33 months (95% CI: 19-47), p=0.006 log rank) and the median RFS (83 months (95% CI: 34-132) vs. to 24 months (95% CI: 13-35), p=0.004 log rank) were significantly longer in patients with high NFD compared to patients with low NFD. More details regarding the group comparisons are presented in table 1.

Survival analysis

After a median follow-up of 53 months, the median CSS of the whole cohort was 49 months (95% CI: 29-69), the median OS 33 months (95% CI: 19-47) and the median RFS 37 months (95% CI: 18-56, Figure 2A and 2B). A Kaplan-Meier analysis with respect to NFD showed a median CSS of 90 months (95% CI: 48-132, 3-year-CSS=77%, 5-year-CSS=72%) in patients with high NFD compared to 33 months (95% CI: 19-47, 3-year-CSS=46%, 5-year-CSS=32%) in patients with low NFD (p=0.006 log rank, Figure 2C). Further, RFS was significantly lower in patients with low NFD (24 months (95% CI: 13-35)) compared to patients with high NFD (83 months (95% CI: 34-132), p=0.004 log rank, Figure 2D). Interestingly, in a subsequent Kaplan-Meier analysis the combination of NFD with nodal status resulted in a median CSS of 90 months (95% CI: 57-123, 3-year-CSS=88%, 5-year-CSS=80%) in patients with high NFD and negative lymph nodes, 51 months (95% CI: 38-64, 3-year-CSS=59%, 5-year-CSS=45%) in patients with either positive lymph nodes or low NFD but not both and 24 months (95% CI: 14-32, 3-year-CSS=26%, 5-year-CSS=16%) in patients with both positive lymph nodes and low NFD (p=0.001 log rank, Figure 2E). Accordingly, the median RFS was 83 months (95% CI: 42-124) in patients with high NFD and negative lymph nodes, 45 months (95% CI: 8-82) in patients with either positive lymph nodes or low NFD and 10 months (95% CI: 0-21) in patients with both positive lymph nodes and low NFD (p=0.001 log rank, Figure 2F).

Cox regression analysis

In univariate analysis, intraoperative blood (p=0.011) and FFP transfusion (p=0.010), R1 resection (p=0.019), nodal status (p=0.002), tumor grading (p=0.004), MVI (p=0.022), LVI (p=0.026) and NFD (p=0.009) were significantly associated with CSS. All variables showing p-value <0.05 were included in a multivariable Cox regression model. Here, intraoperative FFP transfusion (HR=2.90, p=0.004), nodal status (HR=2.84, p=0.001) and NFD (HR=0.41, p=0.024) were identified as independent predictors of CSS (Table 2).

In univariate analysis, intraoperative blood (p = 0.034) and FFP transfusion (p = 0.009), R1 resection (p = 0.006), nodal status (p = 0.003), tumor grading (p = 0.001), MVI (p = 0.008), LVI (p = 0.022), NFD (p = 0.007), and adjuvant therapy (p = 0.028) showed significant associations with RFS. In the corresponding multivariable Cox regression model, intraoperative FFP transfusion (HR = 3.10, p = 0.002), nodal status (HR = 2.92, p = 0.001), MVI (HR = 1.98, p = 0.048) and NFD (HR = 0.42, p = 0.031) were identified as independent predictors of RFS (Table 3).

Table 2 Univariate and multivariable analysis of CSS in pCCA

	Univariate analysis		Multivariable analysis	
	HR (95% CI)	*p* value	HR (95% CI)	*p* value
Demographics				
Sex (male = 1)	1.28 (0.71–2.29)	0.411		
Age (≤65 years = 1)	1.13 (0.64–2.00)	0.683		
BMI (≤25 kg/m^2 = 1)	1.17 (0.66–2.06)	0.591		
PVE (no = 1)	1.01 (0.57–1.80)	0.972		
ASA (I/II = 1)	1.27 (0.72–2.27)	0.411		
Preoperative cholangitis (no = 1)	0.82 (0.44–1.53)	0.526		
EBD (no = 1)	1.29 (0.60–2.76)	0.515		
PBD (no = 1)	0.95 (0.50–1.84)	0.889		
Clinical chemistry				
Albumin (≤40 g/L = 1)	0.68 (0.36–1.28)	0.238		
AST (≤40 U/L = 1)	1.34 (0.72–2.48)	0.739		
ALT (≤40 U/L = 1)	0.87 (0.40–1.93)	0.354		
GGT (≤400 U/L = 1)	1.20 (0.66–2.20)	0.555		
Bilirubin (≤1 mg/dL = 1)	1.26 (0.72–2.23)	0.423		
Alkaline phosphatase (≤250 U/L = 1)	1.01 (0.56–1.86)	0.964		
Platelet count (≤300/nL = 1)	1.08 (0.59–1.96)	0.813		
INR (≤1 = 1)	1.57 (0.84–2.95)	0.162		
Hemoglobin (≤13 g/dL = 1)	0.63 (0.34–0.1.17)	0.144		
CRP, mg/L (≤10 mg/L = 1)	1.08 (0.59–1.95)	0.813		
Operative data				
Operative time (≤360 min = 1)	1.68 (0.87–3.27)	0.125		
Type of hepatectomy				
Right-sided hepatectomy	1	0.965		
Left-sided hepatectomy	0.97 (0.53–1.74)	0.907		
Blood transfusion (no = 1)	2.11 (1.19–3.75)	**0.011**	Excluded	
FFP transfusion (no = 1)	2.38 (1.23–4.61)	**0.010**	2.90 (1.39–6.02)	**0.004**
Arterial resection (no = 1)	1.85 (0.66–5.19)	0.242		
Pathological data				
R1 resection (no = 1)	2.42 (1.16–5.06)	**0.019**	Excluded	
pT category (T1/T2 = 1)	1.53 (0.85–2.78)	0.159		
pN category (N0 = 1)	2.52 (1.32–4.47)	**0.002**	2.84 (1.52–5.31)	**0.001**
Tumor grading (G1/G2 = 1)	2.86 (1.39–5.88)	**0.004**	Excluded	
MVI (no = 1)	2.10 (1.16–3.96)	**0.022**	Excluded	
LVI (no = 1)	2.14 (1.09–4.18)	**0.026**	Excluded	
PNI (no = 1)	1.72 (0.67–4.42)	0.260		
NFD (low = 1)	0.37 (0.18–0.78)	**0.009**	0.41 (0.19–0.89)	**0.024**
Oncological data				
Neoadjuvant therapy (no = 1)	0.58 (0.08–4.21)	0.589		
Adjuvant therapy (yes = 1)	1.52 (0.78–2.97)	0.219		

Various parameters are associated with overall survival. Bold numbers indicate statistical significance ($p < 0.05$). CSS, cancer-specific survival; pCCA, perihilar cholangiocarcinoma; ALT, alanine aminotransferase; ASA, American Society of Anesthesiologists classification; AST, aspartate aminotransferase; CCI, comprehensive complication index; CRP, C-reactive protein; EBD, endoscopic biliary drainage; FFP, fresh frozen plasma; GGT, gamma glutamyltransferase; INR, international normalized ratio; LVI, lymphovascular invasion; MVI, microvascular invasion; NFD, nerve fiber density; PBD, percutaneous biliary drainage; PNI, perineural invasion; PVE, portal vein embolization.

Table 3 Univariate and multivariable analysis of RFS in pCCA

	Univariate analysis		Multivariable analysis	
	HR (95% CI)	*p* value	HR (95% CI)	*p* value
Demographics				
Sex (male = 1)	1.12 (0.62–2.02)	0.704		
Age (≤65 years = 1)	0.89 (0.51–1.56)	0.691		
BMI (≤25 kg/m^2 = 1)	1.46 (0.83–2.58)	0.189		
PVE (no = 1)	1.23 (0.70–2.16)	0.478		
ASA (I/II = 1)	1.00 (0.57–1.75)	0.990		
Preoperative cholangitis (no = 1)	1.71 (0.94–3.09)	0.077		
EBD (no = 1)	1.23 (0.60–2.54)	0.576		
PBD (no = 1)	1.12 (0.58–2.14)	0.741		
Clinical chemistry				
Albumin (≤40 g/L = 1)	0.61 (0.33–1.13)	0.114		
AST (≤40 U/L = 1)	1.49 (0.81–2.74)	0.200		
ALT (≤40 U/L = 1)	1.00 (0.46–2.17)	0.997		
GGT (≤400 U/L = 1)	1.25 (0.69–2.28)	0.463		
Bilirubin (≤1 mg/dL = 1)	1.26 (0.72–2.23)	0.423		
Alkaline phosphatase (≤250 U/L = 1)	0.96 (0.53–1.75)	0.901		
Platelet count (≤300/nL = 1)	1.26 (0.68–2.31)	0.464		
INR (≤1 = 1)	1.75 (0.94–3.27)	0.077		
Hemoglobin (≤13 g/dL = 1)	0.56 (0.30–1.05)	0.069		
CRP, mg/L (≤10 mg/L = 1)	1.34 (0.74–2.43)	0.343		
Operative data				
Operative time (≤360 min = 1)	1.67 (0.85–3.27)	0.136		
Type of hepatectomy				
Right-sided hepatectomy	1	0.466		
Left-sided hepatectomy	0.81 (0.45–1.44)			
Blood transfusion (no = 1)	1.84 (1.05–3.24)	**0.034**	Excluded	
FFP transfusion (no = 1)	2.33 (1.23–4.40)	**0.009**	3.10 (1.42–6.30)	**0.002**
Arterial resection (no = 1)	0.88 (0.21–3.67)	0.862		
Pathological data				
R1 resection (no = 1)	2.69 (1.33–5.44)	**0.006**	Excluded	
pT category (T1/T2 = 1)	1.64 (0.92–2.94)	0.095		
pN category (N0 = 1)	2.33 (1.32–4.10)	**0.003**	2.92 (1.55–5.48)	**0.001**
Tumor grading (G1/G2 = 1)	3.51 (1.82–6.76)	**0.001**	Excluded	
MVI (no = 1)	2.27 (1.23–4.19)	**0.008**	1.98 (1.01–3.89)	**0.048**
LVI (no = 1)	2.13 (1.11–4.08)	**0.022**	Excluded	
PNI (no = 1)	2.41 (0.86–6.80)	0.096		
NFD (low = 1)	0.35 (0.16–0.75)	**0.007**	0.42 (0.19–0.93)	**0.031**
Oncological data				
Neoadjuvant therapy (no = 1)	0.49 (0.07–3.55)	0.479		
Adjuvant therapy (yes = 1)	0.50 (0.27–0.93)	**0.028**	Excluded	

Various parameters are associated with disease-free survival. Bold numbers indicate statistical significance ($p < 0.05$). RFS, recurrence-free survival; pCCA, perihilar cholangiocarcinoma; ALT, alanine aminotransferase; ASA, American Society of Anesthesiologists classification; AST, aspartate aminotransferase; CCI, comprehensive complication index; CRP, C-reactive protein; EBD, endoscopic biliary drainage; FFP, fresh frozen plasma; GGT, gamma glutamyltransferase; INR, international normalized ratio; LVI, lymphovascular invasion; MVI, microvascular invasion; NFD, nerve fiber density; PBD, percutaneous biliary drainage; PNI, perineural invasion; PVE, portal vein embolization.

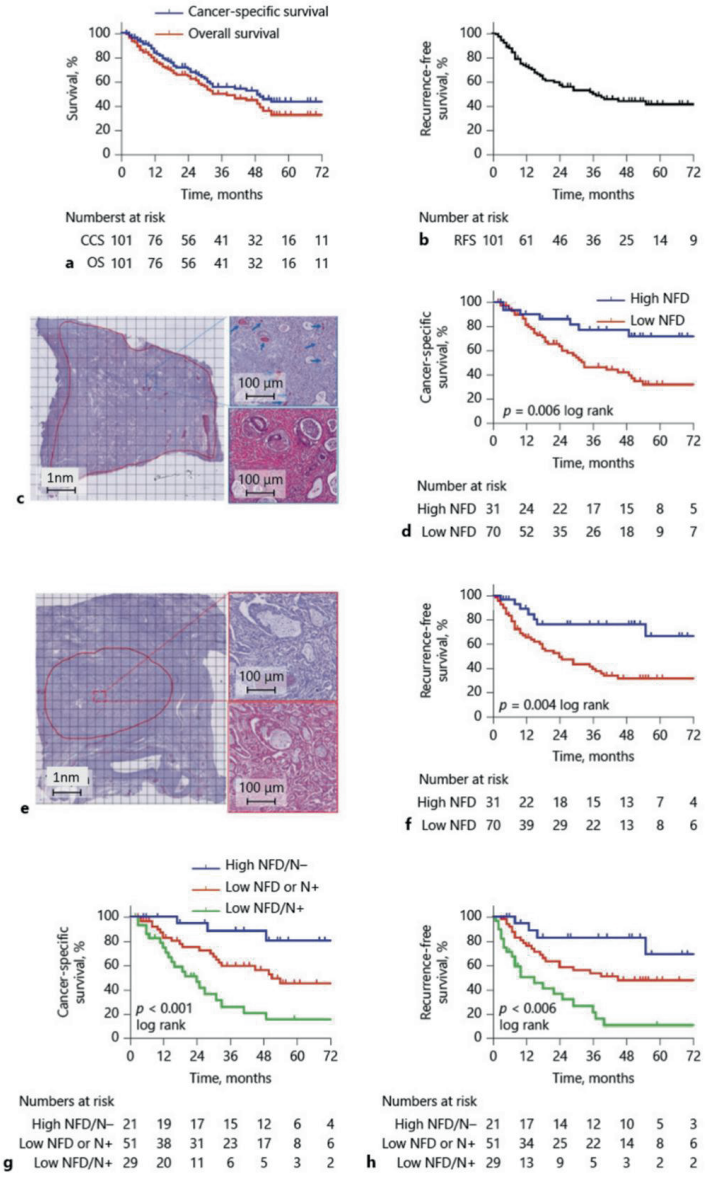

Figure 2. *Oncological survival in pCCA.* a CSS and OS in pCCA. The median CSS was 49 months (95% CI: 29–69) and the median OS 33 months (95% CI: 19–47), respectively. b RFS in pCCA. The median RFS was 37 months (95% CI: 18–56). c PGP staining of pCCA with high NFD. Zoomed in image of the tumor with a lot of small nerves in the stroma between the tumor glands (blue arrows). On the zoomed in image of the routine HE staining, these small nerve fibers are not visible. These results occur in patients corresponding to the blue line in the Kaplan-Meier curve in d and f (high NFD). d CSS in pCCA stratified by NFD. The median CSS was 90 months (95% CI: 48–132) in patients with high NFD compared to 33 months (95% CI: 19–47) in patients with low NFD (p = 0.006 log rank). e PGP staining of pCCA with low NFD. Zoomed in image of the tumor without any small nerves in the stroma between the tumor glands. The zoomed in image of PGP shows a positive bigger nerve trunk with perineural invasion. These big nerve fibers are also easily recognized on the zoomed in routine HE staining.

f RFS in pCCA stratified by NFD. The median RFS was 83 months (95% CI: 34–132) in patients with high NFD compared to 24 months (95% CI: 13–35) in patients with low NFD (p = 0.004 log rank). g CSS in pCCA stratified by NFD and pN category. The median CSS was 90 months (95% CI: 57–123) in patients with high NFD and negative lymph nodes, 51 months (95% CI: 38–64) in patients with either positive lymph nodes or low NFD but not both, and 24 months (95% CI: 14–32) in patients with both positive lymph nodes and low NFD (p = 0.001 log rank). h RFS in pCCA stratified by NFD and pN category. The median RFS was 83 months (95% CI: 42–124) in patients with high NFD and negative lymph nodes, 45 months (95% CI: 8–82) in patients with either positive lymph nodes or low NFD but not both, and 10 months (95% CI: 0–21) in patients with both positive lymph nodes and low NFD (p = 0.001 log rank). CI, confidence interval; CSS, cancer-specific survival; RFS, recurrence-free survival; OS, overall survival; pCCA, perihilar cholangiocarcinoma; PGP, protein gene product 9.5; NFD, nerve fiber density.

Analysis of nerve fiber origin

To further investigate the origin of the counted NFD, immunohistochemistry was carried out in a representative subset of patients (n=20). Here, small nerve fibers counted to assess NFD were stained positive for vasoactive intestinal peptide (VIP; to indicate parasympathetic origin) but negative for neuropeptide Y (NPY; to indicate sympathetic origin). The larger pre-existing nerve fibers which also stain positive in the PGP marker, showed expression of the NPY marker and those nerve fibers were observed to be invaded by tumor cells (Figure 3).

Discussion and conclusion

Radical surgery with lymphadenectomy represents the current gold standard therapy of resectable pCCA [15]. However, oncological outcome remains heterogeneous after curative-intent surgery with some patients displaying long-term survival while other individuals suffer from early tumor recurrence [3]. Therefore, the identification of prognostic factors is of clinical and academic significance as it provides implications for clinical management and may give insights in the underlying tumor biology of the disease [24]. In this large European cohort of pCCA patients, we identified NFD as a novel and important prognostic biomarker for oncological outcome in these patients. The combination of NFD and nodal status demonstrated an excellent ability to stratify pCCA regarding their oncological prognosis after curative-intent surgery for pCCA.

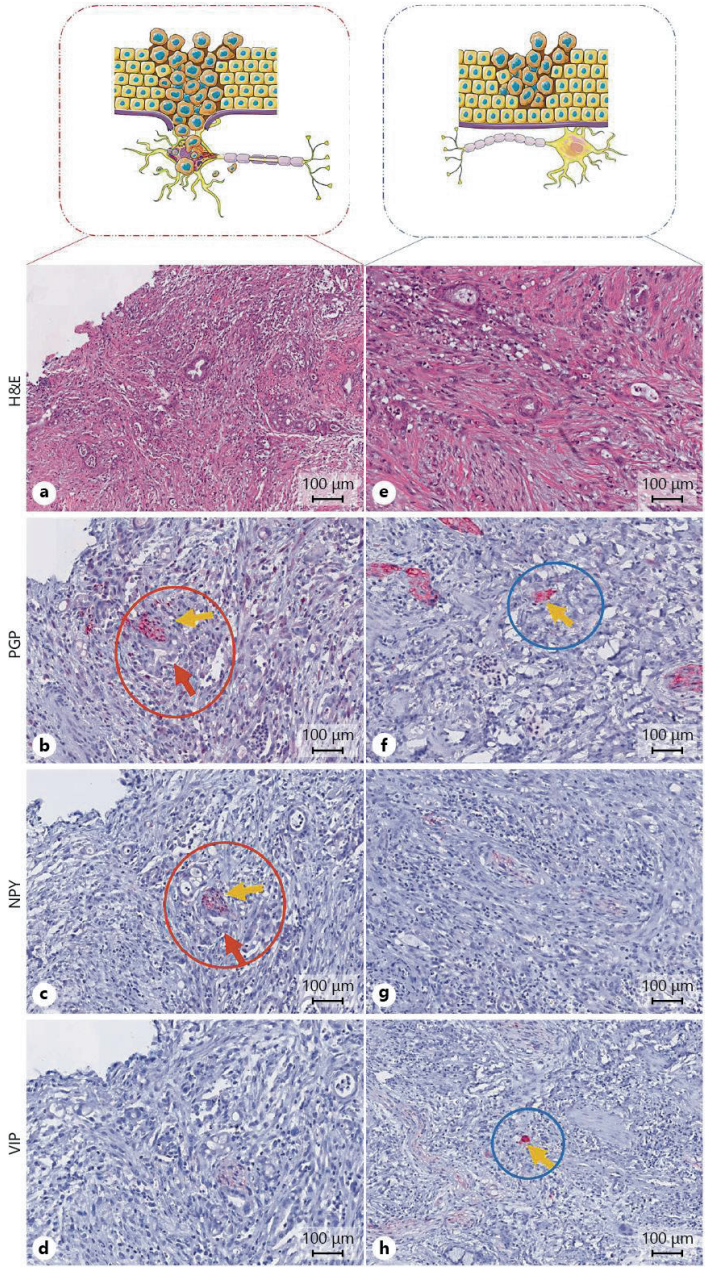

Figure 3. *Origin of the nerve fibers. Schematic overview of tissue with cancers cells invading the nerve.* **a** Routine HE staining showing perineural invasion of cancer cells invading a large nerve trunk (red arrow). **b** PGP immunohistochemistry staining being expressed in this cancer-invaded nerve (yellow arrow). NPY immunohistochemistry (sympathetic origin) is expressed (**c**), and VIP immunohistochemistry (parasympathetic) is not expressed in this large nerve trunk (**d**). Schematic overview of tissue with cancer cells not invading the nerve. **e** Routine HE staining showing the yellow arrow to the localization of the small nerve fibers that are not visible on the HE staining. **f** Those small nerve fibers stain positive in the PGP immunohistochemistry. **g** Negative staining of these small nerve fibers in the VPN

immunohistochemistry. **h** Yellow arrow points to the positive staining in the VIP immunohistochemistry of these small nerve fibers. NPY, neuropeptide Y; VIP, vasoactive intestinal peptide.

CCA is considered to be a "neurotopic" cancer with a high frequency of PNI which is associated with impaired outcomes [17,25]. The biliary tree is surrounded by a complex nerve fiber network being the basis for an intense crosstalk between nerve fibers and tumor cells as well as other parts of the TME e.g. immune cells or cancer-associated fibroblasts (CAF) [26-28]. Neurotransmitters are known to directly interact with the cancer cells and conversely, cancer cells release neurotransmitters activating receptors on the nerve fibers [29-32]. Intra-tumor CAFs are remodeling the extracellular matrix (ECM) and leading to a production of hyaluronic acid, fibronectin and collagen. Those ECM components are known to influence neuron growth [26,27]. Also, the co-localization and interaction of immune cells and nerve fibers drive tissue protection and play a critical immune-regulatory role [28]. In this study, we have further identified the origin of these nerve fibers to be parasympathetic and specifically those nerve fibers predict a better outcome. Of note, from a clinical point of view NFD has already been investigated in various other malignancies e.g. gastric and colorectal carcinomas [33,34]. Here, high NFD has been associated with a higher pathological staging and subsequently decreased survival. Interestingly, Iwasaki et al. have recently reported on the role of NFD in PDAC and found an inverse relationship with low NFD being independently associated with reduced survival after surgical resection [19]. This observation is in line with our present findings, identifying low NFD as an important predictor of inferior CSS in pCCA. In our study, we were able to demonstrate a 5-year-CSS of 72% in patients with high NFD compared to a 5-year-CSS of 32% in patients with low NFD (figure 2C).

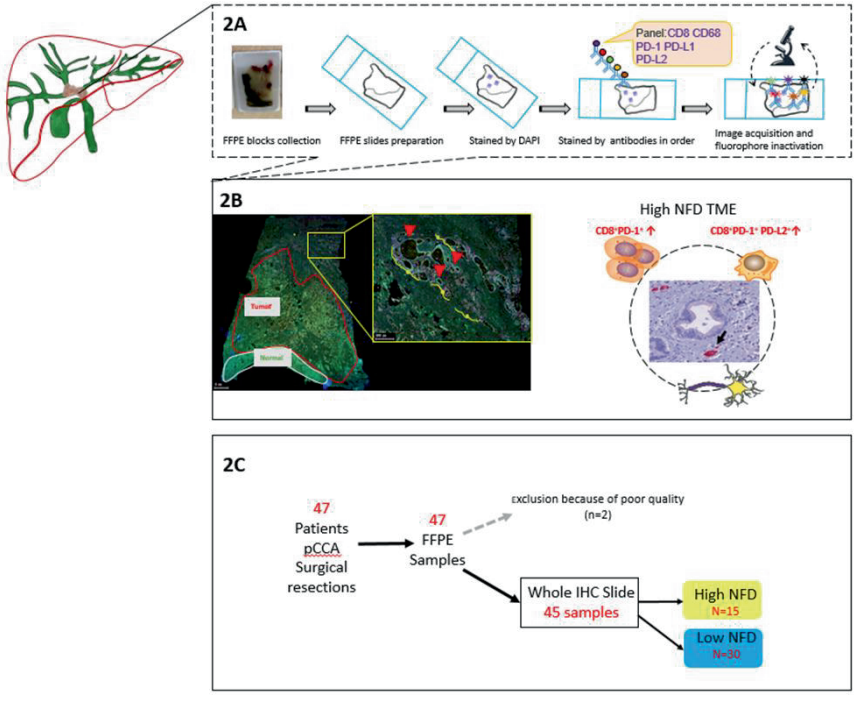

Figure 2: Overview of study workflow. 2A The formalin-fixed paraffin-embedded (FFPE) blocks were collected from the pathology archives. The slides were cut and stained with DAPI and 5 antibodies. The immunofluorescence-stained slides were scanned. 2B The digital scans were annotated for different regions: Tumor and Tumor-free. Cells were subsequently counted in these separate regions. For the NFD patients, the slides were selected based on the small nerve fiber count from previous work and the cell counting was done in the tumor region. 2C In total we included 47 patients in this study. From 45 patients we were able to analyze the digital scans.

DAPI, diamidino-2-phenylindole, FFPE; formalin-fixed paraffin-embedded

Statement of ethics

The study was conducted in accordance with the requirements of the Institutional Review Board of the RWTH-Aachen University (EK 106/18), the current version of the Declaration of Helsinki, and the good clinical practice guidelines (ICH-GCP).

Conflict of interest statement

The authors have no conflicts of interest to declare.

Reference

1. Torre LA, Bray F, Siegel RL, Ferlay J, Lortet-Tieulent J, Jemal A. Global cancer statistics, 2012. *CA: a cancer journal for clinicians* 2015; **65**(2): 87-108.
2. Neumann UP, Schmeding M. Role of surgery in cholangiocarcinoma: From resection to transplantation. *Best practice & research Clinical gastroenterology* 2015; **29**(2): 295-308.
3. Lurje G, Bednarsch J, Czigany Z, et al. The prognostic role of lymphovascular invasion and lymph node metastasis in perihilar and intrahepatic cholangiocarcinoma. *European journal of surgical oncology : the journal of the European Society of Surgical Oncology and the British Association of Surgical Oncology* 2019; **45**(8): 1468-78.
4. Miyazaki M, Ito H, Nakagawa K, et al. Aggressive surgical approaches to hilar cholangiocarcinoma: hepatic or local resection? *Surgery* 1998; **123**(2): 131-6.
5. Neuhaus P, Jonas S, Bechstein WO, et al. Extended resections for hilar cholangiocarcinoma. *Annals of surgery* 1999; **230**(6): 808-18; discussion 19.
6. Becker T, Lehner F, Bektas H, et al. [Surgical treatment for hilar cholangiocarcinoma (Klatskin's tumor)]. *Zentralblatt fur Chirurgie* 2003; **128**(11): 928-35.
7. Petrowsky H, Wildbrett P, Husarik DB, et al. Impact of integrated positron emission tomography and computed tomography on staging and management of gallbladder cancer and cholangiocarcinoma. *Journal of hepatology* 2006; **45**(1): 43-50.
8. Neuhaus P, Thelen A, Jonas S, et al. Oncological superiority of hilar en bloc resection for the treatment of hilar cholangiocarcinoma. *Annals of surgical oncology* 2012; **19**(5): 1602-8.
9. Bednarsch J, Czigany Z, Lurje I, et al. Left- versus right-sided hepatectomy with hilar en-bloc resection in perihilar cholangiocarcinoma. *HPB : the official journal of the International Hepato Pancreato Biliary Association* 2020; **22**(3): 437-44.
10. Clavien PA, Petrowsky H, DeOliveira ML, Graf R. Strategies for safer liver surgery and partial liver transplantation. *The New England journal of medicine* 2007; **356**(15): 1545-59.
11. Bednarsch J, Czigany Z, Lurje I, et al. Insufficient future liver remnant and preoperative cholangitis predict perioperative outcome in perihilar cholangiocarcinoma. *HPB : the official journal of the International Hepato Pancreato Biliary Association* 2020.
12. Nagino M, Ebata T, Yokoyama Y, et al. Evolution of surgical treatment for perihilar cholangiocarcinoma: a single-center 34-year review of 574 consecutive resections. *Annals of surgery* 2013; **258**(1): 129-40.
13. Kimura N, Toyoki Y, Ishido K, et al. Perioperative blood transfusion as a poor prognostic factor after aggressive surgical resection for hilar cholangiocarcinoma. *Journal of gastrointestinal surgery : official journal of the Society for Surgery of the Alimentary Tract* 2015; **19**(5): 866-79.
14. Waghray A, Sobotka A, Marrero CR, Estfan B, Aucejo F, Narayanan Menon KV. Serum albumin predicts survival in patients with hilar cholangiocarcinoma. *Gastroenterology report* 2017; **5**(1): 62-6.
15. Valle J, Wasan H, Palmer DH, et al. Cisplatin plus gemcitabine versus gemcitabine for biliary tract cancer. *The New England journal of medicine* 2010; **362**(14): 1273-81.
16. Shirai K, Ebata T, Oda K, et al. Perineural invasion is a prognostic factor in intrahepatic cholangiocarcinoma. *World journal of surgery* 2008; **32**(11): 2395-402.
17. Fisher SB, Patel SH, Kooby DA, et al. Lymphovascular and perineural invasion as selection criteria for adjuvant therapy in intrahepatic cholangiocarcinoma: a multi-institution analysis. *HPB : the official journal of the International Hepato Pancreato Biliary Association* 2012; **14**(8): 514-22.

18. Zhang L, Guo L, Tao M, Fu W, Xiu D. Parasympathetic neurogenesis is strongly associated with tumor budding and correlates with an adverse prognosis in pancreatic ductal adenocarcinoma. *Chinese journal of cancer research = Chung-kuo yen cheng yen chiu* 2016; **28**(2): 180-6.
19. Iwasaki T, Hiraoka N, Ino Y, et al. Reduction of intrapancreatic neural density in cancer tissue predicts poorer outcome in pancreatic ductal carcinoma. *Cancer science* 2019; **110**(4): 1491-502.
20. Bednarsch J, Czigany Z, Heise D, et al. Leakage and Stenosis of the Hepaticojejunostomy Following Surgery for Perihilar Cholangiocarcinoma. *Journal of clinical medicine* 2020; **9**(5).
21. Neuhaus P, Jonas S, Settmacher U, et al. Surgical management of proximal bile duct cancer: extended right lobe resection increases resectability and radicality. *Langenbeck's archives of surgery / Deutsche Gesellschaft fur Chirurgie* 2003; **388**(3): 194-200.
22. Jonas S, Benckert C, Thelen A, Lopez-Hanninen E, Rosch T, Neuhaus P. Radical surgery for hilar cholangiocarcinoma. *European journal of surgical oncology : the journal of the European Society of Surgical Oncology and the British Association of Surgical Oncology* 2008; **34**(3): 263-71.
23. Primrose JN, Fox RP, Palmer DH, et al. Capecitabine compared with observation in resected biliary tract cancer (BILCAP): a randomised, controlled, multicentre, phase 3 study. *The lancet oncology* 2019; **20**(5): 663-73.
24. Banales JM, Marin JJG, Lamarca A, et al. Cholangiocarcinoma 2020: the next horizon in mechanisms and management. *Nature reviews Gastroenterology & hepatology* 2020.
25. Chen SH, Zhang BY, Zhou B, Zhu CZ, Sun LQ, Feng YJ. Perineural invasion of cancer: a complex crosstalk between cells and molecules in the perineural niche. *Am J Cancer Res* 2019; **9**(1): 1-21.
26. Preston M, Sherman LS. Neural stem cell niches: roles for the hyaluronan-based extracellular matrix. *Front Biosci (Schol Ed)* 2011; **3**: 1165-79.
27. Gritsenko PG, Ilina O, Friedl P. Interstitial guidance of cancer invasion. *The Journal of pathology* 2012; **226**(2): 185-99.
28. Godinho-Silva C, Cardoso F, Veiga-Fernandes H. Neuro-Immune Cell Units: A New Paradigm in Physiology. *Annu Rev Immunol* 2019; **37**: 19-46.
29. Liu HP, Tay SS, Leong S, Schemann M. Colocalization of ChAT, DbetaH and NADPH-d in the pancreatic neurons of the newborn guinea pig. *Cell and tissue research* 1998; **294**(2): 227-31.
30. Dang N, Meng X, Song H. Nicotinic acetylcholine receptors and cancer. *Biomedical reports* 2016; **4**(5): 515-8.
31. Sha M, Cao J, Sun HY, Tong Y, Xia Q. Neuroendocrine regulation of cholangiocarcinoma: A status quo review. *Biochim Biophys Acta Rev Cancer* 2019; **1872**(1): 66-73.
32. Franchitto A, Onori P, Renzi A, et al. Recent advances on the mechanisms regulating cholangiocyte proliferation and the significance of the neuroendocrine regulation of cholangiocyte pathophysiology. *Annals of translational medicine* 2013; **1**(3): 27.
33. Albo D, Akay CL, Marshall CL, et al. Neurogenesis in colorectal cancer is a marker of aggressive tumor behavior and poor outcomes. *Cancer* 2011; **117**(21): 4834-45.
34. Zhao CM, Hayakawa Y, Kodama Y, et al. Denervation suppresses gastric tumorigenesis. *Science translational medicine* 2014; **6**(250): 250ra115.

Chapter 4

Chapter 4

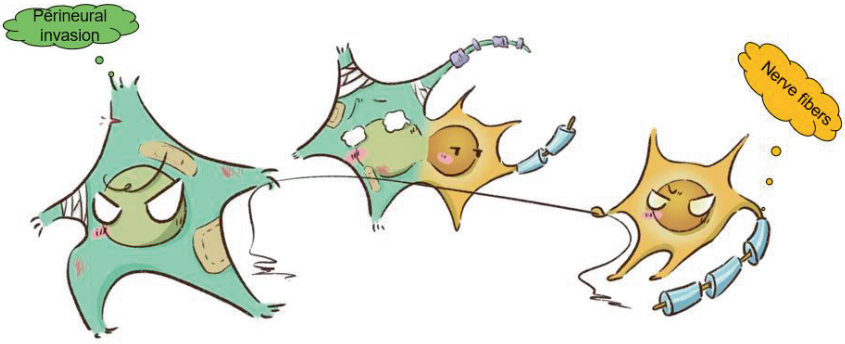

CHAPTER 5

The Presence of Small Nerve Fibers in the Tumor Microenvironment as Predictive Biomarker of Oncological Outcome Following Partial Hepatectomy for Intrahepatic Cholangiocarcinoma

Jan Bednarsch †, Xiuxiang Tan †, Zoltan Czigany, Dong Liu, Sven Arke Lang, Shivan Sivakumar,Jakob Nikolas Kather, Simone Appinger, Mika Rosin, Shiva Boroojerdi, Edgar Dahl, Nadine Therese Gaisa 6, Marcel den Dulk 7, Mariëlle Coolsen 7, Tom Florian Ulmer, Ulf Peter Neumann, and Lara Rosaline Heij

1st shared author

Cancers, 21 July 2021, 13(15):366

Chapter 5

Abstract: The oncological role of the density of nerve fibers (NFs) in the tumor microenvironment (TME) in intrahepatic cholangiocarcinoma (iCCA) remains to be determined. Therefore, data of 95 iCCA patients who underwent hepatectomy between 2010 and 2019 was analyzed regarding NFs and long-term outcome. Extensive group comparisons were carried out and the association of cancer-specific survival (CSS) and recurrence-free survival (RFS) with NFs were assessed using Cox regression models. Patients with iCCA and NFs showed a median CSS of 51 months (5-year-CSS = 47%) compared to 27 months (5-year-CSS = 21%) in patients without NFs (p = 0.043 log rank). Further, NFs (hazard ratio(HR) = 0.39, p = 0.002) and N-category (HR = 2.36, p = 0.010) were identified as independent predictors of CSS. Patients with NFs and without nodal metastases displayed a mean CSS of 89 months (5-year-CSS = 62%), while patients without NFs or with nodal metastases but not both showed a median CCS of 27 months (5-year-CSS = 25%) and patients with both positive lymph nodes and without NFs showed a median CCS of 10 months (5-year-CSS = 0%, p = 0.001 log rank). NFs in the TME are, therefore, a novel and important prognostic biomarker in iCCA patients. NFs alone and in combination with nodal status is suitable to identify iCCA patients at risk of poor oncological outcomes following curative-intent surgery.

Keywords: intrahepatic cholangiocarcinoma; nerve fibers; tumor microenvironment; oncological outcome; biomarker

---

Abbreviations

ALPPS	Associating Liver Partition and Portal Vein Ligation for Staged Hepatectomy
AUC	area under the curve
BILCAP	Capecitabine compared with observation in resected biliary tract cancer
CA	carbohydrate antigen
CCA	cholangiocarcinoma
CI	confidence interval
CSS	cancer-specific survival
CT	computed tomography
dCCA	distal CCA
FFPE	Formalin fixed paraffin embedded
FLR	future liver remnant
H&E	hematoxylin and eosin
HR	hazard ratio
iCCA	intrahepatic cholangiocarcinoma
MRI	magnetic resonance imaging
NFs	nerve fibers
pCCA	perihilar CCA
PDAC	pancreatic ductal adenocarcinoma
PNI	perineural invasion
PVE	portal vein embolization
PVE	portal vein embolization
RFS	recurrence-free survival
ROC	receiver operating characteristic
TME	tumor microenvironment

1. Introduction

Based on the anatomical localization of the primary tumor, cholangiocellular carcinomas (CCA) can be devided into intrahepatic CCA (iCCA), perihilar CCA (pCCA) and distal CCA (dCCA) [1]. Even though iCCA is the least common subtype of CCA, it still comprises about 15% of all primary liver tumors [2]. The ever-increasing global incidence of iCCA underlines

the oncological significance of this disease [3,4]. Although, in some cases, the etiology of CCA remains unclear, cholestatic conditions and diseases associated with chronic inflammation are considered to be the major traditional risk factors in the oncogenesis of CCA [5]. In iCCA patients in particular, etiological factors such as parenchymal disease related to hepatic cirrhosis, viral hepatitis or chronic alcohol consumption may play a pronounced role, illustrating distinct differences compared to the extrahepatic subtypes of CCA [5]. Irrespective of the CCA subentity, radical surgery with lymphadenectomy followed by adjuvant chemotherapy is considered as the current gold-standard approach as it provides improved long-term outcomes in comparison to merely medical or interventional treatment [6-8].

Radical resection of iCCA often requires extended liver resections as iCCA is often diagnosed in advanced disease stages. This may often result in increased perioperative morbidity and mortality [9]. Over the past decades, new surgical techniques have entered the clinical arena (e.g., Associating Liver Partition and Portal Vein Ligation for Staged Hepatectomy (ALPPS), preoperative portal vein embolization (PVE)), allowing surgery in patients even with a large tumor burden. Furthermore, as modern perioperative management facilitated surgery in elderly or patients with multiple comorbidities, more patients become candidates for radical surgical therapy [7,10,11]. Despite these advancements, the overall oncological prognosis in iCCA remains poor even after "curative-intent" surgery, with early tumor recurrence in many patients [10-13]. Identifying patients with particularly favorable oncological prognosis may allow individualized post-resection surveillance and therapy and is, therefore, of upmost clinical and scientific importance.

Our group has recently reported the significant prognostic value of nerve fibers (NFs) in the tumor microenvironment (TME) in a cohort pCCA patients [14] (Figure 1). CCAs often show perineural invasion (PNI), which can be recognized on routine H&E staining. Nevertheless, there is an important difference between traditional PNI and NFs concerning the size of the nerve fibers. The nerve fibers included in the NF count have a smaller diameter and are usually not visible on H&E routine staining and require additional immunohistochemical staining (Figure 2). Although NFs, as prognostic biomarkers, have also been investigated not just in pCCA but also in other malignancies, e.g., colorectal or gastric cancer and pancreatic ductal adenocarcinoma (PDAC) [15-18], their role in iCCA remains to be determined. Therefore, in the present study, we aimed to investigate NFs as a prognostic marker in a European cohort of iCCA patients undergoing curative-intent surgery.

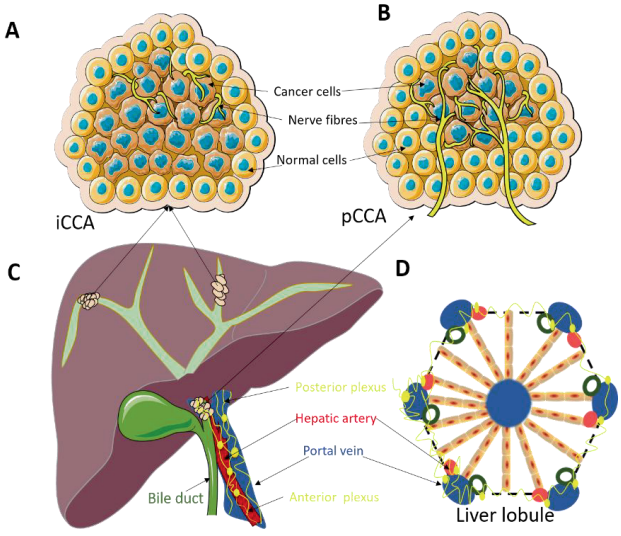

Figure 1. (**A**): Nerve fibers in the tumor microenvironment in intrahepatic cholangiocarcinoma (iCCA). The small nerve fibers are mainly distributed at the edge of the tumor. (**B**): Nerve fibers in the tumor microenvironment in perihilar cholangiocarcinoma (pCCA). The small nerve fibers are growing in between the tumor glands and not just at the edge of the tumor as in iCCA. (**C**): Localization of iCCA and pCCA tumors. ICCA is located centrally in the liver and usually presents with a big tumor mass. PCCA are located at the liver hilum and usually present as smaller tumors. (**D**): Architecture of the normal liver lobule. The normal innervation of the liver lobule can possibly explain the observation of the presence of the small nerve fibers at the edge of the tumor in iCCA and the pattern of mixed distribution of small nerve fibers in pCCA.

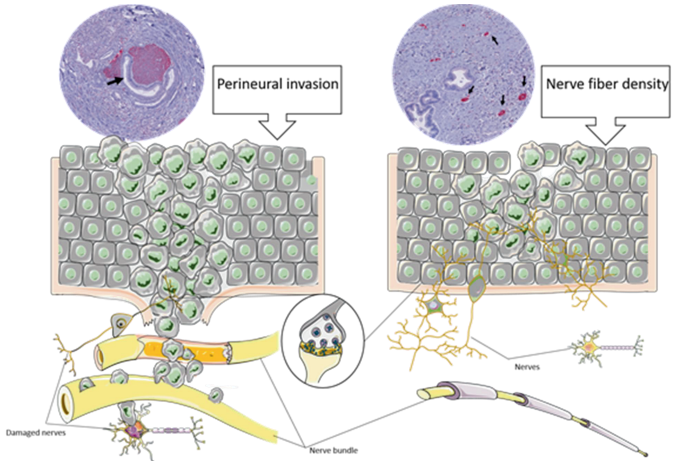

Figure 2. The difference between nerve fiber density and perineural invasion (PNI). (**A**): Graphical overview of perineural invasion. The cancer cells invade the endoneurial or epineurial sheeth of a larger nerve fiber. The immunohistochemical PGP9.5 staining illustrates the nerve fiber with cancer tissue around it. (**B**): Graphical overview of nerve fiber density. The small nerve fibers grow in the tumor microenvironment but are usually not invaded by cancer cells. The immunohistochemical PGP9.5 staining shows small positive (red) dots.

2. Materials and Methods

2.1. Patient Cohort

All consecutive patients scheduled for surgical resection for iCCA at the University Hospital RWTH Aachen (UH-RWTH) between 2010 and 2019 were considered for inclusion in this study. Out of the complete cohort of patients (n = 120), a subset of individuals (n = 24) were excluded (n = 10 cases of perioperative mortality; n = 14 with missing NF data). Subsequently, a final cohort of 96 patients was analyzed. The study was evaluated and approved by the Institutional Review Board of the Medical Faculty of the RWTH-Aachen University (EK 106/18) and conducted in accordance with the principles of the Declaration of Helsinki, and good clinical practice guidelines (ICH-GCP).

2.2. Oncological Staging and Surgical Technique

All patients included in this study underwent a detailed clinical work-up as previously described [7,15,16]. Briefly, resection planning was carried out, and the presence of distant metastases was ruled out using magnetic resonance imaging (MRI) and/or multiphase computed tomography imaging (CT). Further, the preoperative work-up comprised liver volumetry and portal vein embolization (PVE) in patients with insufficient future liver remnant (FLR) scheduled for right-sided hepatectomy. The indication for surgical resection as the primary treatment was based on the final clinical evaluation by one of the senior hepatobiliary staff surgeons and approved by the local multidisciplinary tumor board in all

cases. Surgery was carried out as previously described [7,13]. Depending on the local tumor extent, surgical procedures ranged from limited atypical resections to extended liver resections as well as vascular resections and reconstructions in cases with tumors extending to the liver hilum and ALPPS or PVE in individuals with insufficient FLR (Table 1). A systematic lymphadenectomy including the celiac, the posterior pancreaticoduodenal, the common hepatic, the periportal and pericholedochal lymph nodes was routinely carried out in all cases. All specimens were routinely evaluated by a trained pathologist.

Table 1. Patients' characteristics. Data presented as median and interquartile range if not noted otherwise. ALT, alanine aminotransferase; ASA, American society of anesthesiologists classification; AST, aspartate aminotransferase; BMI, body mass index; CSS, cancer-specific survival; GGT, gamma glutamyltransferase; INR, international normalized ratio; LVI, lympho-vascular invasion; MVI, microvascular invasion; NF, nerve fibers; PNI, perineural invasion, RFS, disease-free survival.

Demographics	Overall Cohort (*n* = 96)	NF Positive (*n* = 45)	NF Negative (*n* = 51)	*p* Value
Gender, m/f (%)	41 (43)/55 (57)	18 (40)/27 (60)	23 (45)/28 (55)	0.614
Age (years)	65 (58–73)	66 (60–75)	62 (56–72)	0.330
BMI (kg/m^2)	25 (22–29)	25 (22–29)	25 (23–29)	0.733
ASA, n (%)				0.230
I	3 (3)	1 (2)	2 (4)	
II	42 (44)	21 (47)	21 (41)	
III	48 (50)	20 (44)	28 (55)	
IV	3 (3)	3 (7)	0	
V	0	0	0	
Clinical chemistry				
Albumin (g/dL)	44 (41–46)	43 (40–46)	44 (41–46)	0.314
AST (U/L)	34 (26–47)	32 (24–44)	37 (29–53)	0.077
ALT (U/L)	29 (20–53)	25 (17–50)	31 (22–57)	0.169
GGT (U/L)	114 (65–304)	88 (65–501)	118 (62–265)	0.876
Total bilirubin (mg/dL)	0.5 (0.4–0.7)	0.5 (0.4–0.7)	0.6 (0.4–0.8)	0.117
Platelet count (/nL)	245 (197–307)	251 (194–303)	238 (198–315)	0.925
Alkaline Phosphatase (U/L)	117 (90–258)	108 (78–301)	125 (91–246)	0.628
Prothrombin time (%)	100 (95–109)	100 (96–111)	102 (94–108)	0.942
INR	0.98 (0.95–1.03)	0.97 (0.93–1.03)	0.99 (0.96–1.03)	0.386
Hemoglobin (g/dL)	13 (12–14)	13 (12–14)	13 (12–14)	0.248
Operative Data				
Operative time (minutes)	285 (221–345)	285 (227–338)	285 (212–345)	0.895
Operative procedure, *n* (%)				0.410
Monosegmentectomy/atypical	9 (9)	6 (13)	3 (6)	

Bisegmentectomy	7 (7)	4 (9)	3 (6)	
Right/left hepatectomy	31 (32)	17 (38)	14 (28)	
Ext. right/left hepatectomy	20 (21)	7 (16)	13 (26)	
Right/left trisectionectomy	13 (14)	4 (9)	9 (18)	
Others	16 (17)	7 (16)	9 (18)	
Intraoperative blood transfusion	0 (0–2)	0 (0–2)	0 (0–2)	0.750
Pathological examination				
R0 resection, *n* (%)	88 (93)	41 (93)	47 (92)	0.849
pT category, *n* (%)				0.400
1	38 (40)	23 (51)	15 (29)	
2	41 (42)	15 (34)	26 (51)	
3	12 (13)	5 (11)	7 (14)	
4	5 (5)	2 (4)	3 (6)	
pN category				0.854
N0	63 (70)	29 (69)	34 (71)	
N1	27 (30)	13 (31)	14 (29)	
Tumor grading, *n* (%)				0.114
G1	0	0	0	
G2	66 (76)	35 (83)	31 (69)	
G3	21 (24)	7 (17)	14 (31)	
G4	0	0	0	
MVI, *n* (%)	32 (35)	12 (28.6)	20 (40)	0.252
LVI, *n* (%)	17 (19)	7 (17)	10 (21)	0.618
PNI, *n* (%)	22 (46)	11 (58)	11 (38)	0.175
Postoperative Data				
Intensive care, days	1 (1–2)	1 (1–1)	1 (1–2)	0.114
Hospitalization, days	13 (8–24)	14 (8–26)	12 (8–22)	0.769
Postoperative complications, *n* (%)				0.898
No complications	36 (38)	15 (33)	21 (41)	
Clavien–Dindo I	2 (2)	1 (2)	1 (2)	
Clavien–Dindo II	24 (25)	13 (29)	11 (22)	
Clavien–Dindo IIIa	19 (20)	10 (22)	9 (18)	
Clavien–Dindo IIIb	9 (9)	4 (9)	5 (10)	
Clavien–Dindo IVa	6 (6)	2 (4)	4 (8)	

Clavien–Dindo IVb	0	0	0	
Clavien–Dindo V	0	0	0	
Oncologic Data				
Adjuvant therapy	30 (31)	10 (22)	20 (39)	0.073
Neoadjuvant therapy, *n* (%)	8 (8)	3 (7)	5 (10)	0.579
Median RFS, months (95% CI)	12 (8–16)	20 (0–41)	8 (5–11)	**0.006**
Median CSS, months (95% CI)	30 (23–37)	51 (12–90)	27 (19–35)	**0.043**

2.3. Adjuvant Therapy and Patient Follow-Up

Adjuvant therapy was advised by the multidisciplinary tumor board for patients diagnosed with high-risk characteristics (e.g., R1 resection or positive nodal status) from 2010 to 2017. From 2017 on, adjuvant therapy was recommended in every case in accordance with findings of the (Capecitabine compared with observation in resected biliary tract cancer) BILCAP trial [8]. Each patient underwent a regular follow-up by the referring oncologist or the local outpatient clinic including standard laboratory blood tests with tumor markers (carbohydrate antigen (CA) 19–9), clinical examinations and cross-sectional imaging. Additional diagnostics, e.g., imaging and/or biopsy, were performed if tumor recurrence was suspected, as described previously [14].

2.4. Assessment of Nerve Fibers

Formalin fixed paraffin embedded (FFPE) blocks were retrieved from the archive of the local institute of pathology and slides were cut to perform immunohistochemistry staining with the neuronal marker PGP9.5. For this, we used sections (2.5 µm) deparaffinized in xylene and rehydrated in graded alcohols. The tissue was heated in citrate buffer (Agilent, Santa Clara, CA, USA) (pH 6.0) at 95–100 °C for 5 min and colled down for 20 min. The immunostaining anti-rabbit PGP9.5 (Dako antibody 1:100, (Agilent, Santa Clara, CA, USA)) was incubated overnight at 4 °C. All slides contained tumor tissue and the peritumoral region and were scanned with a Ventana digital slide scanner (Roche, Rotkreuz, Switzerland). A single digital image was uploaded in Qupath 0.1.6 (Centre for Cancer Research & Cell Biology at Queen's University Belfast, United Kingdom). As previously described, nerve fiber count was analyzed by a trained pathologist who was blinded to the clinical outcomes of the individual patients. The presence of nerve fascicles at the invasive tumor margin with diameters of <100 µm was determined in 20 continuous visual fields at ×200 magnification by manual counting without the utilization of computer methods [14,17].

2.5. Statistical Analysis

The statistical endpoint of this study was cancer-specific survival (CSS), which was defined from the date of resection to the date of tumor-specific death. Deaths not associated with the tumor, e.g., cardiovascular events etc., were censored at the time of death. The secondary endpoint was recurrence-free survival (RFS), which was defined as the period from surgery to the date of first recurrence. Patients without tumor recurrence were censored at the time of death or at the last follow-up. Perioperative mortality was defined as in-hospital mortality. For NF categorization, a cut-off level was calculated by the receiver operating characteristic (ROC)-analysis of CCS with respect to NFs, as previously described [14,17]. Differences between the groups were evaluated by the Mann–Whitney-U-Test in case of continuous variables, while the chi-squared test, fisher's exact test or linear-by-linear association in accordance with scale and number count were used in case of categorical variables. The associations of CSS and RFS with clinico-pathological variables were determined using univariate and multivariable Cox regression analyses in a backward selection model. Survival curves were generated by the Kaplan–Meier method and

compared with the log-rank test. Median follow up was calculated with the reverse Kaplan–Meier method. p-values were given for two-sided testing and the level of significance was set to $p < 0.05$. All analyses were performed using SPSS Statistics 24 (IBM Corp., Armonk, NY, USA)).

3. Results

3.1. Patient Cohort

The patient cohort consisted of 55 women (57%) and 41 men (43%) with a median age of 65 years and the majority being assessed as ASA (American Society of Anesthesiologists classification) III or higher (53%, 51/96). Neoadjuvant therapy was applied in a small number of patients (8%, 8/96). Most of the patients underwent major liver surgery (66%, 64/96) to achieve R0 resections. Accordingly, an R0 status was observed in 93% (88/96) of the cohort. Further, nodal metastases were present in 30% of the patients (27/90). Major complications, as defined by Clavien–Dindo ≥ IIIa, were observed in 35% (34/96) of the cases. Patients displaying perioperative mortality were excluded from the analysis, as stated above. Further general demographic and clinico-pathological characteristics of the study cohort are presented in Table 1.

3.2. Group Categorization and Comparative Analysis with Respect to Nerve Fiber Density

A ROC analysis evaluating the total number of NFs (median number NFs in the cohort: 0 (range: 0–35)) for patients who survived at least 3 years versus patients who died during follow up was conducted. The corresponding area under the curve (AUC) was 0.618 (95% confidence interval (CI): 0.502–0.775). A cut-off value for NFs was determined with respect to optimized accuracy and equal weight for sensitivity and specificity errors (0 NF and ≥1 NF). Using the established cut-off value, the median CSS was 51 months in patients with NFs and 27 months in patients without NFs ($p = 0.043$ log rank).

A comparative group analysis regarding NFs was further carried out between patients with NFs ($n = 45$) and without NFs ($n = 51$). Here, no clinical differences were observed. Of note, no statistical differences in pathological characteristics, e.g., pT category ($p = 0.400$), pN category ($p = 0.854$), tumor grading ($p = 0.114$), lymphovascular invasion (LVI, $p = 0.618$), microvascular invasion (MVI, $p = 0.252$) and PNI ($p = 0.175$), were detected between the groups. However, the median CSS (51 months (95% CI: 12–90) vs. 27 months (95% CI: 19–35), $p = 0.043$ log rank) and the median RFS (20 months (95% CI: 0–41) vs. 8 months (95% CI: 5–11), $p = 0.043$ log rank) were significantly longer in patients with NFs compared to patients without NFs. A detailed overview of the cohort and both subgroups is outlined in Table 1.

3.3. Cox Regression Analysis

To investigate predictors of CSS and RFS in the overall cohort, univariate and multivariable Cox regressions were carried out. Here, in univariate analysis, postoperative complications ($p = 0.007$), N-category ($p = 0.001$), tumor grading ($p = 0.014$), LVI ($p = 0.001$), PNI ($p = 0.011$) and NFs ($p = 0.048$) were significantly associated with CSS. All variables showing p-value <0.10 were included in a multivariable Cox regression model. Here, preoperative hemoglobin (hazard ratio (HR)= 0.51, $p = 0.024$), N-category (HR = 4.78, $p = 0.001$), NFs (HR = 0.47, $p = 0.024$) and neoadjuvant therapy (HR = 8.84, $p = 0.002$) were identified as independent predictors of CSS (Table 2).

In univariate analysis, postoperative complications ($p = 0.028$), intraoperative blood transfusions ($p = 0.034$), duration of hospitalization ($p = 0.031$), N-category ($p = 0.001$), microvascular invasion (MVI, $p = 0.012$), LVI ($p = 0.013$) and NFs ($p = 0.009$) showed significant associations with RFS. In the following multivariable Cox regression model, duration of hospitalization (HR = 1.78, $p = 0.049$), N-category (HR = 2.36, $p = 0.010$) and NFs (HR = 0.39, $p = 0.002$) were identified as independent predictors of RFS (Table 3).

Table 2. Univariate and multivariable analysis of cancer-specific survival in intrahepatic cholangiocarcinoma. Various parameters are associated with cancer-specific survival. ALT, alanine aminotransferase; ASA, American society of anesthesiologists classification; AST, aspartate

aminotransferase; BMI, body mass index; GGT, gamma glutamyltransferase; INR, international normalized ratio; LVI, lympho-vascular invasion; MVI, microvascular invasion; NF, nerve fibers; PNI, perineural invasion.

	Univariate Analysis		Multivariable Analysis	
	HR (95% CI)	***p* Value**	**HR (95% CI)**	***p* Value**
Demographics				
Sex (male = 1)	0.76 (0.45–1.27)	0.297		
Age (≤65 years = 1)	1.30 (0.77–2.15)	0.330		
BMI (≤25 kg/m^2 = 1)	1.17 (0.67–1.96)	0.549		
ASA (I/II = 1)	1.31 (0.79–2.19)	0.299		
Clinical chemistry				
Albumin (≤45 g/L = 1)	0.86 (0.52–1.43)	0.560		
AST (≤35 U/L = 1)	1.15 (0.69–1.93)	0.588		
ALT (≤30 U/L = 1)	1.38 (0.82–2.35)	0.228		
GGT (≤120 U/L = 1)	1.39 (0.83–2.34)	0.214		
Bilirubin (≤0.5 mg/dL = 1)	1.53 (0.91–2.57)	0.105		
Alkaline phosphatase (≤115 U/L = 1)	1.69 (0.99–2.89)	0.054	excluded	
Platelet count (≤250/nL = 1)	0.82 (0.49–1.37)	0.445		
INR (≤1 = 1)	1.54 (0.91–2.61)	0.107		
Hemoglobin (≤13 g/dL = 1)	0.61 (0.37–1.03)	0.063	0.51 (0.27–0.93)	**0.024**
Operative data				
Operative time (≤300 min = 1)	1.11 (0.68–1.80)	0.682		
Type of hepatectomy		0.935		
Right/left hepatectomy	1			
Others	0.92 (0.541–1.62)			
Blood transfusion (no = 1)	1.52 (0.91–2.57)	0.113		
Postoperative data				
Clavien–Dindo Score (CD I/II = 1)	2.05 (1.22–3.47)	**0.007**	exlcuded	
Intensive care (≤1 day = 1)	1.49 (0.85–2.62)	0.168		
Hospitalization (≤13 days = 1)	1.52 (0.91–2.54)	0.106		
Pathological data				
R1 resection (no = 1)	1.58 (0.63–3.96)	0.329		
pT category (T1/T2 = 1)	1.49 (0.81–2.77)	0.203		
pN category (N0 = 1)	4.32 (2.48–7.52)	**0.001**	4.78 (2.54–9.01)	**0.001**
Tumor grading (G1/G2 = 1)	2.13 (1.16–3.89)	**0.014**	excluded	
MVI (no = 1)	1.59 (0.95–2.68)	0.078	excluded	
LVI (no = 1)	3.60 (1.92–6.76)	**0.001**	excluded	
PNI (no = 1)	2.49 (1.23–5.01)	0.**011**		
NF (no = 1)	0.58 (0.34–0.99)	**0.048**	0.47 (0.24–0.90)	**0.024**
Oncological data				
Neoadjuvant therapy (no = 1)	2.18 (0.87–5.50)	0.098	8.84 (2.20–35.49)	**0.002**
Adjuvant therapy (no = 1)	1.17 (0.67–2.04)	0.587		

Table 3. Univariate and multivariable analysis of recurrence-free survival in intrahepatic cholangiocarcinoma. Various parameters are associated with recurrence-free survival. ALT, alanine aminotransferase; ASA, American society of anesthesiologists classification; AST, aspartate aminotransferase; BMI, body mass index; GGT, gamma glutamyltransferase; INR, international normalized ratio; LVI, lympho-vascular invasion; MVI, microvascular invasion; NF, nerve fibers; PNI, perineural invasion.

	Univariate Analysis		Multivariable Analysis	
	HR (95% CI)	***p* Value**	**HR (95% CI)**	***p* Value**
Demographics				
Sex (male = 1)	1.00 (0.60–1.66)	0.993		
Age (≤65 years = 1)	0.92 (0.56–1.52)	0.755		

BMI (≤25 kg/m^2 = 1)	0.84 (0.51–1.38)	0.486		
ASA (I/II = 1)	1.25 (0.76–2.05)	0.383		
Clinical chemistry				
Albumin (≤45 g/L = 1)	0.96 (0.59–1.58)	0.872		
AST (≤35 U/L = 1)	0.97 (0.59–1.60)	0.916		
ALT (≤30 U/L = 1)	1.34 (0.81–2.24)	0.258		
GGT (≤120 U/L = 1)	1.47 (0.89–2.45)	0.137		
Bilirubin (≤0.5 mg/dL = 1)	1.31 (0.79–2.17)	0.302		
Alkaline phosphatase (≤115 U/L = 1)				
Platelet count (≤250/nL = 1)	0.79 (0.48–1.32)	0.373		
INR (≤1 = 1)	1.56 (0.92–2.65)	0.099	excluded	
Hemoglobin (≤13 g/dL = 1)	0.67 (0.40–1.10)	0.112		
Operative data				
Operative time (≤300 min = 1)	1.05 (0.64–1.74)	0.837		
Type of hepatectomy		0.538		
Right/left hepatectomy	1			
Others	1.18 (0.68–2.03)			
Blood transfusion (no = 1)	1.74 (1.04–2.90)	**0.034**	excluded	
Postoperative data				
Clavien–Dindo Score (CD I/II = 1)	1.78 (1.06–2.99)	**0.028**	excluded	
Intensive care (≤1 day = 1)	1.27 (0.73–2.21)	0.410		
Hospitalization (≤13 days = 1)	1.73 (1.05–2.85)	**0.031**	1.78 (1.00–3.15)	**0.049**
Pathological data				
R1 resection (no = 1)	1.62 (0.64–4.07)	**0.**310		
pT category (T1/T2 = 1)	0.98 (0.48–1.98)	0.943		
pN category (N0 = 1)	2.84 (1.61–5.03)	**0.001**	2.36 (1.23–4.52)	**0.010**
Tumor grading (G1/G2 = 1)	1.32 (0.71–2.47)	0.386		
MVI (no = 1)	1.93 (1.15–3.21)	**0.012**	excluded	
LVI (no = 1)	2.22 (1.19–4.17)	**0.013**	excluded	
PNI (no = 1)	1.38 (0.69–2.87)	0.382		
NF (no = 1)	1.98 (1.19–3.31)	**0.009**	0.39 (0.21–0.71)	**0.002**
Oncological data				
Neoadjuvant therapy (no = 1)	1.96 (0.84–4.60)	0.121		
Adjuvant therapy (no = 1)	1.15 (0.68–1.95)	0.597		

3.4. Suvival Analysis

After a median follow-up of 67 months, the median CSS of the whole cohort was 30 months (95% CI: 23–37), the median OS 28 months (95% CI: 20–36) and the median RFS 12 months (95% CI: 8–16, Figure 3A,B). A Kaplan–Meier analysis with respect to NFs showed a median CSS of 51 months (95% CI: 48–132, 3-year-CSS = 54%, 5-year-CSS = 47%) in patients with NFs compared to 27 months (95% CI: 19–47, 3-year-CSS = 35%, 5-year-CSS = 21%) in patients without NFs (p = 0.043 log rank, Figure 3C). Further, RFS was significantly lower in patients without NFs (8 months (95% CI: 5–11)) compared to patients with NFs (20 months (95% CI: 0–41), p = 0.006 log rank, Figure 3D). As both NF and N-category were independent predictors of CCS in the multivariable Cox regressions, a combined Kaplan–Meier analysis was conducted and showed a mean CSS of 89 months (95% CI: 65–111, 3-year-CSS = 73%, 5-year-CSS = 62%) in patients with NFs and negative lymph nodes, a median CCS of 27 months (95% CI: 17–37, 3-year-CSS = 36%, 5-year-CSS = 25%) in patients with either positive lymph nodes or no NFs but not both, and 10 months (95% CI: 6–14, 3-year-CSS = 0%, 5-year-CSS = 0%) in patients with both positive lymph nodes and no NFs (p = 0.001 log rank, Figure 3E). Accordingly, the median RFS was 36 months (95% CI: 24–48) in patients with NFs and negative lymph nodes, 10 months (95% CI: 6–15) in patients with either positive lymph nodes or no NFs but not both, and 5 months (95% CI: 3–6) in patients with both positive lymph nodes and no NFs (p = 0.001 log rank, Figure 3F).

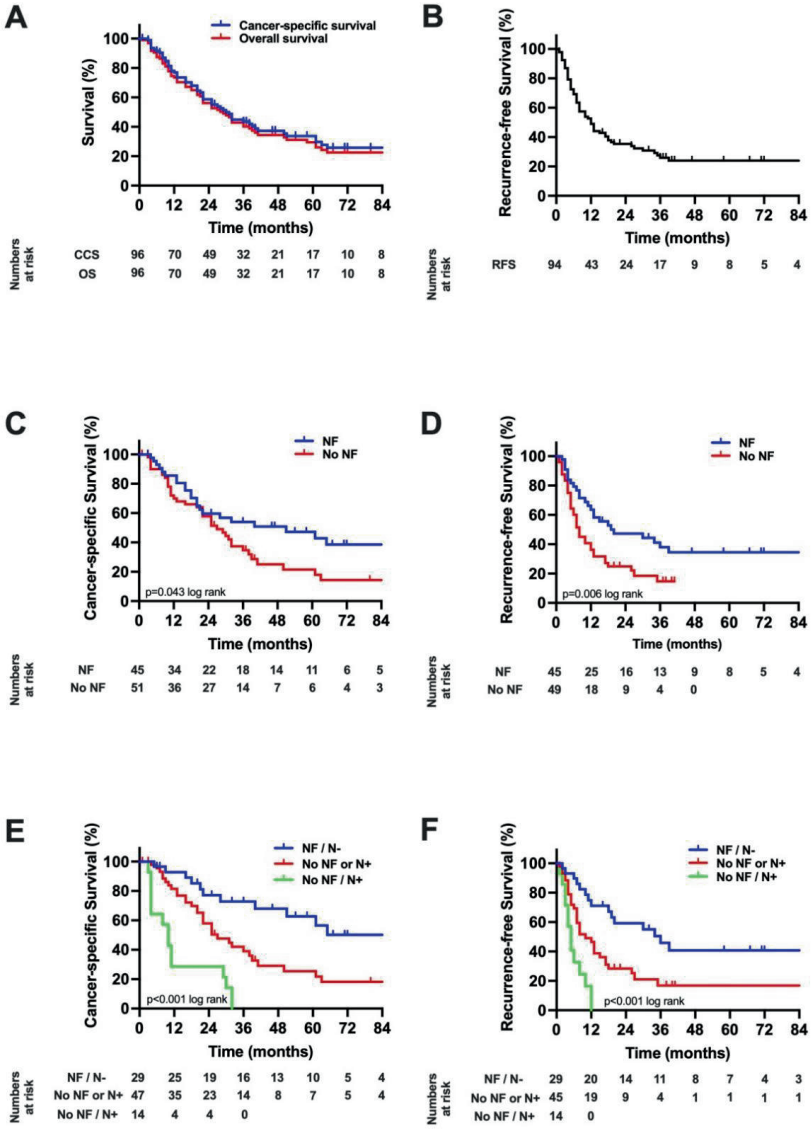

Figure 3. Oncological survival in intrahepatic cholangiocarcinoma (**A**): Cancer-specific and overall survival. The median CSS was 30 months and the median OS 28 months, respectively. (**B**): Recurrence-free survival. The median RFS was 12 months. (**C**): Cancer-specific survival stratified by nerve fibers. The median CSS was 51 months in patients with NF compared to 27 months (p = 0.043 log rank). (**D**): Recurrence-free survival stratified by nerve fibers. The median RFS was 20 months in patients with NF compared to 8 months in patients without NF (p = 0.006 log rank). (**E**): Cancer-specific survival stratified by nerve fibers and pN category. The mean CSS was 89 months in patients with NF and negative lymph nodes, while the median CCS was 27 months (95% CI: 38–64) in patients with either positive lymph nodes or without NF but not both, and 10 months in patients with both positive lymph nodes and low NF (p = 0.001 log rank). (**F**): Recurrence-free survival stratified by nerve fibers and pN category. The median RFS was 36 months in patients with NF and negative lymph nodes, 10 months (95% CI: 8–82) in patients with either positive lymph nodes or no NF but not both, and 5 months in patients with both positive lymph

nodes and no NF (p = 0.001 log rank). CI, confidence interval; CSS, cancer-specific survival; RFS, recurrence-free survival; OS, overall survival.

3.5. Histological Characteristics

Scanned images of the H&E and PGP9.5 were descriptively analyzed. The region marked as tumor on the H&E staining was identified on the PGP immunostaining as well. Nerve fibers in the TME were observed and counted according to the previously described method. We observed that the small nerve fibers were mainly located at the periphery of the tumor and not in the center (Figure 4).

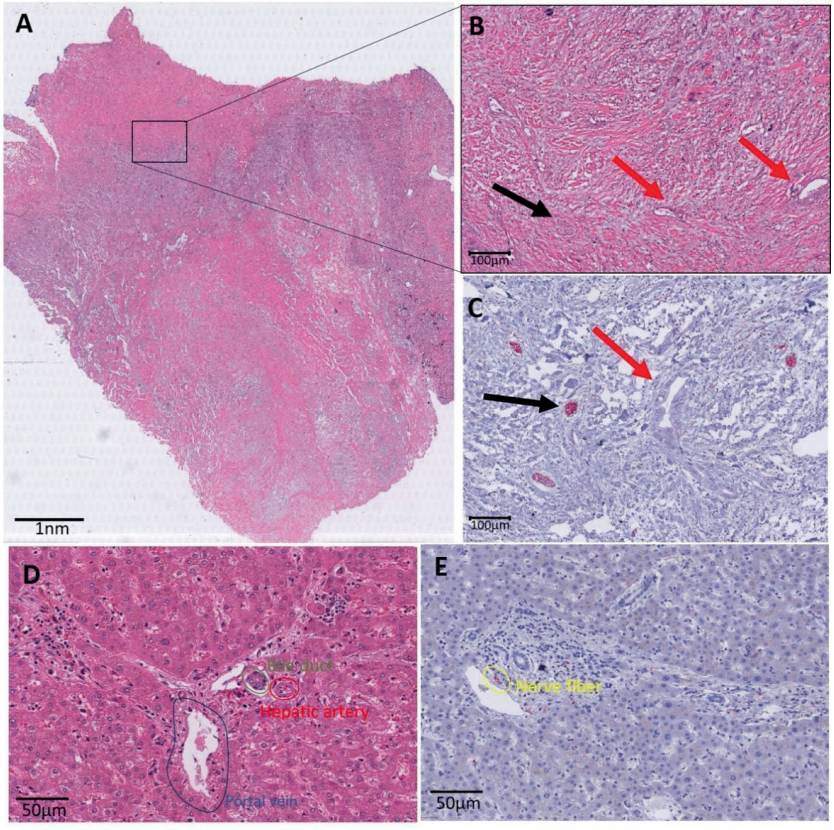

Figure 4. Histology overview of iCCA. (**A**): Whole slide H&E image of an iCCA. At the edge of the slide, normal liver parenchyma is displayed. More centrally, a lesion is shown with a rim of vital tumor cells, and centrally, a pale area corresponding with necrosis. (**B**): Zoomed in image of the black marked box in A. This H&E image shows small tumor glands in abundant stroma marked with red arrows. The black arrow points to a nerve fiber, which is not easily visible on this HE staining. (**C**): Black box area in the immunohistochemical PGP9.5 staining. This staining makes it easier to recognize the small nerve fibers (red in the PGP9.5 immunohistochemistry and marked with a black arrow). The red arrow is pointed at the tumor. (**D**): Zoomed in image of a portal tract. The portal tract illustrates the bile duct (marked in green), the hepatic artery (marked in red) and the portal vein (marked in blue). (**E**): Zoomed in image of a portal tract with PGP9.5 staining. In this zoomed in image, the small nerve fiber is nicely illustrated in red (positive immunohistochemical staining) and marked in yellow.

4. Discussion

ICCA is commonly diagnosed in advanced disease stages and associated with dismal oncological survival [1]. Despite recent advances in diagnosis, operative and systemic therapy, the 5-year-survival has not substantially improved and rarely reaches over 20%, with high

rates of tumor recurrence being the main reason for these discouraging results [1,21,22]. Based on this, the identification of novel prognostic (bio)markers may provide insight into the underlying tumor biology of the disease and has the potential to further improve individualized medical management of these complex patients [13]. In this translational retrospective study, we identified NFs as a powerful novel prognostic biomarker for long-term oncological outcome in iCCA patients. Further, we could also demonstrate that the combination of NFs and traditional nodal status shows an excellent ability to stratify these patients regarding the overall prognosis after curative-intent liver resection.

NFs are believed to play an essential role in the crosstalk between tumor cells and other components of the TME such as immune cells or cancer-associated fibroblasts (CAF) [19-22]. This inter-cellular cross talk is partly based on neurotransmitters from NFs interacting with tumor cells, or ones that are released from cancer cells binding to receptors located on NFs [23-26].

From a clinical-oncological point of view, our results are in line with previous findings. The analyzed cohort of iCCA patients showed a 5-year-CCS of 34% and 5-year-OS of 29%. In a systematic review of 57 studies including more than 4500 patients undergoing liver resection for iCCA, 5-year-OS ranged from 5% to 56% depending on the frequency of typical risk factors, e.g., age, pathological characteristics or lymph node metastases [27]. In our cohort, absence of NFs, nodal metastases, low preoperative hemoglobin and neoadjuvant therapy were independent predictors of inferior CCS. In fact, neoadjuvant therapy (HR = 8.84) had the most pronounced impact on survival followed by lymph node metastases (HR = 4.78) and NFs (HR = 0.47). The role of neoadjuvant therapy in iCCA is a matter of an ongoing debate and its role remains to be defined. In a large multicentric analysis, no difference in oncological survival between patients undergoing upfront surgery versus patients who underwent preoperative chemotherapy was observed; however, patients scheduled for neoadjuvant therapy displayed significantly more advanced tumors in this study [28]. This reflects common international standards and also the clinical routine in our center proceeding with upfront surgery in patients with resectable disease [1,29]. Neoadjuvant therapy in our study cohort was, therefore, applied to a small subset of patients (n = 8) presenting with a large tumor mass and/or major vascular involvement. The biased selection of this high-risk subgroup of patients does certainly explain the high hazard ratio in our analysis.

The presence of NFs, in particular, resulted in a prominent division of our cohort according to long-term outcome, with a median CCS of 51 months (5-year-CSS = 47%) in patients with NFs in the TME and a median CCS of 27 months (5-year-CSS = 21%) in patients without NFs in the TME, indicating an important predictive value of this histological marker. This large difference in survival can be attributed to the good predictive value of NFs in terms of tumor recurrence. Here, the absence of NFs among lymph node metastases and long duration of hospitalization were associated with inferior RFS. The median RFS was 20 months (3-year-RFS 38%) in patients with NFs and 8 months (3-year-RFS 15%) in patients without NFs. This well-illustrates that tumor recurrence remains the major problem in iCCA patients. Repeated liver resections which provide appropriate long-term outcome are unfortunately only applicable for the minority of patients experiencing tumor recurrence [30,31]. Most patients still undergo systemic therapy, which is characterized by limited response and resistance to chemotherapy, thus resulting in early disease progression [6].

The prognostic role of nodal status in iCCA is abundantly discussed elsewhere [15,48,49]. As nodal status was not associated with the presence of NFs in the TME in our group comparison (Table 1) and both variables showed significant risks in our multivariable Cox regression models for RFS and CCS, we created subgroups based on NFs and the N status to stratify patients regarding long-term outcome. Here, patients with low oncological risk (presence of NFs and negative lymph nodes) displayed a compelling outcome with a 5-year-CCS of 62%, while patients with medium risk (absence of NFs or positive lymph nodes but not both) showed an "average" outcome with a 5-year-CCS of 25%, followed by patients with high risk (absence of NFs and positive lymph nodes) yielding a dismal long-term outcome with a 3-year-CCS of 0%. This observation is novel and interesting with a potential impact

on the clinical management of these patients. Surgical resection in patients with positive lymph nodes alone is usually associated with inferior outcome and the survival benefit appears marginally to systemic therapy alone in some previous reports [32,33]. Therefore, some authors suggest a very critical approach to surgery in iCCA with nodal metastases [1]. Our department strategy comprises a radical approach to iCCA that does not deny patients the possibility of radical surgery even in cases where lymph node positivity is confirmed in intraoperative frozen sections [7,13]. However, it has to be acknowledged that our high-risk subgroup (absence of NFs and positive lymph nodes) showed a median CCS of 10 months, which is indeed inferior to the results of systemic therapy, as shown in the ABC-02 trial evaluating Gemcitabine and Cisplatin in the palliative setting displaying a median OS of 12 months [6]. As iCCA does usually present with a notable tumor mass at the time of diagnosis, tissue for preoperative histological analysis is more easily obtainable by biopsy compared to pCCA [14]. If the absence NFs is, therefore, known preoperatively and other oncological risk factors are present in the individual patient, e.g., positive lymph nodes determined by preoperative endoscopic ultrasound-guided fine-needle biopsy, staging laparoscopy or by intraoperative frozen sections, liver resection should be carefully evaluated in these patients as the oncological benefit might not justify the perioperative risks of surgery. This statement represents one of the most important clinical messages of this study.

As with other retrospective translational studies, our analysis has some potential limitations. First, all patients of this study underwent surgery in a single center in accordance with the authors' individual approach to iCCA, and all clinical data were obtained in a retrospective fashion. Second, the retrospective nature of our study resulted in some missing data, which would have been interesting to report in the context of the oncological analysis, e.g., CA19-9. Third, the limited sample size did not allow the division of the cohort into a training and validation set, which would have strengthened our statistical analysis. Further, our data and the resulting observations would certainly require confirmation within a large independent and, optimally, multi-center dataset to reduce the risk of bias, and no amount of reanalysis of the current cohort can eliminate this need. Fourth, it is not possible to deeply investigate the associations of NFs with tumor characteristics using our data. Such investigations focusing on the underlying pathophysiological mechanisms may include extensive radiologic and biological data (e.g., tumor genetics) which were not available for this study but should be the topic of further investigations.

5. Conclusions

Notwithstanding the above-mentioned limitations, we have identified NFs as a novel and important prognostic biomarker in iCCA patients. The presence of NFs alone and in combination with nodal status allow for stratification of iCCA patients in terms of oncological outcome after curative-intent surgery. These findings have the potential to be clinically implemented since the NF count requires only one simple immunohistochemical staining and the nodal status is a routine characteristic in the pathology report. Larger, multi-center studies are needed to confirm and validate our findings.

Author Contributions: Conceptualization, J.B. and L.R.H.; methodology, J.B., U.P.N. and L.R.H.; formal analysis, J.B., X.T., Z.C., D.L., S.A.L., S.S., J.N.K., M.d.D., M.C., T.F.U. and L.R.H.; investigation, J.B., X.T., S.A., M.R., S.B., E.D., N.T.G. and L.R.H.; resources, E.D. and U.P.N.; data curation, J.B., Z.C., M.d.D., M.C. and T.F.U.; writing—original draft preparation, J.B., X.T. and L.R.H.; writing—review and editing, J.B., X.T., Z.C., D.L., S.A.L., S.S., J.N.K., S.A., M.R., S.B., E.D., N.T.G., M.d.D., M.C., T.F.U. and U.P.N.; supervision, U.P.N. and L.R.H.; project administration, U.P.N. and L.R.H. All authors have read and agreed to the published version of the manuscript.

Funding: This particular research received no external funding. X.T. received a scholarship from the China Scholarship Council (CSC Grant No. 201806210074).

Institutional Review Board Statement: The study was conducted according to the guidelines of the Declaration of Helsinki, and approved by the Institutional Review Board of RWTH Aachen University (protocol code: EK 106/18; date of approval: 22 November 2019).

Informed Consent Statement: Informed consent was obtained from all subjects involved in the study.

Data Availability Statement: The data presented in this study are available on request from the corresponding author.

Conflicts of Interest: The authors declare no conflict of interest.

Reference

1. Banales JM, Marin JJG, Lamarca A, et al. Cholangiocarcinoma 2020: the next horizon in mechanisms and management. *Nature reviews Gastroenterology & hepatology* 2020; **17**(9): 557-88.
2. Banales JM, Cardinale V, Carpino G, et al. Expert consensus document: Cholangiocarcinoma: current knowledge and future perspectives consensus statement from the European Network for the Study of Cholangiocarcinoma (ENS-CCA). *Nature reviews Gastroenterology & hepatology* 2016; **13**(5): 261-80.
3. Khan SA, Tavolari S, Brandi G. Cholangiocarcinoma: Epidemiology and risk factors. *Liver international : official journal of the International Association for the Study of the Liver* 2019; **39 Suppl 1**: 19-31.
4. Rizvi S, Khan SA, Hallemeier CL, Kelley RK, Gores GJ. Cholangiocarcinoma - evolving concepts and therapeutic strategies. *Nature reviews Clinical oncology* 2018; **15**(2): 95-111.
5. Clements O, Eliahoo J, Kim JU, Taylor-Robinson SD, Khan SA. Risk factors for intrahepatic and extrahepatic cholangiocarcinoma: A systematic review and meta-analysis. *Journal of hepatology* 2020; **72**(1): 95-103.
6. Valle J, Wasan H, Palmer DH, et al. Cisplatin plus gemcitabine versus gemcitabine for biliary tract cancer. *The New England journal of medicine* 2010; **362**(14): 1273-81.
7. Bednarsch J, Czigany Z, Lurje I, et al. The role of ALPPS in intrahepatic cholangiocarcinoma. *Langenbeck's archives of surgery / Deutsche Gesellschaft fur Chirurgie* 2019; **404**(7): 885-94.
8. Primrose JN, Fox RP, Palmer DH, et al. Capecitabine compared with observation in resected biliary tract cancer (BILCAP): a randomised, controlled, multicentre, phase 3 study. *The lancet oncology* 2019; **20**(5): 663-73.
9. Palen A, Garnier J, Hobeika C, et al. Oncological relevance of major hepatectomy with inferior vena cava resection for intrahepatic cholangiocarcinoma. *HPB : the official journal of the International Hepato Pancreato Biliary Association* 2021.
10. Reames BN, Ejaz A, Koerkamp BG, et al. Impact of major vascular resection on outcomes and survival in patients with intrahepatic cholangiocarcinoma: A multi-institutional analysis. *Journal of surgical oncology* 2017; **116**(2): 133-9.
11. Bagante F, Spolverato G, Weiss M, et al. Defining Long-Term Survivors Following Resection of Intrahepatic Cholangiocarcinoma. *Journal of gastrointestinal surgery : official journal of the Society for Surgery of the Alimentary Tract* 2017; **21**(11): 1888-97.
12. Si A, Li J, Xiang H, et al. Actual over 10-year survival after liver resection for patients with intrahepatic cholangiocarcinoma. *Oncotarget* 2017; **8**(27): 44521-32.
13. Lurje G, Bednarsch J, Czigany Z, et al. The prognostic role of lymphovascular invasion and lymph node metastasis in perihilar and intrahepatic cholangiocarcinoma. *European journal of surgical oncology : the journal of the European Society of Surgical Oncology and the British Association of Surgical Oncology* 2019; **45**(8): 1468-78.
14. Bednarsch J, Kather J, Tan X, et al. Nerve Fibers in the Tumor Microenvironment as a Novel Biomarker for Oncological Outcome in Patients Undergoing Surgery for Perihilar Cholangiocarcinoma. *Liver Cancer* 2021.
15. Albo D, Akay CL, Marshall CL, et al. Neurogenesis in colorectal cancer is a marker of aggressive tumor behavior and poor outcomes. *Cancer* 2011; **117**(21): 4834-45.
16. Zhao CM, Hayakawa Y, Kodama Y, et al. Denervation suppresses gastric tumorigenesis. *Science translational medicine* 2014; **6**(250): 250ra115.
17. Iwasaki T, Hiraoka N, Ino Y, et al. Reduction of intrapancreatic neural density in cancer tissue predicts poorer outcome in pancreatic ductal carcinoma. *Cancer science* 2019; **110**(4): 1491-502.
18. Heij LR, Tan X, Kather JN, et al. Nerve Fibers in the Tumor Microenvironment Are Co-Localized with Lymphoid Aggregates in Pancreatic Cancer. *Journal of clinical medicine* 2021; **10**(3): 490.
19. Preston M, Sherman LS. Neural stem cell niches: roles for the hyaluronan-based extracellular matrix. *Front Biosci (Schol Ed)* 2011; **3**: 1165-79.

20. Gritsenko PG, Ilina O, Friedl P. Interstitial guidance of cancer invasion. *The Journal of pathology* 2012; **226**(2): 185-99.
21. Godinho-Silva C, Cardoso F, Veiga-Fernandes H. Neuro-Immune Cell Units: A New Paradigm in Physiology. *Annu Rev Immunol* 2019; **37**: 19-46.
22. Tan X, Sivakumar S, Bednarsch J, et al. Nerve fibers in the tumor microenvironment in neurotropic cancer-pancreatic cancer and cholangiocarcinoma. *Oncogene* 2020.
23. Liu HP, Tay SS, Leong S, Schemann M. Colocalization of ChAT, DbetaH and NADPH-d in the pancreatic neurons of the newborn guinea pig. *Cell and tissue research* 1998; **294**(2): 227-31.
24. Dang N, Meng X, Song H. Nicotinic acetylcholine receptors and cancer. *Biomedical reports* 2016; **4**(5): 515-8.
25. Sha M, Cao J, Sun HY, Tong Y, Xia Q. Neuroendocrine regulation of cholangiocarcinoma: A status quo review. *Biochim Biophys Acta Rev Cancer* 2019; **1872**(1): 66-73.
26. Franchitto A, Onori P, Renzi A, et al. Recent advances on the mechanisms regulating cholangiocyte proliferation and the significance of the neuroendocrine regulation of cholangiocyte pathophysiology. *Annals of translational medicine* 2013; **1**(3): 27.
27. Mavros MN, Economopoulos KP, Alexiou VG, Pawlik TM. Treatment and Prognosis for Patients With Intrahepatic Cholangiocarcinoma: Systematic Review and Meta-analysis. *JAMA surgery* 2014; **149**(6): 565-74.
28. Buettner S, Koerkamp BG, Ejaz A, et al. The effect of preoperative chemotherapy treatment in surgically treated intrahepatic cholangiocarcinoma patients-A multi-institutional analysis. *Journal of surgical oncology* 2017; **115**(3): 312-8.
29. Bednarsch J, Czigany Z, Heij LR, et al. Compelling Long-Term Results for Liver Resection in Early Cholangiocarcinoma. *Journal of clinical medicine* 2021; **10**(13).
30. Nickkholgh A, Ghamarnejad O, Khajeh E, et al. Outcome after liver resection for primary and recurrent intrahepatic cholangiocarcinoma. *BJS Open* 2019; **3**(6): 793-801.
31. Hyder O, Hatzaras I, Sotiropoulos GC, et al. Recurrence after operative management of intrahepatic cholangiocarcinoma. *Surgery* 2013; **153**(6): 811-8.
32. Groot Koerkamp B, Wiggers JK, Allen PJ, et al. American Joint Committee on Cancer staging for resected perihilar cholangiocarcinoma: a comparison of the 6th and 7th editions. *HPB : the official journal of the International Hepato Pancreato Biliary Association* 2014; **16**(12): 1074-82.
33. Kizy S, Altman AM, Marmor S, et al. Surgical resection of lymph node positive intrahepatic cholangiocarcinoma may not improve survival. *HPB : the official journal of the International Hepato Pancreato Biliary Association* 2019; **21**(2): 235-41.

Chapter 5

Chapter 5

5

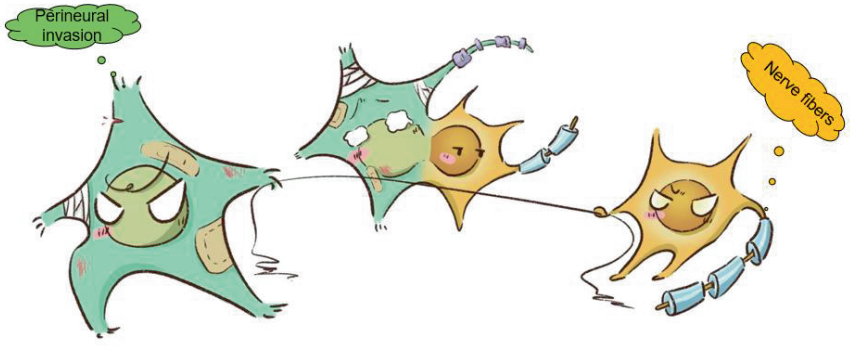

CHAPTER 6

PD-1+ T-cells correlate with Nerve Fiber Density as a prognostic biomarker in patients with resected perihilar cholangiocarcinoma

Xiuxiang Tan, Jan Bednarsch, Mika Rosin, Simone Appinger , Dong Liu, Georg Wiltberger, Juan Garcia Vallejo, Sven Lang, Zoltan Czigany, Shiva Boroojerdi, Nadine T. Gaisa, Peter Boor, Roman David Bülow, Judith de Vos-Geelen, Liselot Valkenburg-van Iersel, Marian Clahsen-van Groningen, Evelien J.M. de Jong, Bas Groot Koerkamp, Michail Doukas , Flavio Rocha, Tom Luedde , Uwe Klinge, Shivan Sivakumar, Ulf Neumann, Lara Heij

1ST author

Published, cancers 2022, 14, 2190

Chapter 6

List of abbreviations

CCA	Cholangiocarcinoma
CHCC-CCA	Combined hepatocellular-cholangiocarcinoma
DCCA	Distal cholangiocarcinoma
FFPE	Formalin fixed paraffin embedded
HCC	Hepatocellular carcinoma
ICCA	Intrahepatic cholangiocarcinoma
MIF	Multiplex Immune Fluorescence
NFD	Nerve fiber density
OS	Overall survival
PCCA	Perihilar cholangiocarcinoma
PD-1	Programmed Death receptor
PD-L1	Programmed Death Ligand 1
PD-L2	Programmed Death Ligand 2
PGP 9.5	Protein gene-product 9.5
PNI	Perineural invasion
RFS	Recurrence-free survival
ROI	Region of interest
TME	Tumor microenvironment

Abstract: *Background & Aims*: Perihilar cholangiocarcinoma (pCCA) is a hepatobiliary malignancy which a dismal prognosis. Nerve fiber density (NFD) – a novel prognostic biomarker – describes the density of small nerve fibers without cancer invasion and is categorized into high numbers and low numbers of small nerve fibers (high vs low NFD). NFD is different than perineural invasion (PNI), defined as nerve fiber trunks invaded by cancer cells. Here, we aim to explore differences in immune cell populations and survival between high and low NFD patients. *Approach & Results*: We applied multiplex immunofluorescence (mIF) on 47 pCCA patients and investigated immune cell composition in the tumor microenvironment (TME) of high and low NFD. Group comparison and oncological outcome analysis was performed. CD8+PD-1 expression was higher in the high NFD than in the low NFD group (12.24 × 10-6 vs. 1.38 × 10-6 positive cells by overall cell count, p=.017). High CD8+PD-1 expression was further identified as an independent predictor of overall (OS; Hazard ratio (HR)=0.41; p=.031) and recurrence-free survival (RFS; HR=0.40; p=.039). Correspondingly, the median OS was 83 months (95% confidence interval (CI): 18 – 48) in patients with high CD8+PD-1+ expression compared to 19 months (95% CI: 5 – 93) in patients with low CD8+PD-1+ expression (p=.018 log rank). Also, RFS was significantly lower in patients with low CD8+PD-1+ expression (14 months (95% CI: 6 – 22)) compared to patients with high CD8+PD-1+ expression (83 months (95% CI:17 – 149), p=.018 log rank). *Conclusions*: PD-1+ T-cells correlate with high NFD as a prognostic biomarker and predict good survival, the biological pathway needs to be investigated.

Keywords: Perihilar cholangiocarcinoma; nerve fibers; tumor microenvironment; oncological outcome; biomarker

---

Introduction

Cholangiocarcinoma (CCA) is a rare and aggressive hepatobiliary malignancy arising from the biliary tract. Based on the cancer location within the biliary tree, CCA is classified into 3 subtypes: intrahepatic cholangiocarcinoma (iCCA), perihilar cholangiocarcinoma (pCCA) and distal cholangiocarcinoma (dCCA). CCA usually has a 5-year overall survival (OS) of less than 10%[1]. Surgical resection remains the only curative treatment for these patients, however, only a minority of patients is eligible for surgery as CCA is often diagnosed at an advanced stage and resection is no longer an option. For almost all CCA patients, conventional cytotoxic chemotherapy is the mainstay treatment option[2], resulting in a survival benefit of only months in comparison to best supportive care and causing toxic side-effects. The upcoming treatment options within personalized medicine has not brought much for the group of patients with pCCA[3]. Recent trials have opened the field of immunotherapy as a treatment option displaying the possibility of long-term survival in some patients[4]. For CCA patients this is a developing field and results from phase 3 trials are

expected [5-7]. Based on phase 1 clinical trials there is hope that immunotherapy in combination with chemotherapy regimens might improve outcomes in CCA patients as well[8].

The low success rate of CCA treatment is caused by many factors, and limited knowledge of its tumor microenvironment (TME) contributes to this problem. CCA has a high heterogeneity at the genomic, epigenetic and molecular level, hence, primary CCA contains a diverse range of cell types[9-14]. Also, the TME is host for many different immune cells and stimulatory and inhibitory effects take place. PCCA shows abundant desmoplastic stroma which contains many immune cells, providing either a host protective immune environment or tumor progression is facilitated[15]. Immune cell compositions play an important role in the immune response to the cancer and different phenotypes have been suggested in combined hepatocellular-cholangiocarcinoma patients (cHCC-CCA)[16] and in iCCA[17].

From a histopathological point of view, pCCA characteristically has an extensive stromal component in which complex microenvironment interactions take place[15]. In the past decade, great efforts have been made to explore complexity of the TME and to develop novel therapies that might help to improve oncological outcomes. However, more needs to be discovered about the spatial relationship among cells within the complex TME and their expression patterns of co-stimulatory and inhibitory signals to understand the response to immune checkpoint blockades in clinical trials. However, not every patient responds equally and response rates differ from <5% to >40% depending on the cancer type. There is an urgent need for biomarkers to better predict response to immunotherapy[18]. Predictors for an anti-tumour response to ICIs currently are: high PD-L1 expression, microsatellite instable cancers or microsatellite high (MSI-H) cancers, tumour infiltrating lymphocytes (TILs) at the edge of the tumour and high mutational burden (TMB). Unfortunately, even in presence of one of these markers not all patients seem to respond to ICIs[14,19-22]. Also, new biomarkers to predict response to checkpoint inhibitors are of urgent need to facilitate patient selection.

We have recently shown that nerve fiber density (NFD) in the TME functions as an important prognostic biomarker in CCA patients. NFD is associated with clinical outcomes in pCCA and iCCA patients[23] and patients with presence of small nerve fibers in the TME display a better survival. The underlying mechanisms of this clinical observation are not discovered yet. Of main importance is the difference of a well-known aggressive feature perineural invasion (PNI), which shows invasion of cancer cells into the nerve fibers (figure 1). This histological feature is detectable on a routine H&E staining and it is thought that the perineurium of the nerve fiber is a barrier for the chemotherapy to reach the cancer. Also, the nerve fiber environment provides a way of least resistance for the tumor to spread and progress. NFD has an opposite effect on outcome and consists of nerve fibers growing in the TME. In case of high NFD, small nerve fibers grow into the TME. These nerve fibers are only visualized by a special staining and the nerve fibers are smaller in diameter and usually don't show any tumor invasion.

Given this prognostic value of NFD in pCCA, we hypothesized NFD might also be associated with different immunophenotypes and therefore used multiplex immunofluorescence (mIF) to reveal the differences in immune cell composition and distribution combined with the expression of co-stimulatory and co-inhibitory checkpoint markers.

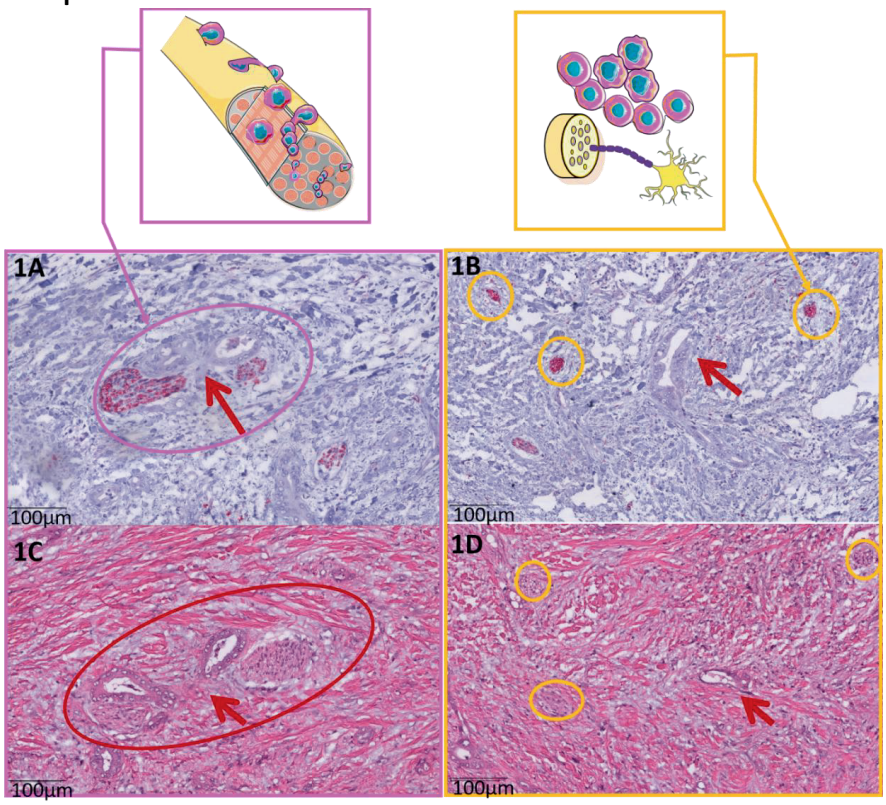

Figure 1: The difference between Perineural Invasion (PNI) and Nerve Fiber Density (NFD). 1A PNI is defined as tumor cells invading the perineurium of the nerve. In the neuronal marker (PGP9.5) staining, the nerve fiber in red (red arrow) surrounded and invaded by tumor cells and glandular structures. 1B NFD shows the presence of small nerve fibers in the tumor microenvironment (TME). These nerve fibers are small in diameter (<100 µm) and do not show any invasion of tumor cells. The red arrow points to the tumor cells and the yellow circles mark the presence of small nerve fibers stained with the neuronal marker (PGP9.5). 1C Corresponding H&E staining of PNI. PNI is recognizable for the pathologist. 1D On the H&E, the cancer is recognizable but the small nerve fibers are not detectable on this routine staining.
H&E, hematoxylin and eosin; NDF, nerve fiber density; PNI, perineural invasion; TME, tumor microenvironment.

Materials and Methods

Patient Cohort

In total 47 pCCA formalin fixed paraffin embedded (FFPE) tissue blocks were selected from the archive of the University Hospital RWTH Aachen. All patients were treated and operated on in our hospital between 2010 and 2019. Of the 47 patients, 2 individuals were excluded due to poor quality of the slide after staining, resulting in 45 patients being eligible for this analysis. The study was conducted in accordance with the requirements of the Institutional Review Board of the RWTH-Aachen University (EK 106/18), the Declaration of Helsinki, and good clinical practice guidelines (ICH-GCP).

Surgical techniques, adjuvant treatment and follow-up

All patients who were referred for surgical treatment of CCA to our institution underwent a detailed clinical work-up which included an oncological staging in accordance with common standards and radical surgery with lymphadenectomy as previously described[23-25] Patients treated between 2010-2017 were recommended for adjuvant therapy in case of positive lymph nodes or a R1 resection. After 2017 every patient was recommended

for adjuvant therapy in line with the BILCAP trial[26]. The postoperative follow up consisted of clinical follow up at the local hospital or oncologist with laboratory testing (CA19-9) and imaging. Confirmation of recurrence was performed by histology or radiology.

Whole slide immunohistochemistry (IHC) and nerve fiber counts

All samples were checked for the presence of tumor region by hematoxylin and eosin-stained sections. Slides were cut in tissue sections (2.5 μm thick) from formalin-fixed blocks, deparaffinized in xylene and rehydrated in graded alcohols. Slides were boiled in citrate buffer (pH 6.0) at 95–100°C for 5 min and were cooled for 20 min at room temperature with endogenous peroxide in methanol for 10 min. Then, these slides were incubated with rabbit anti-human PGP 9.5 (DAKO 1:100) overnight at 4°C to mark the nerve fibers. Histological Slides were scanned using the whole-slide scanners Aperio AT2 with ×40 objective (Leica Biosystems, Wetzlar, Germany), corresponding to a pixel-edge-length of = 0.252. A single digital image per case was uploaded in Qupath 0.1.6.

NFD nerve fiber counts from our previous study were used for immune cell phenotyping[24]. The NFD method was evaluated by manually counting the number of nerve fascicles with diameters of <100 μm in 20 continuous visual fields at ×200 magnification[27]. Based on NFD results, patients were categorized into a low NFD group (<10 nerve fibers) and a high NFD group (≥10 nerve fibers) as previously described[24].

Whole slide multiplex immunofluorescence (mIF)

All FFPE samples were subjected to multiplex immunofluorescence (mIF) in serial 5,0 μm histological tumor sections obtained from representative FFPE tumor blocks. The FFPE block were carefully selected with presence of the tumor region. The sections were labeled by using the Opal 7-Color fIHC Kit (PerkinElmer, Waltham, MA). The antibody fluorophores were grouped into a panel of 5 antibodies. The order of antibodies staining was always kept constant on all sections and sections were firstly counterstained with DAPI (Vector Laboratories). The multiplex immunofluorescence panel consisted of CD8, CD68, PD-1, PD-L1, and PD-L2 (table 1). All antibodies were diluted with Antibody Diluent (with Background Reducing Components, Dako, Germany). Secondary antibodies were applied with ImmPRESS™ HRP (Peroxidase) Polymer Detection Kit (Vector Laboratories, US). TSA reagents were diluted with 1× Plus Amplification Diluent (PerkinElmer/Akoya Biosciences, US).

Table 1: Monoclonal antibodies in the multiplex immunofluorescence panel

Antibody	Marker	Dilution	Incubation	Theme	Manufacturer
CD8	Cytotoxic T	1:500	30 min	CySO	Dako
CD68	Macrophage	1:6000	30 min	Cy7E	Dako
PD-1/CD279	Checkpoint	1:250	Over night	Cy47	Abcam
PD-L1/CD274	Checkpoint	1:200	Over night	46HE	Dako
PD-L2/CD273	Checkpoint	1:400	Over night	43HE	Abcam

The manual for mIF is described as Edwin R. Parra's protocol[28]: in short, the first marker was incubated after the FFPE sections were deparaffinized in xylene and rehydrated in graded alcohols. The second marker was applied on the following day. And the third marker was applied on the third day. After all five sequential reactions, sections were finally cover-slipped with VECTRASHIELD® HardSet™ Antifade Mounting Medium.

The slides were then digitally scanned with the TissueFAXS PLUS system (TissueGnostics, Austria). Image analysis was performed in 2 regions of interest (ROI) in each image only if present in the slide: tumor region and tumor free region. The size of the ROI varying per slide. Immune cell expression was calculated in percentages throughout the whole project (figure 2).

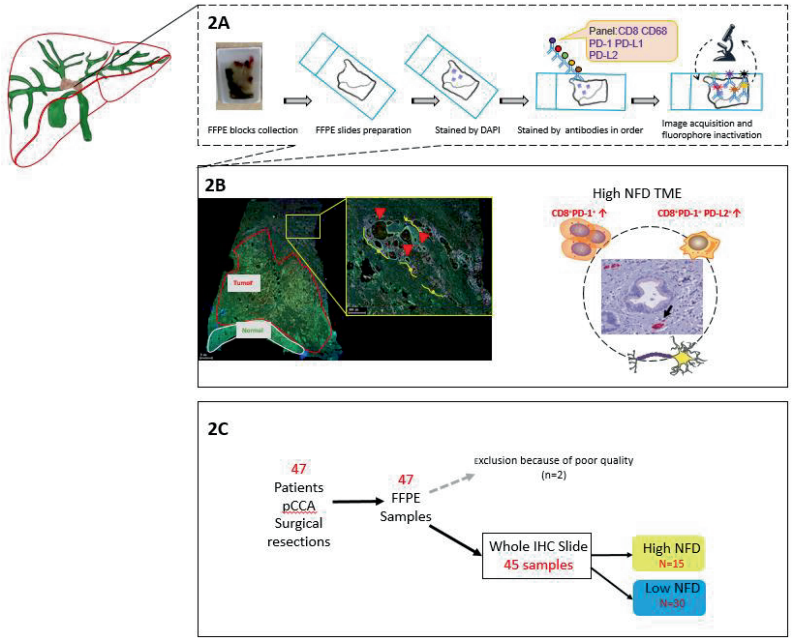

Figure 2: Overview of study workflow. 2A The formalin-fixed paraffin-embedded (FFPE) blocks were collected from the pathology archives. The slides were cut and stained with DAPI and 5 antibodies. The immunofluorescence-stained slides were scanned. 2B The digital scans were annotated for different regions: Tumor and Tumor-free. Cells were subsequently counted in these separate regions. For the NFD patients, the slides were selected based on the small nerve fiber count from previous work and the cell counting was done in the tumor region. 2C In total we included 47 patients in this study. From 45 patients we were able to analyze the digital scans.
DAPI, diamidino-2-phenylindole, FFPE; formalin-fixed paraffin-embedded

Strataquest software was used to analyse the antibody staining and cell counts. The library information was used to associate each fluorochrome component with a mIF marker. All immune cell populations were quantified as positive cells divided by overall cell count using the cell segmentation, thresholds were set manually under supervision of two pathologists (LH/MC). Positive cell count was categorized based on thresholds, a value above the threshold was considered as positive. Checks were performed by the pathologists (LH/MC).

Statistical analysis

Clinical variables and immune cell data and the difference between patients with high and low NFD were investigated by Mann-Whitney U test for continuous variables and the $\chi 2$ test or Fisher's exact test in accordance with scale and number count. Further, overall survival (OS) and recurrence-free survival (RFS) of the cohort were determined by the Kaplan-Meier method. OS was defined as the date of surgery to the date of death based on any cause, while RFS was defined as the date of surgery to the date of first tumor recurrence. Associations between OS or RFS and clinical or multiplex variables were determined by univariate and multivariate Cox Regression analyses. Survival curves were generated by the Kaplan-Meier method and compared with the log-rank test. The cut-off level for group categorization for survival analysis was determined by the receiver operating characteristic (ROC)-analysis of OS with respect to the analyzed continues variable as previously described[24]. The level of significance was set to alpha= 0.05, and p-values were calculated 2-sided testing.

Results

Patients' characteristics

The study cohort comprised of 45 individuals with 15 patients in the high NFD and 30 patients in the low NFD group. Demographical features e.g. gender (p=.664), age (p=.563) and American College of Anesthesiologists (ASA) status (p=.850) displayed no difference between the groups. Also, no statistical differences were observed with respect to basic pathological features as T category (p=.324), N category (p=.832), vascular invasion (p=.225), lymphatic invasion (p=.611), perineural invasion (p=.773) and tumor grading (p=.085). More details on clinicopathological features are displayed in table 2.

Table 2: Comparative analysis surgically treated patients with respect to nerve fiber density

Variables	NFD group		
	High (n=15)	**Low (n=30)**	**p-value**
Demographics			
Gender, m/f (%)	10 (66.7) / 5 (33.3)	18 (60) / 12 (40)	.664
Age (years)	70 (58 – 72)	64 (55 – 73)	.563
ASA, n (%)			.850
I	1 (6.7)	1 (3.3)	
II	8 (53.3)	15 (50.0)	
III	6 (40.0)	13 (43.3)	
IV	0	1 (3.3)	
Pathological examination			
T category, n (%)			.324
T1	0	0	
T2	8 (53.4)	20 (66.6)	
T3	6 (40.0)	6 (20.0)	
T4	1 (6.7)	4 (13.3)	
N category			.832
N0	7 (46.7)	13 (43.6)	
N1	8 (53.3)	17 (56.7)	
Vascular invasion, n (%)	2 (13.3)	10 (33.3)	.225
Lymphatic invasion, n(%)	5 (33.3)	7 (23.3)	.611
Perineural invasion, n (%)	10 (66.7)	21 (87.5)	.733
Tumor grading, n (%)			.085
G1	0	0	
G2	14 (93.3)	20 (71.4)	
G3	0	7 (25.0)	
G4	0	1 (3.6)	
Multiplex Imaging Data			
CD8-Panel ($\times 10^{-6}$)			
CD8+	319.04 (131.37 – 448.66)	182.51 (118.95 –	.195
CD8+PD-1+	12.24 (1.04 – 23.06)	1.38 (0.73 – 8.02)	**.017**
CD8+PD-1+PD-L1+	0.90 (0.03 – 1.97)	0.27 (0.04 – 0.66)	.228
CD8+PD-1+PD-L1+PD-L2+	0.14 (0.00 – 0.52)	0.02 (0.00 – 0.08)	.150
CD8+PD-1+PD-L2+	0.34 (0.03 – 0.79)	0.04 (0.00 – 0.16)	**.044**
CD8+PD-L1+	6.53 (1.92 – 15.76)	2.83 (1.16 – 10.42)	.306
CD8+PD-L1+PD-L2+	0.58 (0.16 – 5.41)	0.13 (0.05 – 0.80)	.091
CD8+PD-L2+	3.30 (0.81 – 17.37)	2.36 (0.37 – 4.93)	.097
CD68-Panel ($\times 10^{-6}$)			
CD68+	709.33 (348.70 – 1475.20)	505.81 (282.94 –	.087
CD68+PD-1+	5.82 (1.22 – 15.16)	2.52 (0.85 – 5.53)	.140
CD68+PD-1+PD-L1+	1.01 (0.06 – 1.90)	0.37 (0.05 – 1.09)	.363

CD68+PD-1+PD-L1+PLD2+	0.01 (0.00 – 0.47)	0.02 (0.00 – 0.14)	.946
CD68+PD-1+PD-L2+	0.11 (0.02 – 1.39)	0.04 (0.00 – 0.53)	.513
CD68+PD-L1+	15.31 (1.58 – 42.57)	6.64 (3.41 – 13.88)	.195
CD68+PD-L1+PD-L2+	1.18 (0.08 – 4.36)	0.06 (0.34 – 0.97)	.120
CD68+PD-L2+	10.24 (4.03 – 24.87)	4.93 (2.56 – 8.84)	.070
Follow-up Data			
Recurrence-free survival (months)	70 (48 – 93)	15 (3 – 27)	**.014**
Overall survival (months)	90 (0 – 196)	19 (12 – 27)	**.037**

Data presented as median and interquartile range if not noted otherwise. Multiplex data is presented as positive cells per overall cell count of the tumor ROI.Follow-up data is presented as median and 95% CI. Categorical data were compared using the chi-squared test, fisher's exact test or linear-by-linear association according to scale and number of cases. Data derived from continuous variables of different groups were compared by Mann-Whitney-U-Test. Follow-up data was calculated by the Kaplan-Meier-Method and compared by log rank tests. ASA, American society of anesthesiologists classification; CI, confidence interval. ROI, region of interest.

Multiplex data

The 45 slides all included whole slide analysis for the combined for immune cell markers (CD8 and CD68) and immune checkpoint markers (PD-1, PD-L1 and PD-L2). The corresponding H&E slide of the same block was used to annotate the tumor region and positive cells were counted. DAPI nuclei staining was used to generate a total cell count. We assessed differences in immune cell counts (CD8 and CD68) and expressions of checkpoint markers (PD-1, PD-L1 and PD-L2). Interestingly, the CD8+ and CD68+ numbers were not significantly different, but PD-1 expressions were. We note that PD-L1 was not significantly expressed and this marker is used for patient selection for Pembroluzimab.

While the expression of CD8+ and CD68+ as well as the expression of co-stimulatory signals appears to be tangentially higher in the high NFD cohort, a pronounced statistical effect was overserved for CD8+PD-1+ and CD8+PD-1+PD-L2+ cells (figure 3). CD8+PD-1 expression was higher in the high NFD than in the low NFD group (12.24×10^{-6} vs. 1.38×10^{-6}, p=.017) as was CD8+PD-1+PD-L2+ (0.34×10^{-6} vs. 0.04×10^{-6}, p=.044; table 2).

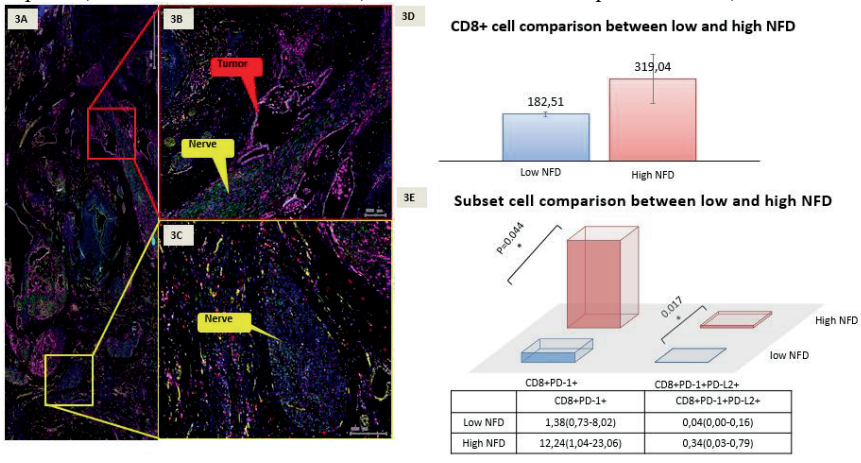

Figure 3: Multiplex immunofluorescence (mIF) digitized images. 3A Zoomed-in image of a slide with perihilar cholangiocarcinoma, with perihilar presence of many big nerve fibers and large vessels. 3B The red box visualizes PNI with the tumor glands highlighted with red and the nerve fiber marked in yellow. For PNI the tumor glands need to be orientated really close to the nerve and invade the perineurium. 3C The yellow box visualizes a large nerve fiber without tumor invasion. The increase of small nerve fibers which are counted to assess NFD are not detectable without a neuronal marker. The positive cell counting was done in the tumor annotation in a patient with high NFD. 3D For high and low NFD, positive cell counts for CD8 were not significantly different the tumor region. 3E Cell subset comparison. CD8+PD-1+

(p=.044) and CD8+PD-1PD-L2 cell counts (p=.017) were significantly higher in patients with high NFD.

NFD, nerve fiber density; PNI, perineural invasion.

Survival analysis

As high expression of CD8+PD-1+ and CD8+PD-1+PD-L2+ were associated with high NFD, these two variables were further included into a survival analysis for the whole cohort. For this purpose, a ROC analysis evaluating CD8+PD-1+ and CD8+PD-1+PD-L2+ expression with respect to OS was carried out and cut-off values for these variables determined with respect to optimized accuracy and equal weight for sensitivity and specificity errors. By this approach the cut-off values determined to be $<1.4 \times 10^{-6}$ (=low expression) vs. $\geq 1.4 \times 10^{-6}$ (=high expression) for CD8+PD-1+ and $<0.1 \times 10^{-6}$ (=low expression) vs. $\geq 0.1 \times 10^{-6}$ (=high expression) for CD8+PD-1+PD-L2+.

After a median follow-up of 70 months, the median OS of the cohort was 28 months (95%Confidence interval (CI): 12 – 43) and the RFS 24 months (95%CI: 0 – 49; Figure 4A and B). A Kaplan-Meier analysis with respect to NFD showed a median OS of 90 months (95% CI: 0 – 196) in patients with high NFD compared to 19 months (95% CI: 12 – 27) in patients with low NFD (p=.037 log rank, Figure 4C). Further, RFS was significantly lower in patients with low NFD (15 months (95% CI: 3 – 37)) compared to patients with high NFD (70 months (95% CI: 48 –93), p=.014 log rank, Figure 4D).

A similar survival analysis was conducted for CD8+PD-1+ expression. Here, A Kaplan-Meier analysis showed a median OS of 83 months (95% CI: 18 – 110) in patients with high CD8+PD-1+ expression compared to 19 months (95% CI: 5 – 93) in patients with low CD8+PD-1+ expression (p=.018 log rank, Figure 4E). Also, RFS was significantly lower in patients with low CD8+PD-1+ expression (14 months (95% CI: 6 – 22)) compared to patients with high CD8+PD-1+ expression (83 months (95% CI:17 – 149), p=.018 log rank, Figure 4F).

Cox Regression Analysis

To further explore independent prognostic markers of survival in our cohort, Cox regression analyses were conducted. Here, in univariate analysis, tumor grading (Hazard ratio (HR)=3.22; p=.010) and high CD8+PD-1+ expression (HR=0.44; p=.029) were significantly associated with OS. All variables showing p-value <0.10 were included in a multivariable Cox regression model. Here, tumor grading (HR=3.67; p=.010) and high CD8+PD-1+ expression (HR=0.42; p=.031) were identified as independent predictors for improved OS (table 3).

Table 3: Uni- and multivariate analysis of overall survival

Variables	Univariate Analysis		Multivariate Analysis	
	HR (95%CI)	p-value	HR (95%CI)	p-value
NFD (low=1)	0.47 (0.21 – 1.06)	.070	excluded	.595
Gender (male=1)	1.22 (0.60 – 2.49)	.576		
Age (<65 years=1)	1.22 (0.61 – 2.46)	.572		
ASA (I/II=1)	1.14 (0.57 – 2.30)	.707		
T category (T1/T2=1)	1.53 (0.76 – 3.09)	.233		
N category (N0=1)	1.70 (0.83 – 3.49)	.149		
Vascular invasion (No=1)	1.75 (0.81 – 3.78)	.154		
Lymphatic invasion (No=1)	1.43 (0.65 – 3.15)	.377		
Perineural invasion (No=1)	1.50 (0.44 – 5.08)	.515		
Tumor grading (G1/G2=1)	3.22 (1.33 – 7.82)	**.010**	3.67 (1.37 – 9.82)	**.010**
CD8+PD-1+ (low=1)	0.44 (0.21 – 0.92)	**.029**	0.42 (0.19 – 0.92)	**.031**
CD8+PD-1+PD-L2+ (low=1)	0.57 (0.26 – 1.22)	.145		

Variables displaying a p-value <0.1 in the univariate Cox Regression were transferred into a multivariable Cox regression model.

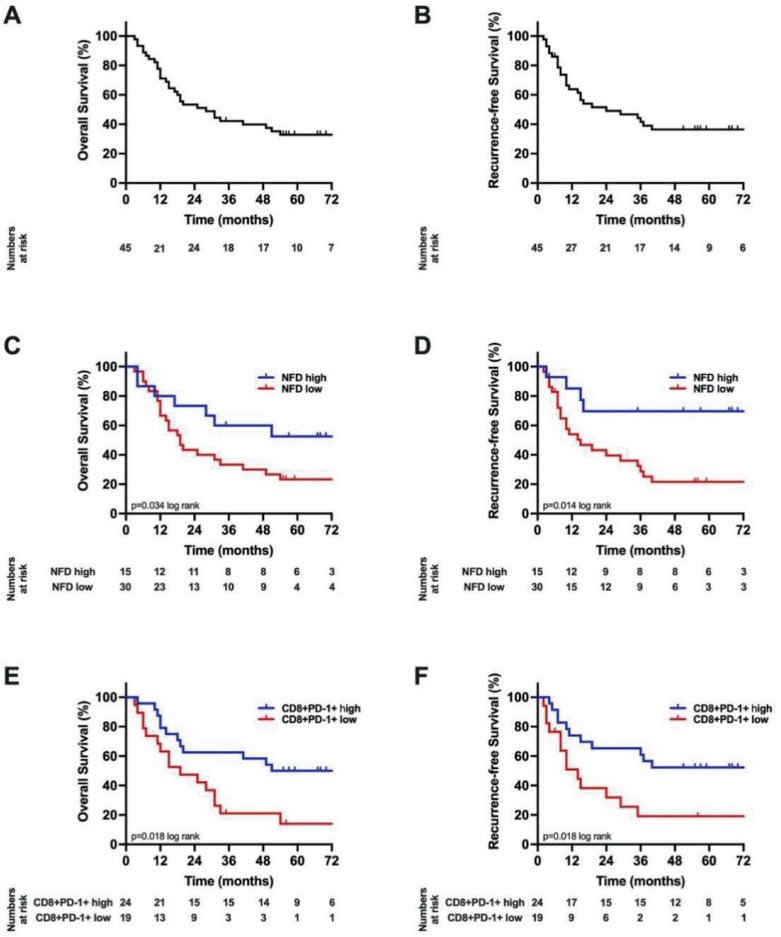

Figure 4: Oncological survival in CCA with respect to CD8+PD1+ count and nerve fiber density.

A Overall survival. The median OS of the cohort was 28 months. B Recurrence-free survival. The median RFS of the cohort was 24 months. C Overall survival stratified by nerve fiber density. The median OS of the cohort was 19 months in patients low NFD and 90 months in patients with high NFD. D Recurrence-free survival stratified by nerve fiber density. The median RFS of the cohort was 15 months in patients low NFD and 83 months in patients with high NFD. E Overall survival stratified by CD8+PD1+ count. The median OS of the cohort was 19 months in patients with low CD8+PD1+ expression and 83 months in patients with high CD8+PD1+≥ expression. F Recurrence-free survival stratified by CD8+PD1+ count. The median RFS of the cohort was 14 months in patients with low CD8+PD1+ expression and 83 months in patients with high CD8+PD1+ expression.

NFD, nerve fiber density; OS, overall survival; RFS, recurrence-free survival.

In an analog univariate analysis, high NFD (HR=0.31; p=.021), tumor grading (HR=4.79; p=.001) and high CD8+PD-1+ expression (HR=0.54; p=.024) showed significant associations with RFS. In the corresponding multivariable Cox regression model, tumor grading (HR=5.51; p=.001) and high CD8+PD-1+ expression (HR=0.40; p=.039) were identified as independent predictors of RFS (table 4).

Table 4: Uni- and multivariate analysis of recurrence-free survival

Variables	Univariate Analysis		Multivariate Analysis	
	HR (95%CI)	p-value	HR (95%CI)	p-value
NFD (low=1)	0.31 (0.12 – 0.84)	**.021**	excluded	.307
Gender (male=1)	1.16 (0.54 – 2.49)	.714		
Age (<65 years=1)	1.03 (0.48 – 2.20)	.941		
ASA (I/II=1)	1.08 (0.51 – 2.31)	.841		
T category (T1/T2=1)	1.24 (.57 – 2.73)	.589		
N category (N0=1)	1.53 (0.71 – 3.31)	.277		
Vascular invasion (No=1)	2.24 (0.97 – 5.16)	.059	excluded	.085
Lymphatic invasion (No=1)	1.46 (0.63 – 3.40)	.377		
Perineural invasion (No=1)	1.68 (0.39 – 7.28)	.486		
Tumor grading (G1/G2=1)	4.79 (1.90 – 12.04)	**.001**	5.51 (1.98 – 15.33)	**.001**
CD8+PD-1+ (low=1)	0.40 (0.18 – 0.89)	**.024**	0.40 (0.17 – 0.96)	**.039**
CD8+PD-1+PD-L2+ (low=1)	0.54 (0.23 – 1.26)	.156		

Variables displaying a p-value <0.1 in the univariate Cox Regression were transferred into a multivariable Cox regression model.

Discussion

PCCA is considered a rare primary biliary tract cancer and therefore it remains understudied. While the literature is short of large cohorts of patients, reported outcomes are entirely poor compared to other solid malignancies, especially for those individuals who are not eligible for a surgical resection.

Immunotherapy remains experimental in the clinical treatment of pCCA and patient stratification for systemic treatment, especially in the context of immunotherapy, is a subject of ongoing investigation. For HCC, as the most common primary liver cancer, immunotherapy in combination with Bevacizumab is already a first line treatment in the palliative setting [29]. First clinical trial results report that pCCA is an immunoresponsive malignancy indicating a potential role of immunotherapy in improving patients survival. However, only a subset of patients might respond to immunotherapy and biomarkers to identify these individuals for immunotherapy are of urgent need[30].

The histology of pCCA usually shows characteristic growth pattern of nerves invaded by cancer cells. Even though most patients have this feature somewhere present in the tumor, not all patients display poor outcome. In this study, we have shown that patients with high NFD is associated with a higher PD-1 expression. These patients do further display significant better oncological outcome survival. The underlying mechanism for this still needs to be further investigated.

NFD is defined as large numbers of small nerve fibers in the TME, these nerve fibers are not invaded by cancer cells. A recent study has demonstrated that CD8+ infiltration was associated with better survival in patients with iCCA[31]. Hence, we evaluated the clinical significance of the main immune cells (T cells and macrophages) in pCCA patients. In our previous publication[24], we investigated the role of NFD in a large pCCA cohort and demonstrated high NFD being independently associated with improved survival after surgical resection. We subsequently hypothesized that the small nerve fibers attract immune cells providing a better immune response to the cancer. Patients with a high NFD have abundant CD8+PD-1+ T-cells.

This finding identifies a subgroup of pCCA patients with a better survival. Further, these might suggest this subgroup for immunotherapy-based adjuvant treatment.

PD-1 checkpoint therapy unleashes the immune cells blocked by PD-1 expanding the T cell population at the interface and in the tumor. Potentially the high NFD subgroup of patients could benefit from immunotherapy, when the CD8+ T-cells blocked with PD-1 are re-activated. Our data are in line with previous findings on HCC patients, where patients with high levels of PD-1 expression showed an improved survival[32] and low counts of CD8 T-cells were indicative for a poorer outcome[33]. Previous work on the immune landscape in

intrahepatic cholangiocarcinoma showed an immunosuppressive environment with low numbers of CD3 and CD4 to be correlated with reduced long-term outcome [34] and low expression of PD-1 to be associated with an improved oncological survival [35-37]. For extrahepatic cholangiocarcinoma high numbers of CD3+ T-cells combined with expression of PD-L1 on the tumor cells was correlated with a more invasive growth[38]. The prognostic relevance of the PD-1 marker is therefore diverse, but expression of this checkpoint receptor usually indicates patients are likely to benefit from immunotherapy[39-41]. Previous work has shown that cholangiocarcinoma patients with high densities of tumor infiltrating lymphocytes also have high expression levels of PD-L1[42]. Besides using the expression of PD-1 and PD-L1 to predict outcome, different immune responses in biliary tract cancer are indicative for a better or worse outcome. The presence of tumor infiltrating lymphocytes are also an important prognostic factor[43]. The different prognostic values of the PD-1 and PD-L1 expression in cholangiocarcinoma patients suggests that expression of this marker by itself is not enough to function as a good biomarker.

The TME is host to many different cell types and nerve fibers seem to play a dual role. The large nerve fiber trunks with tumor invasion are usually a sign of a bad outcome[44] and the small nerve fibers are indicative of a good outcome[23]. The same phenomenon exists for immune cells (Tregs are usually bad for prognosis and CD8 cytoxic T cells are protective to the host[45]) and fibroblasts[46]. In the light of this perspective we hypothesized that nerve fibers have a dual role as well and they potentially can be used to stratify patients for response to immunotherapy.

In the future our findings need to be validated by external cohorts and underlying pathways should be identified. Once the pathways behind high NFD are known, the next step would be to see if high NFD can be influenced by therapeutics. First this needs to be done in 3D models and hopefully later potentially a nerve fiber targeted therapy could be included in a clinical trial and be part of a combination (chemo)therapy.

We have started a functional study to validate our findings in 3D models, hopefully this will be the next step to a clinical implementation.

Our study has limitations, unfortunately our cohort of only 50 surgically resected perihilar patients makes the sample size limited. The study could be validated in a larger sample size, using an external validation cohort would strengthen the study. Since perihilar cholangiocarcinoma (pCCA) is a relatively rare disease we have not managed to achieve this so far. We will collaborate internationally and gather larger cohorts of pCCA slides which we can use for further hypothesis and validation. Also our method could be improved by using a multiplex imaging device with accessibility of a 40-antibody panel, like CODEX or Hyperion.

To our knowledge, this is a first study in pCCA using a wide multiplex antibody panel focusing on immune cells in the TME in combination with checkpoint markers in relation to NFD. PD-1 expression correlates with high NFD patients suggesting NFD can be used as a simple prognostic biomarker. NFD can be easily integrated in the routine workup of the pathology report, since only one neuronal antibody is needed to achieve a nerve fiber count.

References

1. Bertuccio P, Malvezzi M, Carioli G, et al. Global trends in mortality from intrahepatic and extrahepatic cholangiocarcinoma. *Journal of hepatology* 2019; **71**(1): 104-14.
2. Valle J, Wasan H, Palmer DH, et al. Cisplatin plus gemcitabine versus gemcitabine for biliary tract cancer. *The New England journal of medicine* 2010; **362**(14): 1273-81.
3. Marin JJG, Prete MG, Lamarca A, et al. Current and novel therapeutic opportunities for systemic therapy in biliary cancer. *British journal of cancer* 2020; **123**(7): 1047-59.
4. Piha-Paul SA, Oh DY, Ueno M, et al. Efficacy and safety of pembrolizumab for the treatment of advanced biliary cancer: Results from the KEYNOTE-158 and KEYNOTE-028 studies. *International journal of cancer* 2020; **147**(8): 2190-8.
5. Di Federico A, Rizzo A, Ricci AD, et al. Nivolumab: an investigational agent for the treatment of biliary tract cancer. *Expert opinion on investigational drugs* 2021; **30**(4): 325-32.
6. Hack SP, Zhu AX. Atezolizumab: an investigational agent for the treatment of biliary tract cancer. *Expert opinion on investigational drugs* 2021; **30**(10): 1007-15.

7. Rizzo A, Ricci AD, Brandi G. Recent advances of immunotherapy for biliary tract cancer. *Expert review of gastroenterology & hepatology* 2021; **15**(5): 527-36.
8. Ueno M, Ikeda M, Morizane C, et al. Nivolumab alone or in combination with cisplatin plus gemcitabine in Japanese patients with unresectable or recurrent biliary tract cancer: a non-randomised, multicentre, open-label, phase 1 study. *The lancet Gastroenterology & hepatology* 2019; **4**(8): 611-21.
9. Banales JM, Marin JJG, Lamarca A, et al. Cholangiocarcinoma 2020: the next horizon in mechanisms and management. *Nature reviews Gastroenterology & hepatology* 2020; **17**(9): 557-88.
10. Zou S, Li J, Zhou H, et al. Mutational landscape of intrahepatic cholangiocarcinoma. *Nature communications* 2014; **5**: 5696.
11. Andersen JB, Spee B, Blechacz BR, et al. Genomic and genetic characterization of cholangiocarcinoma identifies therapeutic targets for tyrosine kinase inhibitors. *Gastroenterology* 2012; **142**(4): 1021-31.e15.
12. Sia D, Hoshida Y, Villanueva A, et al. Integrative molecular analysis of intrahepatic cholangiocarcinoma reveals 2 classes that have different outcomes. *Gastroenterology* 2013; **144**(4): 829-40.
13. Chaisaingmongkol J, Budhu A, Dang H, et al. Common Molecular Subtypes Among Asian Hepatocellular Carcinoma and Cholangiocarcinoma. *Cancer cell* 2017; **32**(1): 57-70.e3.
14. Jusakul A, Cutcutache I, Yong CH, et al. Whole-Genome and Epigenomic Landscapes of Etiologically Distinct Subtypes of Cholangiocarcinoma. *Cancer discovery* 2017; **7**(10): 1116-35.
15. Sirica AE, Gores GJ. Desmoplastic stroma and cholangiocarcinoma: clinical implications and therapeutic targeting. *Hepatology (Baltimore, Md)* 2014; **59**(6): 2397-402.
16. Nguyen CT, Caruso S, Maillé P, et al. Immune profiling of combined hepatocellular-cholangiocarcinoma reveals distinct subtypes and activation of gene signatures predictive of response to immunotherapy. *Clinical cancer research : an official journal of the American Association for Cancer Research* 2021.
17. Job S, Rapoud D, Dos Santos A, et al. Identification of Four Immune Subtypes Characterized by Distinct Composition and Functions of Tumor Microenvironment in Intrahepatic Cholangiocarcinoma. *Hepatology (Baltimore, Md)* 2020; **72**(3): 965-81.
18. Yuan J, Hegde PS, Clynes R, et al. Novel technologies and emerging biomarkers for personalized cancer immunotherapy. *Journal for immunotherapy of cancer* 2016; **4**: 3.
19. Gutiérrez-Larrañaga M, González-López E, Roa-Bautista A, et al. Immune Checkpoint Inhibitors: The Emerging Cornerstone in Cholangiocarcinoma Therapy? *Liver Cancer* 2021; **10**(6): 545-60.
20. Rizzo A, Ricci AD, Brandi G. Durvalumab: an investigational anti-PD-L1 antibody for the treatment of biliary tract cancer. *Expert opinion on investigational drugs* 2021; **30**(4): 343-50.
21. Kang S, El-Rayes BF, Akce M. Evolving Role of Immunotherapy in Advanced Biliary Tract Cancers. *Cancers* 2022; **14**(7): 1748.
22. Vogel A, Bathon M, Saborowski A. Immunotherapies in clinical development for biliary tract cancer. *Expert opinion on investigational drugs* 2021; **30**(4): 351-63.
23. Bednarsch J, Tan X, Czigany Z, et al. The Presence of Small Nerve Fibers in the Tumor Microenvironment as Predictive Biomarker of Oncological Outcome Following Partial Hepatectomy for Intrahepatic Cholangiocarcinoma. *Cancers* 2021; **13**(15): 3661.
24. Bednarsch J, Kather J, Tan X, et al. Nerve Fibers in the Tumor Microenvironment as a Novel Biomarker for Oncological Outcome in Patients Undergoing Surgery for Perihilar Cholangiocarcinoma. *Liver Cancer* 2021.
25. Bednarsch J, Czigany Z, Heij LR, et al. The prognostic role of in-hospital transfusion of fresh frozen plasma in patients with cholangiocarcinoma undergoing curative-intent liver surgery. *European journal of surgical oncology : the journal of the European Society of Surgical Oncology and the British Association of Surgical Oncology* 2021.
26. Primrose JN, Fox RP, Palmer DH, et al. Capecitabine compared with observation in resected biliary tract cancer (BILCAP): a randomised, controlled, multicentre, phase 3 study. *The Lancet Oncology* 2019; **20**(5): 663-73.
27. Heij LR, Tan X, Kather JN, et al. Nerve Fibers in the Tumor Microenvironment Are Co-Localized with Lymphoid Aggregates in Pancreatic Cancer. *Journal of clinical medicine* 2021; **10**(3): 490.

28. Dievernich A, Achenbach P, Davies L, Klinge U. Tissue remodeling macrophages morphologically dominate at the interface of polypropylene surgical meshes in the human abdomen. *Hernia : the journal of hernias and abdominal wall surgery* 2020; **24**(6): 1175-89.
29. Finn RS, Qin S, Ikeda M, et al. Atezolizumab plus Bevacizumab in Unresectable Hepatocellular Carcinoma. *The New England journal of medicine* 2020; **382**(20): 1894-905.
30. Macias RIR, Kornek M, Rodrigues PM, et al. Diagnostic and prognostic biomarkers in cholangiocarcinoma. *Liver international : official journal of the International Association for the Study of the Liver* 2019; **39 Suppl 1**: 108-22.
31. Tian L, Ma J, Ma L, et al. PD-1/PD-L1 expression profiles within intrahepatic cholangiocarcinoma predict clinical outcome. *World journal of surgical oncology* 2020; **18**(1): 303.
32. Sangro B, Melero I, Wadhawan S, et al. Association of inflammatory biomarkers with clinical outcomes in nivolumab-treated patients with advanced hepatocellular carcinoma. *Journal of hepatology* 2020; **73**(6): 1460-9.
33. Sideras K, Biermann K, Verheij J, et al. PD-L1, Galectin-9 and CD8(+) tumor-infiltrating lymphocytes are associated with survival in hepatocellular carcinoma. *Oncoimmunology* 2017; **6**(2): e1273309.
34. Carapeto F, Bozorgui B, Shroff RT, et al. The Immunogenomic Landscape of Resected Intrahepatic Cholangiocarcinoma. *Hepatology (Baltimore, Md)* 2021.
35. Lu JC, Zeng HY, Sun QM, et al. Distinct PD-L1/PD1 Profiles and Clinical Implications in Intrahepatic Cholangiocarcinoma Patients with Different Risk Factors. *Theranostics* 2019; **9**(16): 4678-87.
36. Kitano Y, Yamashita YI, Nakao Y, et al. Clinical Significance of PD-L1 Expression in Both Cancer and Stroma Cells of Cholangiocarcinoma Patients. *Annals of surgical oncology* 2020; **27**(2): 599-607.
37. Gani F, Nagarajan N, Kim Y, et al. Program Death 1 Immune Checkpoint and Tumor Microenvironment: Implications for Patients With Intrahepatic Cholangiocarcinoma. *Annals of surgical oncology* 2016; **23**(8): 2610-7.
38. Walter D, Herrmann E, Schnitzbauer AA, et al. PD-L1 expression in extrahepatic cholangiocarcinoma. *Histopathology* 2017; **71**(3): 383-92.
39. Xu G, Sun L, Li Y, et al. The Clinicopathological and Prognostic Value of PD-L1 Expression in Cholangiocarcinoma: A Meta-Analysis. *Frontiers in oncology* 2019; **9**: 897.
40. Zhu Y, Wang XY, Zhang Y, et al. Programmed death ligand 1 expression in human intrahepatic cholangiocarcinoma and its association with prognosis and CD8(+) T-cell immune responses. *Cancer management and research* 2018; **10**: 4113-23.
41. Tumeh PC, Harview CL, Yearley JH, et al. PD-1 blockade induces responses by inhibiting adaptive immune resistance. *Nature* 2014; **515**(7528): 568-71.
42. Fontugne J, Augustin J, Pujals A, et al. PD-L1 expression in perihilar and intrahepatic cholangiocarcinoma. *Oncotarget* 2017; **8**(15): 24644-51.
43. Goeppert B, Frauenschuh L, Zucknick M, et al. Prognostic impact of tumour-infiltrating immune cells on biliary tract cancer. *British journal of cancer* 2013; **109**(10): 2665-74.
44. Zhang Z, Zhou Y, Hu K, Wang D, Wang Z, Huang Y. Perineural invasion as a prognostic factor for intrahepatic cholangiocarcinoma after curative resection and a potential indication for postoperative chemotherapy: a retrospective cohort study. *BMC Cancer* 2020; **20**(1): 270.
45. Kitano Y, Okabe H, Yamashita Y-i, et al. Tumour-infiltrating inflammatory and immune cells in patients with extrahepatic cholangiocarcinoma. *British Journal of Cancer* 2018; **118**(2): 171-80.
46. Affo S, Nair A, Brundu F, et al. Promotion of cholangiocarcinoma growth by diverse cancer-associated fibroblast subpopulations. *Cancer Cell* 2021; **39**(6): 866-82.e11.

Chapter 6

Chapter 6

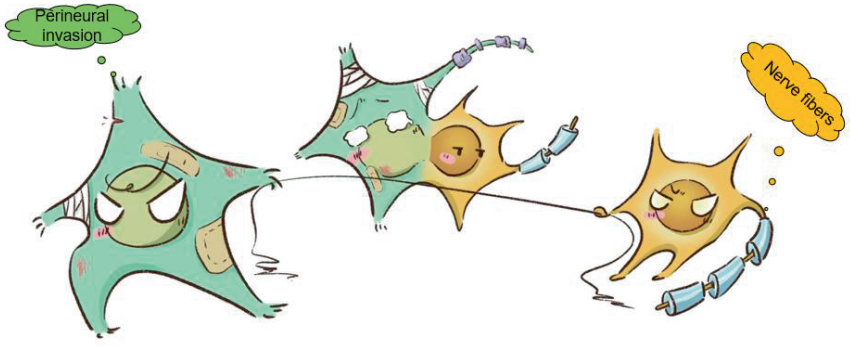

CHAPTER 7

General discussion and future perspectives

Chapter7

General Discussion

In the TME, tumor cells are surrounded by extracellular matrix and various components of the stroma. Known stromal cells under current investigation are fibroblasts, blood vessels and inflammatory cells[1]. Small nerve fibers have not been investigated much up to now. Some cancer types, amongst PDAC and CCA, are known for their characteristic aggressive perineural growth pattern.

In this thesis, we hypothesized that different kind of nerve fibers exist. Besides the large nerve trunks with invasion of cancer cells, small nerve fibers are present in the TME and these nerve fibers have a positive effect on outcome. This thesis provides insight into the prognostic role of the small nerve fibers in patients with PDAC and CCA. We aimed to explore a novel biomarker with prognostic value. In more detail, this thesis starts with the existent knowledge of the neural functions in neurotropic cancer (PDAC and CCA). In addition, potential mechanisms of PNI in PDAC and CCA are discussed. It also summarizes the latest clinical studies that explored the relationship between nerves and patients' survival with PDAC and CCA, respectively. Based on a review of current clinical and molecular studies of neurotropic cancer (PDAC and CCA) (**Chapter 2**), we hypothesized that nerve fibers can be a novel candidate biomarker to predict patients' clinical outcomes, such as cancer-specific survival (CSS) and overall survival (OS). We explored relationships between the nerve fibers and their spatial distribution in PDAC patients in **Chapter 3**. The relationship of nerve fibers in perihilar Cholangiocarcinoma (pCCA) and intrahepatic Cholangiocarcinoma (iCCA) patients with CSS and OS are demonstrated in **Chapter 4** and **Chapter 5**, respectively. Furthermore, we examined the potential correlation with immune cell phenotypes in pCCA patients in **Chapter 6**. We hope to provide some clues for future nerve fiber-cancer-research.

Origin of small nerve fibers in the TME

As presented in **Chapter 2**, autonomic nerves are widely distributed in the TME of PDAC and CCA. It is important to distinguish the phenomenon of PNI and small nerve fibers. PNI has widely attracted attention in the field of cancer research since it is a known feature for an aggressive cancer biology. Clinically, PNI is an independent predictor of poor prognosis and it plays an important role in the development and progression of PDAC.

In recent years, evidence has shown that nerve fibers are a crucial component of the TME and might play a dual role within the TME. In other words, nerve fibers participate in the progression of tumor growth in both PDAC and CCA. Literature has shown that the reactivation of developmental and regenerative pathways allow recruitment of nerves and this is important for cancer growth[2]. Nerve fibers originate from the central nervous system. Depending on the localization of the cancer type from which the malignancy arises as well as its native innervation pattern, different parts of the nervous system are involved. Certain branches of the nervous system are critical in a cancer progression. In the pancreas, the parasympathetic nerves can suppress the growth of pancreatic cancer cells, while the sympathetic nerves stimulate the growth of pancreatic cells. Therefore, there is a balance of neural influence for pancreatic cancer cells[3] (**Chapter 3**). If this mechanism also takes place in CCA remains unknown.

To further investigate the nerve fibers, we conducted immunohistochemistry and identified the small nerve fibers to be of parasympathetic origin. This finding is novel and interesting as the role of the parasympathetic nervous system in cancer initiation and progression is not fully understood. A potential inhibitory effect of the parasympathetic nervous system on cancer initiation was historically observed in patients who underwent vagotomy as a treatment for gastric ulcers and subsequently displayed a higher incidence for gastric cancer[4,5]. A study investigated the impact of subdiaphragmatic vagotomy in a murine PDAC model. Here, vagotomy increased tumor growth and impaired survival in this mouse model which was partly explained by increased expression of tumor necrosis factor alpha in tumor tissue[6]. Kamiya et al. introduced an adeno-associated virus vector enabling the

stimulation or inhibition of parasympathetic and sympathetic nerve fibers localized in the tumor tissue. In a xenograft model, they observed a decreased progression of the primary tumors and attenuation of the development of distant metastases after increasing parasympathetic neurotransmission. Additionally, the vector also showed antitumor activity in a chemically induced model of breast cancer[7,8]. While the investigation of the mechanism of our observation regarding the protective effect of parasympathetic nerve fibers is beyond the scope of our clinically oriented analysis, these observations provide further evidence for the significant interaction of the parasympathetic nervous system and cancer cells and warrants further research. In pancreatic cancer, low NFD indicates a poor survival[9]. Observational studies have shown differences in the role of an increased sympathetic innervation of tumors. For prostate cancer[10], breast cancer[11], and hepatocellular carcinoma[12], the presence of sympathetic nerve fibers was indicative for cancer progression. For gastric cancer[13] and colorectal cancer[14], the opposite has been described. This dual role of nerve fibers and their exact origin in pCCA are important research questions of ongoing studies of our group.

At present, the emerging field of targeted therapies is evolving. Many components in TME are now undergoing investigation and promising targets of drug therapies are ongoing. Due to the close relationship between nerve fibers and tumor cells, this might provide novel treatment strategies for highly innervated tissues, such as the pancreas. There is a need to understand the complex role of nerve fibers within the TME before new treatment strategies can be tested.

The current knowledge of the origination of nerve fibers in the TME of cancer, in particular PDAC and CCA, is still under investigation and the mechanism behind the positive effect on survival of the small nerve fibers in the TME needs to be further investigated as well. We hope our work contributes to further studies in the field of cancer and neuroscience.

Small nerve fibers and their potential interaction with B-cells in PDAC

Up to now, in PDAC the research on neural-cancer interactions has been ongoing. Previous work on the "influence of nerves on PNI" has shown that PNI is thought to be an indicator of aggressive tumor behavior and this correlates with a poor prognosis of patients with PDAC[15]. Iwasaki et al. have reported on the role of neural density in PDAC and found an inverse relationship with neural density being independently associated with reduced survival after surgical resection[9]. It is also known that the neural system provides an alternative route for PDAC metastatic spread and pain generation in this cancer. The aggressiveness of PDAC and its resistance to therapeutics possibly can be explained by the complex role of the TME in this cancer type. We initiated a retrospective cohort study (**Chapter 3**), in which we aimed to explore whether the density of nerve fibers was associated with OS in patients with PDAC. Furthermore, this study was designed to investigate the co-localization of immune cells and nerve fibers. After a pilot analysis of 166 PDAC patients', we concluded that a high density of nerve fibers is associated with a better survival in patients with PDAC. This conclusion is opposite to PNI in PDAC. Nerve fiber density and PNI are independent of each other, meaning a patient can have both nerve fibers in one histology slide. Further, we observed that the small nerve fibers were co-localized with lymphoid aggregates.

This clinical retrospective study in PDAC patients explored the influence of small nerve fibers on patients' survival. According to our primary analysis of the location of nerve fibers and the co-localization of lymphoid aggregates, we hypothesized that an immune cell interaction plays a role.

PDAC is known for its abundant stroma, and here, crosstalk takes place between the tumor and the host. The immune environment is influenced by the tumor and the host. The immune system is known to have a crucial role in cancer, and this is possibly regulated by genetic and morphological features of the tumor. It is known that PDAC patients with higher levels of CD4+ and CD8+ T cells have a better survival[16]. The surrounding stromal

cells support tumor budding of the cancer cells and promote aggressive behavior; it is described that this phenotype contains a depletion of tumor-infiltrating lymphocytes (TILs)[17]. The presence of TILs is a predictor of a better prognosis. In breast and ovarian cancer, a major component of TILs are the tumor-infiltrating lymphocytic B cells (TIL-B)[18]. In our study, we demonstrated that when lymphoid aggregates were co-localized together with small nerve fibers these patients demonstrated a better survival. Previous literature has shown that B cells and tertiary lymphoid structures promote immunotherapy response in melanoma and sarcoma[19,20] and are of main importance for better survival. The role of nerve fibers in the co-localization with these lymphoid aggregates has the potential to discover new pathways for a better survival and it paves the way for new possible targets for (combination) therapy. We expect that these data may be broadly applicable to other malignancies.

Small nerve fibers used as a prognostic biomarker in CCA

Similar with PDAC, the TME of CCA is characterized by a large desmoplastic stromal component. We hypothesized that the characteristic large desmoplastic stromal component might be a reason to explain the poor response to systemic therapy[4]. The biliary tree is surrounded by a complex nerve fiber network being the basis for an intense crosstalk between nerve fibers and tumor cells as well as other parts of the TME (**Chapter 5**). For example, immune cells or cancer-associated fibroblasts[7,21,22]. CCA is also considered to be a "neurotropic" cancer with a high frequency of PNI which is associated with poor oncological outcomes[23,24]. To explore the role of nerve fibers in CCA, we explored the association between nerve fibers and patients' clinical outcome in pCCA and iCCA patients. Our studies identified nerve fiber density to be a potential novel prognostic biomarker in both pCCA and iCCA patients. Nerve fiber density alone and in combination with nodal status allows to stratify patients based on their risk for inferior oncological outcome after curative-intent surgery. We applied the parameters cancer-specific survival (CSS) and recurrence-free survival (RFS) to value the oncological outcome.

The prognostic role of lymph node metastases in pCCA is abundantly discussed in other studies[25-28]. In line with these previous observations, nodal status was also of major predictive value in our multivariable analysis of oncological outcome. As nodal status was not associated with the presence of nerve fibers in our pCCA cohort and the combination of both major oncological predictors, might therefore be of value. An interesting observation was the compelling outcome of the above mentioned low-risk cohort (high NFD and nodal negative), while our median-risk group (low NFD or node positive) is in line with previous reports and the high-risk group (low NFD and nodal positive) below the commonly reported outcome figures. This underlines the oncological role of nerve fibers in pCCA[29-35]. As such, the combination of nerve fibers (which is assessable by immunohistochemistry) and nodal status (which is routinely provided by the pathology report) does provide an easily applicable risk stratification for pCCA patients undergoing curative-intent surgery. This observation is in line with our PDAC cohort, identifying low NFD as an important predictor of inferior CSS in PDAC patients.

Tumor recurrence remains the major problem in pCCA patients who underwent surgery with curative-intent[36,37]. Local recurrence is commonly diagnosed concomitantly with a stenosis at the surgically performed hepaticojejunostomy resulting in recurrent cholangitis and life-threatening biliary sepsis[35]. In contrast, survival after metastatic recurrence is usually determined by the limited response and resistance to chemotherapy resulting in early disease progression and associated fatal outcome[38]. These limitations in the treatment of tumor relapse were also observed in our cohort with most of the individuals experiencing tumor recurrence deceasing shortly after the diagnosis. This close relationship between RFS and CSS also explains our finding that NFD is also associated with RFS in multivariable analysis.

Interestingly, adjuvant therapy was a risk factor for RFS in univariate analysis. This might be explained by our historic approach to apply adjuvant therapy in patients with a high risk for tumor recurrence (e.g., positive nodal status or R1 resection) in the early study

period[39,40]. From 2018, patients with adequate performance status were subjected to adjuvant capecitabine-based therapy or referred for inclusion to the currently recruiting ACCTICA trial (Adjuvant Chemotherapy with Gemcitabine and Cisplatin Compared to Standard of Care After Curative Intent Resection of Biliary Tract Cancer, NCT02170090). In all cases if the patient was willing to participate in a clinical trial[41,42] .

Unfortunately, nerve fibers cannot be assessed prior to surgery and is therefore up to now not available for preoperative patient selection. However, NFD displayed a good prognostic ability for recurrence and reduced survival after surgery and might therefore be used for postoperative risk stratification. Adjuvant therapy in biliary tract cancer is considered the standard of care in Europe after the results of the BILCAP trial[42]. In other countries, patients are selected for adjuvant therapy when high-risk features as positive lymph nodes or residual tumor are present[43]. In this context, the NFD status could be a high-risk feature similar to the nodal status.

Limitations

Our analysis has limitations. All patients included in this study were treated at a single institution reflecting the authors' individual surgical approach, and all data were collected and analyzed retrospectively. This retrospective nature of our study resulted in some missing data which would have been interesting in the context of the oncological analysis, for example, CA19-9 levels in blood samples. The monocentric approach also results in a limited sample size, external validation cohorts are still missing.

Notwithstanding the above-mentioned limitations, we have identified small nerve fibers as a novel and important prognostic biomarker. Nerve fibers alone and in combination with nodal status allows to stratify CCA patients in terms of oncological outcome after curative-intent surgery. Larger, multicenter studies are needed to confirm and validate our findings.

In these three oncological studies investigating the role of nerve fibers, the identification of low-risk and high-risk cohorts and the selection of nerve fiber cutoffs appears to differ largely between various tumor entities. In breast cancer, nerve fiber density was categorized into no nerve fibers, weak expression with 1–10 nerve fibers and moderate/strong expression with >10 nerve fibers by Zhao et al[44]. In PDAC, intrapancreatic neural density was defined as low with ≤7 nerve fibers and as high with >7 nerve fiber[9]. In our study focusing on pCCA, we defined nerve density as low in cases with <10 nerve fibers and a high in individuals with ≥10 nerve fibers [45]. The distinct observations made in this iCCA cohort (nerve fibers vs. no nerve fibers) and in our study analysis regarding pCCA must be discussed critically. PCCA and iCCA share morphological similarities but these entities are also different. The histological characteristics of pCCA are basically conventional mucin-producing adenocarcinomas or papillary tumors[46,47]. In contrast, iCCA can be divided into several histological subtypes with a conventional type, cholangiolocarcinomas and rare variants. Conventional iCCA can be subdivided into large duct type and small duct type cancers. Large duct iCCA arises from large intrahepatic bile ducts and is histologically a mucin-producing tumor arranged in a large duct or papillary architecture, similarly to pCCA. Small duct iCCA, in contrast, is a tubular or acinar adenocarcinoma with a nodular growth and no or minimal mucin production, which originates from smaller intrahepatic bile ducts[7,48]. Notably, these histological differences also reflect the molecular heterogeneity of iCCA[49]. Small duct iCCA can often show isocitrate dehydrogenase (IDH1, IDH2) mutations or fibroblast growth factor receptor 2 (FGFR2) fusions[50,51]. In contrast, large duct iCCA shows a high frequency of mutations in Kirsten Rat Sarcoma (KRAS) and/or Tumor Protein 53 (TP53) genes similar to pCCA[52]. Given the similarities of one iCCA subtype with pCCA and the considerable differences of some iCCA subtypes in molecular and histological characteristics to pCCA, it might lead us to the assumption that the whole entity of iCCA demonstrates a

heterogeneous population. A specific nerve fiber cut-off to stratify high- and low-risk patients in the future is needed between the different entities and possibly between subtypes. Unfortunately, molecular data was not available for analysis in our cohort to correlate the nerve fibers characteristics with separate genetic subtypes of iCCA.

Main findings

- Nerve fibers can be used as a powerful prognostic biomarker for oncological outcome in PDAC, iCCA and pCCA.
- This thesis illustrates the co-localization of nerve fibers and lymphoid aggregates in the TME of PDAC.
- The combination of NFD and nodal status demonstrates an excellent ability to stratify patients regarding their prognosis after curative-intent surgery for pCCA and iCCA patients.
- This thesis identifies that small nerve fibers are of parasympathetic origin rather than sympathetic origin in pCCA.
- This thesis identifies that high NFD is associated with a high CD8_PD-1 expression. These patients demonstrate a significant better oncological outcome survival.
- NFD can be integrated in the routine workup of the pathology report, since only one neuronal antibody is needed to achieve a nerve fiber count.

Future perspectives

High nerve fiber density is described in PDAC, pCCA and iCCA patients to be associated with a better outcome. In this thesis, we conclude that our results provide basic evidence for exploration of future nerve fiber research in cancer patients. The underlying pathway still must be identified, and further research is needed. The next step would be to further unravel the spatial context of the small nerve fibers combined with a spatial genomic approach. New techniques allow single cell RNA sequencing on FFPE blocks. Using these methods, it will allow to closely investigate the transcriptomic status of the patients with high and low NFD within the context of the surrounding structures. Another method would be to use confocal microscopy and analyze the architecture of the small nerve fibers in a 3D manner. Increasing knowledge on the role of nerve fibers in cancer is important to improve personalized medicine for cancer patients.

Abbreviation

CCA	Cholangiocarcinoma
CSS	Cancer-specific survival
ICCA	Intrahepatic Cholangiocarcinoma
NFD	Nerve fiber density
OS	Overall survival
PCCA	Perihilar Cholangiocarcinoma
PDAC	Pancreatic cancer
PNI	Perineural invasion
TME	Tumor microenvironment

Reference

1. Wang M, Zhao J, Zhang L, et al. Role of tumor microenvironment in tumorigenesis. *J Cancer* 2017; **8**(5): 761-73.
2. Zahalka AH, Frenette PS. Nerves in cancer. *Nature Reviews Cancer* 2020; **20**(3): 143-57.
3. Renz BW, Tanaka T, Sunagawa M, et al. Cholinergic Signaling via Muscarinic Receptors Directly and Indirectly Suppresses Pancreatic Tumorigenesis and Cancer Stemness. 2018; **8**(11): 1458-73.

4. Weigt J, Malfertheiner P. Cisplatin plus gemcitabine versus gemcitabine for biliary tract cancer. *Expert review of gastroenterology & hepatology* 2010; **4**(4): 395-7.
5. Caygill CPJ, Knowles RL, Hall R. Increased risk of cancer mortality after vagotomy for peptic ulcer: a preliminary analysis. *European Journal of Cancer Prevention* 1991; **1**(1): 35-8.
6. Ivo Partecke L, Käding A, Nguyen Trung D, et al. Subdiaphragmatic vagotomy promotes tumor growth and reduces survival via TNFα in a murine pancreatic cancer model. *Oncotarget* 2017; **8**(14).
7. Godinho-Silva C, Cardoso F, Veiga-Fernandes H. Neuro–Immune Cell Units: A New Paradigm in Physiology. *Annual Review of Immunology* 2019; **37**(1): 19-46.
8. Tibensky M, Mravec B. Role of the parasympathetic nervous system in cancer initiation and progression. *Clinical & translational oncology : official publication of the Federation of Spanish Oncology Societies and of the National Cancer Institute of Mexico* 2021; **23**(4): 669-81.
9. Iwasaki T, Hiraoka N, Ino Y, et al. Reduction of intrapancreatic neural density in cancer tissue predicts poorer outcome in pancreatic ductal carcinoma. *Cancer Sci* 2019; **110**(4): 1491-502.
10. Magnon C, Hall SJ, Lin J, et al. Autonomic Nerve Development Contributes to Prostate Cancer Progression. *Science* 2013; **341**(6142): 1236361.
11. Kamiya A, Hayama Y, Kato S, et al. Genetic manipulation of autonomic nerve fiber innervation and activity and its effect on breast cancer progression. *Nature Neuroscience* 2019; **22**(8): 1289-305.
12. Zhang L, Wu LL, Huan HB, et al. Sympathetic and parasympathetic innervation in hepatocellular carcinoma. *Neoplasma* 2017; **64**(6): 840-6.
13. Bae GE, Kim HS, Won KY, Kim GY, Sung JY, Lim SJ. Lower Sympathetic Nervous System Density and β-adrenoreceptor Expression Are Involved in Gastric Cancer Progression. *Anticancer research* 2019; **39**(1): 231-6.
14. Zhou H, Shi B, Jia Y, et al. Expression and significance of autonomic nerves and α9 nicotinic acetylcholine receptor in colorectal cancer. *Molecular medicine reports* 2018; **17**(6): 8423-31.
15. Wang J, Chen Y, Li X, Zou X. Perineural Invasion and Associated Pain Transmission in Pancreatic Cancer. *Cancers* 2021; **13**(18).
16. Bankhead P, Loughrey MB, Fernández JA, et al. QuPath: Open source software for digital pathology image analysis. *Scientific Reports* 2017; **7**(1): 16878.
17. Karamitopoulou E. Tumour microenvironment of pancreatic cancer: immune landscape is dictated by molecular and histopathological features. *British Journal of Cancer* 2019; **121**(1): 5-14.
18. Roghanian A, Fraser C, Kleyman M, Chen J. B Cells Promote Pancreatic Tumorigenesis. *Cancer discovery* 2016; **6**(3): 230-2.
19. Petitprez F, de Reyniès A, Keung EZ, et al. B cells are associated with survival and immunotherapy response in sarcoma. *Nature* 2020; **577**(7791): 556-60.
20. Cabrita R, Lauss M, Sanna A, et al. Tertiary lymphoid structures improve immunotherapy and survival in melanoma. *Nature* 2020; **577**(7791): 561-5.
21. Preston M, Sherman LS. Neural stem cell niches: roles for the hyaluronan-based extracellular matrix. *FBS* 2011; **3**(3): 1165-79.
22. G. Gritsenko P, Ilina O, Friedl P. Interstitial guidance of cancer invasion. *The Journal of Pathology* 2012; **226**(2): 185-99.
23. Fisher SB, Patel SH, Kooby DA, et al. Lymphovascular and perineural invasion as selection criteria for adjuvant therapy in intrahepatic cholangiocarcinoma: a multi-institution analysis. *HPB : the official journal of the International Hepato Pancreato Biliary Association* 2012; **14**(8): 514-22.
24. Chen SH, Zhang BY, Zhou B, Zhu CZ, Sun LQ, Feng YJ. Perineural invasion of cancer: a complex crosstalk between cells and molecules in the perineural niche. *American journal of cancer research* 2019; **9**(1): 1-21.
25. Zhao C-M, Hayakawa Y, Kodama Y, et al. Denervation suppresses gastric tumorigenesis. *Science Translational Medicine* 2014; **6**(250): 250ra115-250ra115.
26. Ito T, Ebata T, Yokoyama Y, et al. The Pathologic Correlation Between Liver and Portal Vein Invasion in Perihilar Cholangiocarcinoma: Evaluating the Oncologic Rationale for the American Joint Committee on Cancer Definitions of T2 and T3 Tumors. *World Journal of Surgery* 2014; **38**(12): 3215-21.

27. Ebata T, Mizuno T, Yokoyama Y, Igami T, Sugawara G, Nagino M. Surgical resection for Bismuth type IV perihilar cholangiocarcinoma. *British Journal of Surgery* 2017; **105**(7): 829-38.
28. Zhang XF, Beal EW, Chakedis J, et al. Defining Early Recurrence of Hilar Cholangiocarcinoma After Curative-intent Surgery: A Multi-institutional Study from the US Extrahepatic Biliary Malignancy Consortium. *World journal of surgery* 2018.
29. Neumann UP, Schmeding M. Role of surgery in cholangiocarcinoma: From resection to transplantation. *Best Practice & Research Clinical Gastroenterology* 2015; **29**(2): 295-308.
30. Torre LA, Bray F, Siegel RL, Ferlay J, Lortet-Tieulent J, Jemal A. Global cancer statistics, 2012. *CA: A Cancer Journal for Clinicians* 2015; **65**(2): 87-108.
31. Lurje G, Bednarsch J, Czigany Z, et al. The prognostic role of lymphovascular invasion and lymph node metastasis in perihilar and intrahepatic cholangiocarcinoma. *European Journal of Surgical Oncology* 2019; **45**(8): 1468-78.
32. Neuhaus P, Jonas S, Bechstein WO, et al. Extended Resections for Hilar Cholangiocarcinoma. *Annals of Surgery* 1999; **230**(6).
33. Petrowsky H, Wildbrett P, Husarik DB, et al. Impact of integrated positron emission tomography and computed tomography on staging and management of gallbladder cancer and cholangiocarcinoma. *Journal of Hepatology* 2006; **45**(1): 43-50.
34. Neuhaus P, Thelen A, Jonas S, et al. Oncological Superiority of Hilar En Bloc Resection for the Treatment of Hilar Cholangiocarcinoma. *Annals of Surgical Oncology* 2012; **19**(5): 1602-8.
35. Bednarsch J, Czigany Z, Lurje I, et al. Left- versus right-sided hepatectomy with hilar en-bloc resection in perihilar cholangiocarcinoma. *HPB* 2020; **22**(3): 437-44.
36. Hyder O, Hatzaras I, Sotiropoulos GC, et al. Recurrence after operative management of intrahepatic cholangiocarcinoma. *Surgery* 2013; **153**(6): 811-8.
37. Komaya K, Ebata T, Yokoyama Y, et al. Recurrence after curative-intent resection of perihilar cholangiocarcinoma: analysis of a large cohort with a close postoperative follow-up approach. *Surgery* 2018; **163**(4): 732-8.
38. Valle J, Wasan H, Palmer DH, et al. Cisplatin plus Gemcitabine versus Gemcitabine for Biliary Tract Cancer. *New England Journal of Medicine* 2010; **362**(14): 1273-81.
39. de Jong MC, Nathan H, Sotiropoulos GC, et al. Intrahepatic cholangiocarcinoma: an international multi-institutional analysis of prognostic factors and lymph node assessment. *Journal of clinical oncology : official journal of the American Society of Clinical Oncology* 2011; **29**(23): 3140-5.
40. Miura JT, Johnston FM, Tsai S, et al. Chemotherapy for Surgically Resected Intrahepatic Cholangiocarcinoma. *Ann Surg Oncol* 2015; **22**(11): 3716-23.
41. Stein A, Arnold D, Bridgewater J, et al. Adjuvant chemotherapy with gemcitabine and cisplatin compared to observation after curative intent resection of cholangiocarcinoma and muscle invasive gallbladder carcinoma (ACTICCA-1 trial) - a randomized, multidisciplinary, multinational phase III trial. *BMC cancer* 2015; **15**: 564.
42. Primrose JN, Fox RP, Palmer DH, et al. Capecitabine compared with observation in resected biliary tract cancer (BILCAP): a randomised, controlled, multicentre, phase 3 study. *The Lancet Oncology* 2019; **20**(5): 663-73.
43. Serrablo A, Serrablo L, Alikhanov R, Tejedor L. Vascular Resection in Perihilar Cholangiocarcinoma. *Cancers (Basel)* 2021; **13**(21): 5278.
44. Zhao Q, Yang Y, Liang X, et al. The clinicopathological significance of neurogenesis in breast cancer. *BMC Cancer* 2014; **14**(1): 484.
45. Bednarsch J, Kather J, Tan X, et al. Nerve Fibers in the Tumor Microenvironment as a Novel Biomarker for Oncological Outcome in Patients Undergoing Surgery for Perihilar Cholangiocarcinoma. *Liver Cancer* 2021; **10**(3): 260-74.
46. Liu HP, Tay SS, Leong S, Schemann M. Colocalization of ChAT, DbetaH and NADPH-d in the pancreatic neurons of the newborn guinea pig. *Cell and tissue research* 1998; **294**(2): 227-31.
47. Nakanuma Y, Kakuda Y. Pathologic classification of cholangiocarcinoma: New concepts. *Best practice & research Clinical gastroenterology* 2015; **29**(2): 277-93.
48. Akita M, Fujikura K, Ajiki T, et al. Dichotomy in intrahepatic cholangiocarcinomas based on histologic similarities to hilar cholangiocarcinomas. *Modern pathology : an official journal of the United States and Canadian Academy of Pathology, Inc* 2017; **30**(7): 986-97.

49. Kendall T, Verheij J, Gaudio E, et al. Anatomical, histomorphological and molecular classification of cholangiocarcinoma. *Liver international : official journal of the International Association for the Study of the Liver* 2019; **39 Suppl 1**: 7-18.
50. Borger DR, Tanabe KK, Fan KC, et al. Frequent mutation of isocitrate dehydrogenase (IDH)1 and IDH2 in cholangiocarcinoma identified through broad-based tumor genotyping. *Oncologist* 2012; **17**(1): 72-9.
51. Lowery MA, Ptashkin R, Jordan E, et al. Comprehensive Molecular Profiling of Intrahepatic and Extrahepatic Cholangiocarcinomas: Potential Targets for Intervention. *Clinical cancer research : an official journal of the American Association for Cancer Research* 2018; **24**(17): 4154-61.
52. Nakamura H, Arai Y, Totoki Y, et al. Genomic spectra of biliary tract cancer. *Nature genetics* 2015; **47**(9): 1003-10.

Chapter7

7

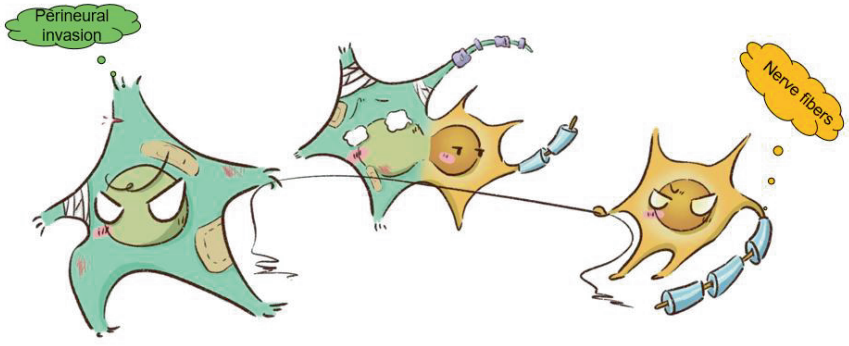

ADDENDUM 8

Summary

Chapter 8

Summary

The overall aim of this thesis is to study the role of nerve fibers in neurotropic cancer, pancreatic cancer (PDAC) and Cholangiocarcinoma (CCA), exploring a novel prognostic biomarker. This thesis provides clinical observational studies focusing on the presence of nerve fibers in PDAC, pCCA and iCCA patients undergoing curative intend surgery.

The role of nerve fibers in neurotropic cancer

Chapter 2 provides an overview of theoretical knowledge of neural systems in neurotropic cancer as well as clinical studies that describe the clinical association between nerves and patients' oncological outcomes in PDAC and CCA. There are evident indications of a close relationship between nerves in the TME and patients' survival in PDAC and CCA. The existing literature shows that perineural invasion is an independent prognostic factor of poor outcome in neurotropic cancer. This chapter focuses on the shared signaling pathways of the mechanisms behind perineural invasion in PDAC and CCA. Hereby we focus on signaling neurotransmitters and neuropeptides which may be a target for future cancer therapies. Small nerve fiber crosstalk with other components of the TME, participate in the interaction of cancer progression.

The role of nerve fibers in PDAC

In **Chapter 3**, we present our retrospective study about the influence of nerve fibers in PDAC patients. This study aimed to explore whether NFD is associated with oncological outcome of PDAC patients after surgery. In this study design, NFD is determined as the number of small nerve fibers, not to be confused by nerves which are invaded by tumor cells. We have used single immunohistochemistry to define which immune cells were co-localized with the nerve fibers. The results demonstrate that high NFD is associated with a better survival in PDAC patients, while NFD was not associated with tumor invasion into the nerve fibers. In addition, these small nerve fibers are co-localized with lymphoid aggregates, mostly containing CD20+ B cells and a small rim of T cells.

The conclusion from **Chapter 3** is that small nerve fibers can be a potential biomarker to improve clinical outcome. Though, more studies are needed to confirm the positive function of small nerve fibers in PDAC, we expect that these results will provide reference for further studies, potentially our results may even be broadly applicable to other malignancies.

The role of nerve fibers in pCCA

Chapter 4 presents a retrospective study about the role of nerve fibers in CCA on survival. Based on the results of our PDAC cohort, we aim to investigate nerve fibers as a prognostic marker in a large European cohort of pCCA patients undergoing surgical resection. In this study design, extensive group comparison between patients with high and low NFD were carried out. The association of cancer-specific survival (CSS) and recurrence-free survival (RFS) with NFD and other clinic pathological characteristics were assessed using univariate and multivariable analysis. Results suggest patients with high NFD have better CSS and RFS. Furthermore, in this study we have conducted immunohistochemistry to identify the small nerve fibers origin to be parasympathetic. **Chapter 4** suggests that nerve fiber are identified as an important novel prognostic biomarker in pCCA patients. High NFD is associated with a better outcome. Nerve fibers alone or in combination with nodal status in particular allows to stratify pCCA patients based on their risk for inferior oncological outcomes after curative-intent surgery.

The role of nerve fibers in iCCA

In **Chapter 5**, we aimed to determine the role of nerve fibers in iCCA. Therefore, the impact of nerve fibers on long term survival is investigated in a large European cohort of patients with iCCA. All patients were admitted to the University Hospital RWTH Aachen for curative-intent surgical resection. By univariate and multivariate analysis, the absence of

nerve fibers is determined to be an independent predictor of impaired long-term survival. A group comparison between patients with and without the presence of small nerve fibers demonstrated a better outcome in patients with presence of small nerve fibers compared to patients without small nerve fibers. In **Chapter 5**, we suggested the presence of nerve fibers in the TME of iCCA to be a novel prognostic biomarker.

Based on clinical observational studies, we further aimed to explore differences in immune cell composition and spatial distribution on survival between high and low NFD patients. In **chapter 6**, we applied multiplexed immunofluorescence (mIF) on pCCA patients and investigated the immune cell composition and distribution in the TME of high and low NFD patients. Group comparison and oncological outcome analysis was performed. Results demonstrated high CD8+PD-1 expression is associated with a better OS and RFS. Thus, High CD8+PD-1 expression is further identified as an independent predictor of OS of pCCA patients, potentially after validation and further research this can be of importance in patient selection for PD-1 blockade therapeutics.

Abbreviations

CCA	Cholangiocarcinoma
CSS	Cancer-specific survival
ICCA	Intrahepatic Cholangiocarcinoma
NFD	Nerve fiber density
OS	Overall Survival
PCCA	Perihilar Cholangiocarcinoma
PDAC	Pancreatic cancer
RFS	Recurrence-free survival
TME	Tumor microenvironment

Chapter 8

ADDENDUM

中文摘要

Chapter 8

胰腺癌和胆管癌都是恶性度极高的侵袭性肿瘤，诊断和治疗困难，预后差。早期诊断和早期治疗是提高和改善胰腺癌和胆管癌预后的关键。目前，手术并辅以放化疗综合治疗仍然是有望根治的唯一方法。但由于大多数病人诊断较晚，已经丧失手术根治的机会，还没有一种高效且可完全应用的有效综合治疗方案。本论文旨在探索神经纤维在胰腺癌和胆管癌的肿瘤微环境中充当的角色并探讨结合免疫和分子等生物治疗的新方法。评估其作为胰腺癌和胆管癌诊断，预后的新型生物标记物的潜能。

胰腺癌和胆管癌被认为是嗜神经性癌，**第二章** 综述了近年有关神经侵袭和神经纤维在胰腺癌和胆管癌的实验和临床研究进展，对胰腺癌和胆管癌的周围神经侵袭潜在分子机制中的共同信号通路进行概述。值得注意的是，在本论文中，我们更关注的是肿瘤微环境中神经纤维在癌症进程中的作用。在**第二章**中，我们讨论了胰腺癌和胆管癌肿瘤微环境中神经纤维、免疫细胞、成纤维细胞以及肿瘤细胞等主要不同成分的串扰，专注于信号传导神经递质和神经肽，这可能是未来治疗的目标。此外，我们总结了现有关于 胰腺癌和 胆管癌患者神经纤维的临床研究文献的回顾性结果。

研究表明肿瘤微环境中各种间质成分对胰腺癌的免疫逃逸起作用，而神经纤维在胰腺癌的相关进展中的作用尚未得到充分研究。我们假设神经纤维在胰腺癌进展中起着关键作用。为了确定神经纤维在胰腺癌中的作用及其在肿瘤微环境中的空间分布，我们在**第三章**对 166 例手术后的胰腺癌病例做了回顾性研究。结果显示高密度神经纤维的病人比低密度神经纤维的病人具有更长的生存时间，肿瘤微环境中的神经纤维似乎是胰腺癌病人有利的预后因素。同时，这些神经纤维位于淋巴聚集体周围， 被 B 淋巴细胞包围。 在这项研究表明神经纤维也在肿瘤进展中发挥作用，神经纤维可能是癌症发生、进展和转移的新兴调节因子。

在胰腺癌回顾性研究中，我们发现神经纤维密度与病人的总生存期相关。然而，其在胆管癌中的作用未知。**第四章** 纳入了 2010 年至 2019 年间接受根治性手术的 101 名 肝门部胆管癌进行回顾性研究，探索神经纤维密度是否与临床预后相关。结果显示高密度神经纤维与病人的癌症特异性生存期和无复发生存期特异性相关，高密度的神经纤维组病人具有更长的癌症特异性生存期和无复发生存期。同时，我们用免疫组化方法对神经纤维进行免疫染色，探索其来源，发现这些神经纤维来源于副交感神经。

基于**第四章**的结论：在肝门胆管癌中，神经纤维可作为肝门胆管癌患者潜在的新型预后生物标记物，神经纤维密度和患者临床生存期相关，肿瘤微环境中神经纤维密度高的患者具有更长的癌症特异性、生存期和无复发生存期，但目前这种临床现象的潜在机制没有研究做出解释。在**第六章**我们进一步对其潜在的分子机制进行研究。我们假设 神经纤维密度可能与免疫细胞表型相关。因此使用多重免疫荧光技术来表征不同的免疫细胞表型，及其共刺激和共抑制免疫检查点，来揭示肝门胆管癌中高神经纤维密度组和低神经纤维密度组的免疫细胞组成和分布的差异。 研究显示 PD-1+ T 细胞与高 神经纤维 相关。PD-1+的表达量可作为免疫疗法预后生物标志物并以此预测良好的存活率。

我们几项针对胰腺癌，肝门胆管癌的回顾性病例研究，确认了肿瘤微环境中神经纤维与患者临床预后的关系，但肝内胆管癌肿瘤微环境中神经纤维密度的肿瘤学作用仍有待探索。因此，本论文**第五章**对 2010 年至 2019 年期间，接受肝切除术的 95 名 肝内胆管癌患者的病理学特征及生存数据进行了分析。在我们的队列中，无神经纤维，淋巴结转移，术前血红蛋白低这几项参数都是短期癌症特异性生存期的独立性预测指标。这项研究结果与之前的研究结果一致，肝内胆管癌患者中低神经纤维密度或无神经纤维组患者的总生存期显著短于高神经纤维组，表明神经纤维密度在肝内胆管癌中也具有重要的预测价值。高低两组患者生存率的巨大差异显示了神经纤维密度 在肿瘤复发方面的良好预测价值。

在本论文中，我们提出并确认了我们的假设，即神经纤维有可能被用作“神经性”肿瘤－胰腺癌和胆管癌 患者强有力的生存生物标志物。

Summary

Chapter 8

ADDENDUM 9

Valorization

Chapter 9

Impact paragraph

Societal impact and scientific relevance

Globally, cancer ranks as a leading cause of death and a critical burden of disease. PCA is the 14th most commonly diagnosed malignancy and the 7th leading cause of cancer mortality. Furthermore, research shows the incidence and mortality are overall increasing[1]. The incidence of PCA shows regional differences in distribution: the regions with high incidence are developed countries including North America, Europe, Australia and Asia, the rates in low-income nations are much lower than those in North America and Europe[2].

Although the incidence of CCA shows geographical variation worldwide as well, the global incidence of CCA is < 2/100,000, therefore it is considered a rare cancer globally[3]. The highest incidence of iCCA is in Asia (6.1/100,000), while the lowest incidence of iCCA is in Oceania (1.8/100,000). In general, we need to continue to investigate and improve our understanding of the basic biology of PDAC and CCA to reach more effective personalized treatment approaches for CCA and PDAC patients and potentially extend life expectancy and increase treatment options.

The research field of the TME in cancer is evolving, however we conclude that research focusing on small nerve fibers in PDAC and CCA is still limited. In the current thesis, we propose that high nerve fiber density is a potential prognostic biomarker. This is a valuable finding from a clinical point of view as it might lead to the development of a new reliable prognostic biomarker for CCA and PDAC patients after surgery. The evaluation of nerve fiber density can be easily analyzed with one additional immunohistochemical staining and could be integrated in the routine pathology report.

This thesis provides first steps for further research in neuroscience and PDAC and CCA. Our target population included PDAC and CCA cohorts from the University Hospital RWTH Aachen, because these cohorts were available in the archives of the pathology department. All patients had localized disease and underwent surgical resection with curative intent. The study design in this thesis was retrospective.

Novelty of the concept

In this thesis, we focused on the density of small nerve fibers in different types of "neurotropic cancer" rather than the well-known concept “perineural invasion (PNI)”. Nerve fiber density (NFD) is determined as the number of small nerve fibers in the TME, while perineural invasion refers to larger nerve fibers with the presence of tumor cells invading the perineurium.

PDAC and CCA are in close anatomical location but they have some different histological characteristics. These histological differences reflect the molecular heterogeneity of cancer entities. We observed that high NFD is predictive for a good outcome and can be used as a novel prognostic biomarker in both CCA and PDAC patients. In contrast to this, we could not identify NFD as a prognostic biomarker in Hepatocellular carcinoma (HCC) (not in this thesis)[4].

Nerve fibers are a component of the TME but have not been highlighted much, more is known about the role of fibroblasts and immune cells in cancer initiation and progression. PDAC and CCA are known for the PNI growth pattern, associated with a poor outcome. Here, we presented the novel hypothesis of a dual role of nerve fibers: besides the aggressive PNI, also protective nerve fibers exist. The underlying pathway behind the presence of NFD needs to be further investigated. Also, the potential role for new therapeutically targets is still under investigation.

Future plan

Valorization

We described high nerve fiber density in PDAC, pCCA and iCCA patients to be associated with a better outcome. In this thesis, we conclude that our results provide basic evidence for exploration of future nerve fiber research in cancer patients. The underlying pathway still must be identified, and further research is needed. Next steps would be to further unravel the spatial context of the small nerve fibers combined with a spatial genomic approach. New techniques allow single cell RNA sequencing on FFPE blocks with the advantage the spatial context is kept. Using these methods, it will allow to closely investigate the transcriptomic status of the patients with high and low NFD. Recent work has demonstrated that in a mouse model axonal sprouting from pre-existent nerve fiber trunks is protective in PDAC[5]. Increasing knowledge on the role of nerve fibers in cancer is important to improve personalized medicine for cancer patients.

Reference

1. Huang J, Lok V, Ngai CH, et al. Worldwide Burden of, Risk Factors for, and Trends in Pancreatic Cancer. *Gastroenterology* 2021; **160**(3): 744-54.
2. Klein AP. Pancreatic cancer epidemiology: understanding the role of lifestyle and inherited risk factors. *Nature Reviews Gastroenterology & Hepatology* 2021; **18**(7): 493-502.
3. Krishna M. Pathology of Cholangiocarcinoma and Combined Hepatocellular-Cholangiocarcinoma. *Clin Liver Dis (Hoboken)* 2021; **17**(4): 255-60.
4. Bednarsch J, Tan X, Czigany Z, et al. Limitations of Nerve Fiber Density as a Prognostic Marker in Predicting Oncological Outcomes in Hepatocellular Carcinoma. *Cancers (Basel)* 2022; **14**(9).
5. Guillot J, Dominici C, Lucchesi A, et al. Sympathetic axonal sprouting induces changes in macrophage populations and protects against pancreatic cancer. *Nature communications* 2022; **13**(1): 1985.

Chapter 9

ADDENDUM 10

Curriculum Vitae

Publication

Acknowledgement

Chapter 10

Curriculum Vitae

Xiuxiang Tan was born in Fujian province, China. In July 2011, she graduated from high School and started her bachelor education in Fujian University of Traditional Chinese Medicine (Fuzhou, Fujian province, China) in September of the same year. During the four-year college (2011-2015), she got National Encouragement Scholarship, Prize Scholarship, Outstanding student of Fujian University of Traditional Chinese Medicine. After completing an internship at Fujian Province Hospital (Fuzhou, China), she got his bachelor's degree with a major in biomedical engineering in July, 2015.

Subsequently, she applied on a Master program to the Peking Union Medicine College (Beijing, China) and then participated in the Master program of biomedical engineering in September 2015. The research project of her master's degree was about "Hydrogel Loading ENDOSTAR Combined With Immunotherapy were an Promising Treatment for Colorectal Cancer". From this study experience, she felt researching the field of cancer research was an amazing work and determined to devote her career on this field. She got her master's degree in July 2018 after finishing her master thesis.

Then in the same year, she was awarded a scholarship under the State Scholarship Fund from China Scholarship, this scholarship covered four years (09.2018-09.2022). With this scholarship, she set out her research in the Netherlands. He started her full- time PhD candidate at the department of Surgery within the school of Nutrition and Translational Research in Metabolism (NUTRIM), Maastricht University under the supervision of Prof. dr. Ulf P. Neumann and dr. Lara Heij. The topic of her PhD research was to explore the role of nerve fibers in the tumor microenvironment in pancreatic cancer and cholangiocarcinoma.

List of publications

1. **Tan X**, Sivakumar S, Bednarsch J, Wiltberger G, Kather JN, Niehues J, de Vos-Geelen J, Valkenburg-van Iersel L, Kintsler S, Roeth A, Hao G, Lang S, Coolsen ME, den Dulk M, Aberle MR, Koolen J, Gaisa NT, Olde Damink SWM, Neumann UP, Heij LR. Nerve fibers in the tumor microenvironment in neurotropic cancer-pancreatic cancer and cholangiocarcinoma. Oncogene. 2021 Feb;40(5):899-908. doi: 10.1038/s41388-020-01578-4. Epub 2020 Dec 7. (2021 IF: 9.867)

2. Bednarsch [#], **Tan X**[#], Czigany Z, Liu D, Lang SA, Sivakumar S, Kather JN, Appinger S, Rosin M, Boroojerdi S, Dahl E, Gaisa NT, den Dulk M, Coolsen M, Ulmer TF, Neumann UP, Heij LR. The Presence of Small Nerve Fibers in the Tumor Microenvironment as Predictive Biomarker of Oncological Outcome Following Partial Hepatectomy for Intrahepatic Cholangiocarcinoma. Cancers (Basel). 2021 Jul 21;13(15):3661. (2021 IF: 6.639)

3. Heij LR, **Tan X**, Kather JN, Niehues JM, Sivakumar S, Heussen N, van der Kroft G, Damink SWMO, Lang S, Aberle MR, Luedde T, Gaisa NT, Bednarsch J, Liu DHW, Cleutjens JPM, Modest DP, Neumann UP, Wiltberger GJ. Nerve Fibers in the Tumor Microenvironment Are Co-Localized with Lymphoid Aggregates in Pancreatic Cancer. J Clin Med. 2021 Jan 30;10(3):490. doi: 10.3390/jcm10030490. PMID: 33573277. (2021 IF: 4.24)

4. Bednarsch J, Kather J, **Tan X**, Sivakumar S, Cacchi C, Wiltberger G, Czigany Z, Ulmer F, Neumann UP, Heij LR. Nerve Fibers in the Tumor Microenvironment as a Novel Biomarker for Oncological Outcome in Patients Undergoing Surgery for Perihilar Cholangiocarcinoma. Liver Cancer. 2021 Jun;10(3):260-274. doi: 10.1159/000515303. Epub 2021 May 6. (2021 IF: 11.74)

5. Echle A, Grabsch HI, Quirke P, van den Brandt PA, West NP, Hutchins GGA, Heij LR, **Tan X**, Richman SD, Krause J, Alwers E, Jenniskens J, Offermans K, Gray R, Brenner H, Chang-Claude J, Trautwein C, Pearson AT, Boor P, Luedde T, Gaisa NT, Hoffmeister M, Kather JN. Clinical-Grade Detection of Microsatellite Instability in Colorectal Tumors by Deep Learning. Gastroenterology. 2020 Oct;159(4):1406-1416.e11. doi: 10.1053/j.gastro.2020.06.021. Epub 2020 Jun 17. (2021 IF: 22.687)

6. Muti HS, Heij LR, Keller G, Kohlruss M, Langer R, Dislich B, Cheong JH, Kim YW, Kim H, Kook MC, Cunningham D, Allum WH, Langley RE, Nankivell MG, Quirke P, Hayden JD, West NP, Irvine AJ, Yoshikawa T, Oshima T, Huss R, Grosser B, Roviello F, d'Ignazio A, Quaas A, Alakus H, **Tan X**, Pearson AT, Luedde T, Ebert MP, Jäger D, Trautwein C, Gaisa NT, Grabsch HI, Kather JN. Development and validation of deep learning classifiers to detect Epstein-Barr virus and microsatellite instability status in gastric cancer: a retrospective multicentre cohort study. Lancet Digit Health. 2021 Oct;3(10):e654-e664. doi: 10.1016/S2589-7500(21)00133-3. Epub 2021 Aug 17. Erratum in: Lancet Digit Health. 2021 Oct;3(10):e622. (2021 IF: 24.519)

Poster presentations

- February, 2022: Liver Cancer Summit 2022, online. Title: Nerve Fibers in the Tumor Microenvironment as a Novel Biomarker for Oncological Outcome in Patients Undergoing Surgery for Perihilar Cholangiocarcinoma.
- June, 2022: 105th annual conference of the scientific specialist society in pathology, Münster, Germany. Title: PD1+ T-cells correlate with Nerve Fiber Density as a prognostic biomarker in patients with resected perihilar cholangiocarcinoma.

- July, 2022: ENS-CCA 2022 Edinburgh. Title: Intratumoral PD-1 positive Memory T cells are predictive of response to checkpoint blockade in cholangiocarcinoma.

Acknowledgement

I am truly grateful for my scholarship supporter, China Scholarship Council (CSC), the scholarship covered my four-year study in the Department of Surgery, Maastricht University in the Netherlands. Also, I would like to express my gratitude to many people for their support and encouragement during my PhD and writing this thesis. This scholarship allows me to work less hours.

I am grateful to my assessment committee, prof. dr. Manon van Engeland, prof. Dr. Heike Grabsch, prof. Edgar Dahl, prof. dr. Danny Jonigk . Thank you very much for your effort and time to evaluate this thesis critically. Lots of grateful moments accompany the completion of this thesis. I truly appreciate all the help and support I have received leading to this thesis, from my supervision team, my colleagues, my friends, and my family. I could not have finished it without your help and encouragement.

First and foremost, I am extremely grateful to my supervisors, prof. dr. Ulf P. Neumann and dr. Lara Heij for their invaluable advice, continuous support, and patience during my PhD study. Their immense knowledge and plentiful experience have encouraged me in all the time of my academic research and daily life. My dear daily-supervisor, dr. Lara Heij, this is a note of appreciation for taking time out of your busy day and helping me with all aspects of studies, projects, and lives. I still clearly remember that you always encouraged me and gave me confidence whenever I have difficulties in communication and languages. It really released me from stress and also helped me to adapt into new environment and new research projects. You always patiently to answer my confusion and question no matter during work time or off work time. I still remember that night we worked together on exploring cell suspension technology until midnight. You always kindly drove me between Aachen and Maastricht at the first year. Besides, thanks a lot for your warm care and kind help during my PhD. You often asked me if I need help when we met. These are all great memories for me. I am very happy that have been working with you for the past years, I learned a lot from you not only about the academic knowledge but also the respectful attitude to every communicator. In my mind, you are a great pathologist, a fantastic promotor, an outstanding scientist, and a nice mother, who balances the career and life perfectly.

I would like to express my sincere thanks to all of the members of the Department of Surgery. I received so much support. Thanks for you all warm words and care at the beginning when I joined surgery department. I received so many great comments and brilliant ideals during our Lab Chats. I also enjoyed a lot during our department social activities at the beginning two years, before CoV-19 pandemic. No matter celebrating Sinterklaas day or barbecue were all help me into the new collective. Those are unforgettable memories for my PhD. I really enjoyed being a member of this nice department. I would like to offer my special thanks to Romy Aarnoutse and Jeanine. Many thanks for all the kind help you gave in the first year of my PhD. Romy Aarnoutse, I still remember you picked me up at the station and prepared bedclothes for me when I arrived 4 years ago. All your done help me settle down in Maastricht made a favorable impression of this beautiful city in the mind of me. Jeanine, thank you for your all kind help in Lab work during my first year PhD. Although we only had a short time work together, these detail things made a strong impression on me. Many thanks to Bas, Mo, Hans, Annemarie, Chantal, Loes for your technical support in Lab. Many thanks to Lin, Min, Mirjam, Merel, Rianne, Annet, Kees, Janine, Anne, Romy, Sanaz, and all PhD students both current and former colleagues in Surgery Lab. It is so nice to communicate with all of you.

Yuandi and Peiliang, my dear office roommates and lovely friends. I'm so glad to join your Journey to Paris when I knew you both for the first time. And then we become roommates and had more great journey and nice memories gradually. We celebrated special festival together, had nice dinner, play Majiang, etc. We chatted and shared our hobbies which makes the stressful working time turn to interesting.

Many thanks to all colleagues who participated in my projects in ZBMT surgery lab. Prof. Cramer, Thorsten, thank you for providing a lovely working condition. Mika and Simone, thank you for your computer technological support. Johanna, thank you for the orientation in lab. Jochen, you always patiently and kindly help me in all aspects including lab training and introduction of German lives and culture. Ümran, Merve, and Laura, I am really enjoyed the tour of Aachen Christmas market in 2020. Long and Guanshan, special thanks to you, thank you for your care. I still clearly remember that I used your accounts and keys when I haven't gotten my own stuffs in Aachen at the first year. You are always patient, kind, and enthusiasm. Although we only had two years' time in Lab, you both like my order brother to me. I also participated in your PhD defense, It was like yesterday. Really appreciated all the help you gave to me.

I would like to extend my sincere thanks to my Chinese friends Xinwei, Liuhong, Jianhua, Lin and all my friends. I enjoyed chatting, drinking, sharing experience and vies and having dinner with you. Those activities we had during my living in Netherland help me release my stress and fill in with energy. Jianhua, do you know you are a powerful, efficient, and diligent girl. It is so nice to have deep friendships and travel together with you. Thank you for all your friendship that makes me feel relaxed and warm. I would like to express my special thanks to my new friend, Jiali, thank you for your work for this thesis cover. I really like your cartoon characters. And these cells under your pen look really vivid and vital.

I wish to express my thanks to my family for their unwavering support and belief in me, thank you very much for your warm care within these years. Thanks for always being there with me. I want to say, thank you for your great admiration on my own freedom, you always fully support my life or study choice with no judgment. Every time when I face challenges, you give me a lot of strength, you always supported me financially and mentally. How can I repay your marvelous love? I will share more time together with you.

Chapter 10